การสังเคราะห์อะโรเมติกจากนอร์มัลเฮปเทนโดยใช้ตัวเร่งปฏิกิริยา ซีโอไลต์ชนิดเอ็มเอฟไอที่ถูกดัดแปร

นางสาว นิลเนตร แซ่อึ้ง

วิทยานิพนธ์นี้เป็นส่วนหนึ่งของการศึกษาตามหลักสูตรปริญญาวิศวกรรมศาสตรมหาบัณฑิต

สาขาวิชาวิศวกรรมเคมี ภาควิชาวิศวกรรมเคมี

คณะวิศวกรรมศาสตร์ จุฬาลงกรณ์มหาวิทยาลัย

ปีการศึกษา 2543

ISBN 974-346-984-2

AROMATIC SYNTHESIS FROM N-HEPTANE USING MODIFIED MFI-TYPE ZEOLITE CATALYSTS

Miss Nilnate Oung

A Thesis Submitted in Partial Fulfillment of the Requirements
for the Degree of Master of Engineering in Chemical Engineering
Department of Chemical Engineering
Faculty of Engineering
Chulalongkorn University
Academic Year 2000

ISBN 974-346-984-2

Thesis Title	Aromatic synthesis from n-heptane using modified MFI-type zeolite catalysts
By	Miss Nilnate Oung
Field of Study	Chemical Engineering
Thesis Advisor	Dr. Suphot Phatanasri, Dr. Eng.
Thesis Co-advisor	Professor Piyasan Praserthdam, Dr.Ing.

Accepted by the Faculty of Engineering, Chulalongkorn University in Partial Fulfillment of the Requirements for the Master's Degree

.....……Dean of Faculty of Engineering
(Professor Somsak Panyakeow, Dr.Eng.)

Thesis Committee

.....Chairman
(Associate Professor Kroekchai Sukanjanajtee, Ph.D.)

.....Thesis Advisor
(Suphot Phatanasri, Dr. Eng.)

.....Thesis Co-advisor
(Professor Piyasan Praserthdam, Dr.Ing.)

.....Member
(Assistant Professor Suttichai Assabumrungrat, Ph.D.)

นิลเนตร แซ่อึ้ง : การสังเคราะห์อะโรเมติกจากนอร์มัลเฮปเทนโดยใช้ตัวเร่งปฏิกิริยาซีโอไลต์ชนิดเอ็มเอฟไอที่ถูกดัดแปร (AROMATIC SYNTHESIS FROM N-HEPTANE USING MODIFIED MFI-TYPE ZEOLITE CATALYSTS) อ. ที่ปรึกษา : อ. ดร. สุพจน์ พัฒนะศรี, อ. ที่ปรึกษาร่วม : ศ. ดร. ปิยะสาร ประเสริฐธรรม, 98 หน้า. ISBN 974-346-984-2.

การสังเคราะห์อะโรเมติกจากนอร์มัลเฮปเทนโดยใช้ตัวเร่งปฏิกิริยาซีโอไลต์ชนิดเอ็มเอฟไอที่ถูกดัดแปร พบว่า โลหะแกลเลียม (Ga) และสังกะสี (Zn) จะช่วยเพิ่มทั้งความว่องไวและการเลือกเกิดของการสังเคราะห์อะโรเมติกจากนอร์มัลเฮปเทน โดยทำการเตรียมตัวเร่งปฏิกิริยาแบบอินคอร์เปอร์เรชัน ซึ่งจะช่วยลดขั้นตอนในการเตรียมตัวเร่งปฏิกิริยาลง พบว่า H-Ga.Al-silicate ซึ่งมีอัตราส่วนซิลิกอนต่อแกลเลียมในการสังเคราะห์เท่ากับ 100 และซิลิกอนต่ออะลูมิเนียมเท่ากับ 40 และ H-Zn.Al-silicate ซึ่งมีอัตราส่วนซิลิกอนต่อสังกะสีในการสังเคราะห์เท่ากับ 150 และซิลิกอนต่ออะลูมิเนียมเท่ากับ 40 จะให้ผลการเลือกเกิด เบนซีน โทลูอีน และไซลีนสูงใกล้เคียงกับค่าที่ได้จากแกลเลียมและสังกะสีแลกเปลี่ยนไอออนกับตัวเร่งปฏิกิริยาซีโอไลต์ชนิดเอ็มเอฟไอที่มีปริมาณแกลเลียมและสังกะสีใกล้เคียงกันแต่ขั้นตอนในการเตรียมตัวเร่งปฏิกิริยาน้อยกว่า

สำหรับอิทธิพลของตัวแปรต่างๆ ในการทำปฏิกิริยา เช่น อุณหภูมิในการทำปฏิกิริยา ความเร็วเชิงเสปซ ความเสถียรของตัวเร่งปฏิกิริยา พบว่าค่าการเลือกเกิดอะโรเมติกของตัวเร่งปฏิกิริยาที่เตรียมแบบอินคอร์เปอร์เรชันมีค่าสูงสุดเมื่อทำปฏิกิริยาที่อุณหภูมิ 550 องศาเซลเซียส ความเร็วเชิงเสปซ 2000 ต่อชั่วโมง เป็นเวลา 1 ชั่วโมง ตัวเร่งปฏิกิริยาที่เตรียมแบบอินคอร์เปอร์เรชันเมื่อเสื่อมสภาพแล้วสามารถนำกลับมาใช้ใหม่ได้เมื่อถูกเผาที่อุณหภูมิ 550 องศาเซลเซียส เป็นเวลา 2 ชั่วโมง

ภาควิชา.....วิศวกรรมเคมี..... ลายมือชื่อนิสิต.....

สาขาวิชา.....วิศวกรรมเคมี..... ลายมือชื่ออาจารย์ที่ปรึกษา.....

ปีการศึกษา.....2543..... ลายมือชื่ออาจารย์ที่ปรึกษาร่วม.....

 # #4170376721: MAJOR CHEMICAL ENGINEERING
KEY WORD: ZSM-5 / n-HEPTANE / AROMATIZATION
NILNATE OUNG : AROMATIC SYNTHESIS FROM n-HEPTANE USING MODIFIED MFI-TYPE ZEOLITE CATALYSTS. THESIS ADVISOR: SUPHOT PHATANASRI, Dr. Eng, THESIS COADVISOR: PROF. PIYASAN PRASERTHDAM, Dr. Ing. 98 pp. ISBN 974-346-984-2.

Aromatic synthesis from n-heptane using modified MFI-type zeolite catalysts were investigated. It was shown that gallium and zinc improved both the activity and selectivity of n-heptane aromatization. Gallium and zinc modification was achieved by incorporation method which simplified the catalyst preparation procedure. It has been found that H-Ga.Al-silicate having Si/Ga loading ratio of 100, Si/Al ratio of 40 and H-Zn.Al-silicate having Si/Zn loading ratio of 150, Si/Al ratio of 40 exerted considerably high selectivity for aromatics. This selectivity was comparable to that of Ga or Zn exchanged MFI with the same amount of Ga or Zn loading. However, the bimetalloaluminosilicate catalysts can be prepared in only one step crystallization and thus simplifies the catalyst preparation procedure.

The influence of different reaction parameters such as reaction temperature, space velocity and stability were also studied. The selectivity for aromatic is maximum at 550 ^{o}C and GHSV 2000 h^{-1} for 1 hour on stream. The activity of deactivated H-Ga.Al-silicate and H-Zn.Al-silicate can be restored via the regeneration at 550 ^{o}C for 2 hours.

Department...….Chemical.engineering.. Student 's signature.....…….....….
Field of study.....Chemical engineering.. Advisor signature.....…...
Academic year…**2000**.....…….... Co-advisor 's signature..….....…..

ACKNOWLEDGEMENTS

The author would like to express her greatest gratitude to Dr. Suphot Phatanasri, her advisor, for his continuous guidance, enormous number of invaluable discussions, helpful suggestions and warm encouragement. She wishes to give his gratitude to Professor Dr. Piyasan Praserthdam, the thesis co-advisor, for his kind guidance and encouragement. In addition, she is also grateful to Associate Professor Dr. Kroekchai Sukanjanajtee, as chairman, and Assistant Professor Dr.Suttichai Assabumrungrat, as the thesis committee.

Special thanks also go to Mr. Thana Punsupsawat, Miss Sunee Srihiranpullop, Mr. Sornnarong Theinkaew and many friends who have encouraged and guided her over the years of her study.

Most of all, the author would like to express her highest gratitude to her parents for their inspiration and encouragement during her research.

CONTENTS

PAGE

LIST OF TABLES

LIST OF FIGURES

CHAPTER I
INTRODUCTION

Total lead phase-out and the change in the international petroleum market have led to rapid variations of feed cost and availability. In the present scenario, the major challenge is to take advantage of these variations and develop high value and high demand product. One of the low-value petroleum feedstocks available in excess in petroleum refineries is light naphtha. A profitable way to increase the value of the lower paraffin present in such petroleum feedstocks is to transform them directly into aromatic products which have high octane number and have a wide variety of applications in the petrochemical and chemical industries. They are an important raw material for many intermediates of commodity petrochemicals and valuable fine chemicals, such as monomers for polyesters, engineering plastics, intermediates for detergents, pharmacenticals, agricltural-products and explosives [1]. Among them, benzene, toluene and xylenes (BTX) are the three basic materials for most intermediates of aromatic derivatives (figure 1.1) [2].

Aromatics are usually produced by catalytic reforming which changes low octane number paraffins and naphthas into high octane number products, such as isoparaffin or aromatic. The product yields of this process are normally controlled by thermodynamics and hence result in a substantial mismatch between the supply and the actual market demands (figure 1.2) [3].

During the last decades, many investigation have been carried out on conversion of C_3-C_4 liquefied petroleum gas (LPG) into aromatic hydrocarbon on zeolite catalysts doped with gallium and also with other compounds such as zinc, platinum and bimetallics. The metal may be either incorporated to replace aluminium in the zeolite framwork or ion-exchanged with the existing cation in MFI-type catalyst has been proposed as the suitable catalyst for the reaction. Now light naphthas particularly hexane, heptane and octane are becoming an attractive feed for the production of the aromatic over MFI-type catalyst.

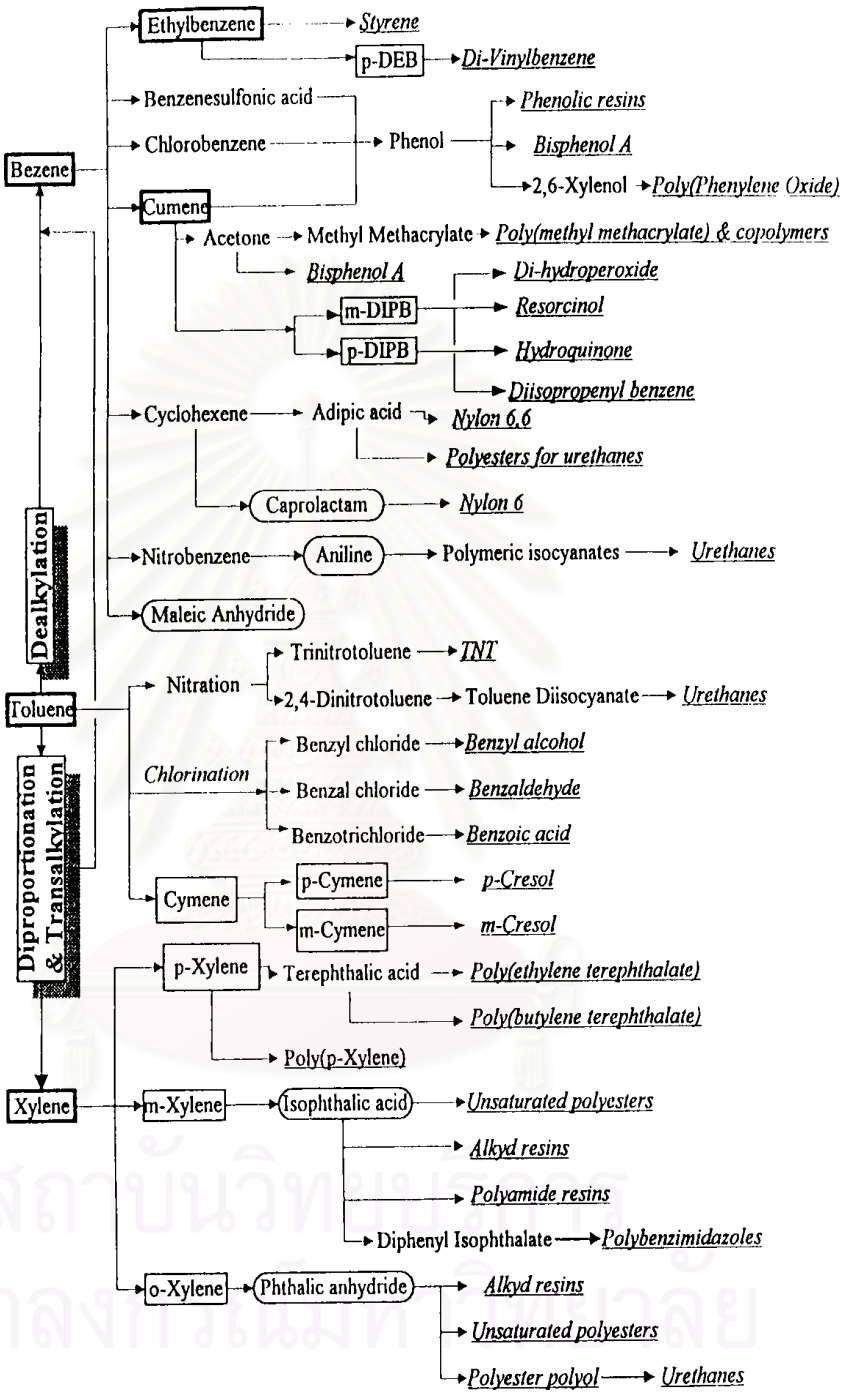

Figure 1.1 Derivatives of benzene, toluene and xylene [1]

Previous studies found that naphtha reforming over modified MFI-type zeolite catalyst had increasing conversion and selectivity. Therefore this research aims to investigate the catalytic performance of various metal containing MFI-type catalysts on heptane aromatization and the optinum method of metal introduction was proposed.

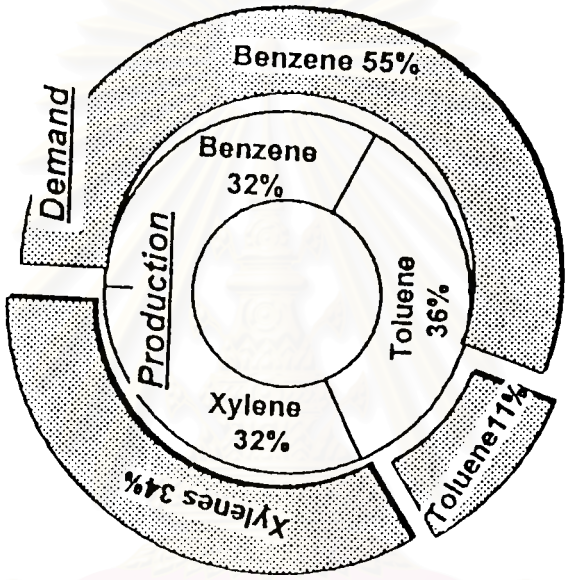

Figure 1.2 Comparison of worldwide BTX distribution patterns of production and market demand [2]

Therefore, this work aims to study synthesis of aromatic from n-heptane using modified MFI-type zeolite. This present work is arranged as follows:

Chapter II presents the literature reviews of investigation on the aromatization of n-heptane.

The theory of this research, the theoretical consideration on ZSM-5 and mechanism of aromatization of n-heptane are presented in chapter III.

Following by the description of the experimental systems and the operational procedures in chapter IV.

The experimental results obtained from a laboratory scale reactor and standard measurement are reported and discussed in chapter V.

Chapter VI gives overall conclusions emerged from this work and present some recommendations for any future works.

Finally, the sample of calculation of catalyst preparation, and product distribution are including in appendix at end of this thesis.

The Objective of This Study

1. To study the preparation method of metal containing MFI-type zeolite catalysts.

2. To characterize the prepared catalysts.

3. To investigate the performance of the prepared catalysts on aromatization of n-heptane.

4. To observe the stability of the prepared catalyst.

The Scope of This Study

1. Study the method to introduce metals such as gallium, zinc into MFI-type zeolite catalyst either by incorporation and/or ion-exchange.

2. Study the characterization of the prepared catalysts by following methods.

- Analyzing structure and crystallity of catalysts by X-ray diffraction (XRD).

- Analyzing amount of metal of catalysts by X-ray fluorescency (XRF).

- Analyzing shape and size of crystallites by Scanning Electron Microscope (SEM).

- Analyzing surface areas of catalysts by Brunauer-Emmett-Teller (BET) Surface Areas Meausurement.

- Analyzing the Acidity of catalysts by IR Spectroscorpy.

3. Investigate the performance of the prepared catalysts on the aromatization of n-heptane under the following condition.

- Atmospheric pressure.
- Reaction temperature 450-600 ^{o}C
- Space velocity 2,000-6,000 h^{-1}
- Reactant feed 6% n-heptane

The reaction products were analyzed by Gas Chromatographs

CHAPTER II
LITERATURE REVIEWS

In 1972, Mobil Oil Corp. published zeolite " ZSM-5" that is the catalyst which synthesized gasoline shape-selectivity from methane (The MTG process) [4]. The investigation of shape-selectivity was undertaken in a lot of laboratories. Some of the more prominent studied on modified ZSM-5 for dehydrogenation and aromatization reactions are summaried below.

Anunziata and Pierella [5] studied LPG transformation to aromatic hydrocarbons on Zn^{2+} modified pentasil zeolite. They found the zinc-zeolite (ZSM-5 and ZSM-11) increased activity and produced more aromatic hydrocarbons than H-MFI with the best BTX selectivity. The primary role of the Zn^{2+} species is in C-H activation and the transformation of the intermediates into aromatic hydrocarbons.

V.R. Choudhary et al. [6] studied direct aromatization of natural gas over H-galosilicate (MFI), H-galloaluminosilicate (MFI) and Ga/H-ZSM-5 zeolites. They found that direct conversion of the C_{2+} hydrocarbons from natural gas to aromatics over H-gallosilicate (MFI), H-galloaluminosilicate (MFI) and Ga/H-ZSM-5 zeolites has been investigated at different temperatures (500-600 ^{o}C) and space velocities (500-6000 $cm^3g^{-1}h^{-1}$). The zeolites are compared for their activity/selectivity and distribution of aromatics formed in the natural gas-to-aromatics conversion at different process conditions. The performance shown by the zeolites is in the following order : H-galloaluminosilicate (MFI) >> H-gallosilicate (MFI) > Ga/H-ZSM-5. Natural gas, containing 27.3% C_{2+} hydrocarbons, can be converted to aromatics with very high selectivity (~90%) at high conversion (70%) of C_{2+} hydrocarbons over H-galloaluminosilicate (MFI) zeolite at 600 ^{o}C and space velocity of 3000 $cm^3g^{-1}h^{-1}$.

M. Guisnet and N.S. Gnep [7] investigated that propane aromatization on H-ZSM-5 pure or loaded with platinum or with gallium. On H-ZSM-5, the selectivity to

aromatics is limited because of the formation of methane by propane cracking and of alkanes by hydrogen transfer. Platinum increase the rate of propane transformation significantly but a higher production of methane and ethane is found on PtH-ZSM-5 catalysts, owing to the hydrogenolysis of alkanes and of alkylaromatics and to the hydrogenation of platinum site. Gallium improves both the rate and the selectivity of propane aromatization. The aromatization occurs, like on PtH-ZSM-5, through a bifunctional to pathway, gallium catalyzing the dehydrogenation of alkane reactant to alkenes and of naphthenic intermediates to aromatics, and the acid sites catalyzing the oligomerization of light alkenes and the cyclization of C_6-C_8 alkane. The better selectivity to aromatics is obtained for GaMFI catalysts with gallium species well dispersed with in the zeolite and being very active for dehydrogenation (eg. with gallosilicates or galloaluminosilicates steams under mild conditions).

Vasant R. Choudhary et al. [8] studied influence of zeolite factors affecting zeolitic acidity on the propane aromatizatiom activity and selectivity of Ga/H-ZSM-5. They found that the acidity of Ga/H-ZSM-5 zeolite catalyst is strongly influenced by its Si/Al ratio and degree of H^+ exchange and calcination temperature but not by its Ga loading. As expected, the acidity is increase with increasing degree of H^+ exchange and it is decreased with increasing Si/Al ratio and calcination temperature. The acidity is also decrease with increasing Ga loading, but the decrease is small. At high Ga loading, only a small part of the gallium may exist as GaO^+ or Ga^+ and there is little or no possibility of the existence of Ga^{3+} species in the zeolite channels. Both the conversion of propane and product selectivity are substantially influenced by the Si/Al ratio, degree of H^+ exchange, calcination temperature and Ga loading of the zeolite catalyst. When the Ga loading of the zeolite of the zeolite catalyst is kept the same, the propane conversion/aromatization activity of the zeolite catalyst is increased markedly with increasingly strong acidity. However, for the zeolite catalyst with higher Ga loading, but somewhat lower acidity, the propane conversion/aromatization activity is higher. Thus, for a better performance in the propane aromatization there should be a proper balance between the acidity and Ga species in the zeolite channel.

Zaihui Fu et al. [9] reported the modified ZSM-5 catalysts for propane aromatization prepared by a solid state reaction. A solid-exchange mechanism is suggested that Zn.ZSM-5 is the most active catalyst for propane conversion and gives a better benzene, toluene and xylenes selectivity. Over Mo-ZSM-5, propane mainly undergoes cracking to methane and ethane, and the loading ZSM-5 with Cr^{5+} enhances the propane dehydrogenation to propene.

The Platinum promoting effects in Pt/Ga zeolite catalysts of n-butane aromatization were study by Shpiro et al. [10] They suggested that the Pt and Ga synergy was also found to increase significantly selectivity to aromatics at the account of rapid dehydrogenation and suppressing such side reactions as hydrogenolysis and hydrogenation (Pt), cracking and isomerization (Ga). Both far distance and reduced Ga(I) ion seem to be responsible for the enhancement of aromatization activity and stability of Pt-Ga zeolite catalysts.

Aromatization of n-butane over Ni-ZSM-5 and Cu-ZSM-5 zeolite catalysts prepared by using Ni and Cu impregnated silica fiber was investigated by N. Kumar et al. [11] It found that the modification of ZSM-5 by Ni and Cu increased the selectivity to aromatic hydrocarbons. The state of Ni and Cu and their stabilization in ZSM-5 structure was highly influenced by the mode of catalyst pretreatment.

Modification of the ZSM-5 zeolite using Ga and Zn impregnated silica fibre for the conversion of n-butane into aromatic hydrocarbon was investigated by N. Kumar and L. E. Lindfors [12]. In this work a silica fibre pre-impregnated with Ga and Zn has been used during the synthesis by which Ga-ZSM-5 and Zn-ZSM-5 zeolite catalysts were prepared. The catalysts synthesised consisted of Brønsted and Lewis types of acid sites with uniform dispersion of Ga and Zn cations. The catalysts were found to be very active for n-butane conversion and for transformation into aromatic hydrocarbons. The Ga and Zn cations balanced together with Brønsted acid sites were the active sites for this reaction. The deactivation due to coke formation was very low for the Ga and Zn modified zeolite catalysts.

Fukase et al. [13] reported on the electronic and geometric effect of platinum on the catalyst activity and decay in the aromatization of n-pentane over platinum ion-exchange zinc-aluminosilicate. They found the deactivation of catalyst decrease with increasing density of strong acid sites of the zeolite. Because platinum atoms become more cationic and were located inside the zeolite pores when platinum was loaded onto zeolites with a higher strong acid site density. Platinum atom were less cationic and trended to migrate to external surface where aggregated when platinum was loaded onto zeolites that had a lower strong acid site density and they assumed to the deactivation of catalyst cause the migration and aggregation of platinum.

The conversion of liquefied petroleum gas to aromatic hydrocarbons over various metals containing MFI-type catalysts was reported by A. Sripusitto [14]. It has been shown that zinc and gallium improved both the activity and selectivity of propane aromatization. Further development was done by preparing Zn.Al- or Ga.Al-silicates with purpose of minimizing the catalyst preparation procedure. It has been found that NH_4-Zn.Al-silicate having and Si/Zn ratio of 150 and H-Ga.Al-silicate having an Si/Ga ratio of 155 and an Si/Al ratio of 40 exerted considerably high selectivity for aromatics, ca. 51% and 64% of BTX respectively. This selectivity was comparable to that of Zn or Ga exchanged MFI with the same amount of Zn or Ga loading. However, the bimetallosilicate catalysts can be prepared in only one step crystallization and thus minimizing the catalyst preparation procedure.

Hu Zeshan et al. [15] studied the modification of HZSM-5 by metal surfactant for aromatization of methylcyclohexane. The modification resulted in an increase in external surface area, a slight decrease in pore window and gave almost unchanged micropore volume as well as internal surface area. Both conversion and selectivity of aromatization were increase by the modification with zinc valerate, while also resulted in an improvement in shape selectivity of the zeolite. There existed an optimal zinc ion ratio of external surface/internal surface of the zeolite for aromatization. The ratio can be obtained by a combination of zinc valerate modification and zinc ion exchange. The modification with magnesium valerate, however, resulted in a decrease of C_1-C_4 hydrocarbon selectivity and its yield.

D. Bhattacharya and S. Sivasanker [16] studied the effect of promoters and added gas on the aromatization of n-hexane over H-ZSM-5. They showed that the aromatization is enhanced by the promoters ZnO and Ga_2O_3, while Fe_2O_3 and Cr_2O_3 decrease the aromatization and both ZnO and Ga_2O_3 containing catalysts deactivate less. The addition of N_2 to the feed increases aromatization over H-ZSM-5, while H_2 decrease aromatization and increasing the total pressure does not significantly decrease the yield of aromatic.

Kanai and Kawata [17] shown the proton forms of galloaluminosilicate and gallosilicate have much activity for the aromatization of n-hexane than Ga^{3+}-exchanged H-ZSM-5 or Ga_2O_3-supported H-ZSM-5. On the other hand, a proton form of gallosilicate exchanged with hydrochloric acid shows lower activity for aromatization of n-hexane, but the activity of the proton form of gallosilicate is increased by a small addition of Ga^{3+}. It is suggested that the active gallium species over galloaluminosilicate and gallosilicate are not gallium species in the framework but those outside the framework.

n-Hexane aromatization on synthetic gallosilicates with MFI structure was studied by H.D. Lanh et al. [18] It found that gallosilicates having the MFI structure were prepared with varying ratio framework-to-non-framwork gallium at constant gallium content. They contain framework gallium only up to 2 Ga/u.c. besides non-framework gallium. In the aromatization of n-hexane the activity of the sample increasing content of framework gallium. However, activity and selectivity increase, too, with samples containing increasing amounts of non-framework gallium but nearly constant amounts of framework. This proves that non-framework gallium is an active species, but only in cooperation with framework gallium. Non-framework gallium alone was inactive. The results support a bifunctional mechanism with L and B sites on gallosilicates similar to what has been suggested previously for aluminosilicates. Observed distributions of the aromatics formed and the selectivity for aromatics are in accordance with the concept of dehydrogenating L sites and cracking B sites.

The interaction between gallium and H-ZSM-5 on gallium supported H-ZSM-5 catalysts were investigated by Lee et al. [19] Gallium was introduced into H-ZSM-5 by impregnation [Ga/Z5 (im)] and physical mixing [Ga/Z5 (mix)]. Temperature-programmed desorption studies of ammonia show that the number of strong acid sites (HTP) of H-ZSM-5 decreased after hydrogen pretreatment, while the number of weak acid site (LTP) increased at the same time. The fall of the HTP is compensated for by the rise of the LTP. If the pretreatment time was long enough, the HTP would disappear completely. The new acid center (Ga-Z) was also an active site for acid catalyzed reaction (cracking, oligomerization and cyclization) as H-Z. The main factor affecting the catalytic activity was the dispersion of gallium rather than the oxidation state. The yield of aromatics on the reduced and reoxidized catalysts were similar. On hydrogen pretreatment, the residual gallium species (probably in the form of Ga_2O) sinter and block the aperture and/or the internal channel of zeolite. Because Ga/Z5 (im) sintered more seriously than Ga/Z5 (mix) were superior to those of Ga/Z5 (im), especially at higher space velocity.

The hydrogen pretreatment effect on catalytic properties of Ga/ZSM-5 has been studied by Chau-Sang Chang and Min-Dar Lee [20]. The interaction between gallium and H-ZSM-5 can improve the dispersity of gallium and at the same time increase the activity for aromatization of n-hexane from 44.2 to 60.3% with simultaneous decrease of the selectivity to aliphatics.

Aromatization of n-heptane over ZSM-5 prepare without the acid of template was investigated by A.R. Pradhan et al. [21] They found that highly crystalline zeolite ZSM-5 could be prepared without the acid of organic template using silica gel as a silica source and addition of seed material increased the crystallinity of the ZSM-5 phase. The catalytic activity was comparable with a sample prepared using an organic template. Formation of higher amount of C_{9+} aromatic was observed over the non-templated zeolite.

Kanai and Kawata [22] also studied coke formation and ageing in the conversion of light naphtha into aromatics over galloaluminosilicate (ZSM-5 type zeolite), the acid density of which was controlled by changing the pretreatment temperature. It was found that the catalyst life depended on the pretreatment temperature of the zeolite and had its maximum at 1053 K. Furthermore, it was found that the acid density of the zeolite decrease, and non-framework gallium species increased, with increasing pretreatment temperature. Thus, it is suggested that the trends in the catalyst life result from: (1) the appropriate combination of the dehydrogenation activity and the acidic activity, (2) the rapid decrease of coke formation with increasing pretreatment temperature, and (3) pore blockage by coke formation inside the crystals.

The effect of the dehydrogenating component of H-ZSM-5 and Zn/H-ZSM-5 catalysts on n-heptane aromatization reaction was studied by N. Viswanadham et al. [23] Incorporation of zinc enhances the concentration of olefin precursors through its effective dehydrogenation action on paraffins, which ultimately results in enhancement in aromatics yield. Zinc also facilitates the formation of C_6-C_8 aromatics from the corresponding oligomers, as in that way suppresses the formation of C_9-C_{12} oligomers, a source for the formation of higher (C_{9+}) aromatics.

From above paper review, gallium and zinc modified ZSM-5 was widely used for light alkane aromatization. Gallium and zinc modification ZSM-5 have more acidity for aromatization. So study the extensive performances of gallium and zinc modified ZSM-5 for aromatic production from the other range of hydrocarbon such as naphtha is attractive.

CHAPTER III
THEORY

3.1 Zeolite

The name “zeolite” comes from the Greek words zeo (to boil) and lithos (stone). The classical definition of a zeolite is a crystalline, porous aluminosilicate. However, some relatively recent discoveries of materials virtually identical to the classical zeolite, but consisting of oxide structures with elements other than silicon and aluminum have stretched the definition. Most researchers now include virtually all types of porous oxide structures that have well-defined pore structures due to a high degree of crystallinity in their definition of a zeolite.

In these crystalline materials we call zeolites, the metal atoms (classically, silicon or aluminum) are surrounded by four oxygen anions to form an approximate tetrahedron consisting of a metal cation at the center and oxygen anions at the four apexes. The tetrahedra metals are called T-atoms for short, and these tetrahedra then stack in beautiful, regular arrays such that channels form. The possible ways for the stacking to occur is virtually limitless, and hundreds of unique structures are known. Graphical depictions of several representative types are given under “Representative Structures”.

The zeolitic channels (or pores) are microscopically small, and in fact, have molecular size dimensions such that they are often termed “molecular sieves”. The size and shape of the channels have extraordinary effects on the properties of these materials for adsorption processes, and this property leads to their use in separation processes. Molecules can be separated via shape and size effects related to their possible orientation in the pore, or by differences in strength of adsorption.

Since silicon typically exits in a 4+ oxidation state, the silicon-oxygen tetrahedra are electrically neutral. However, in zeolites, aluminum typically exists in

the 3+ oxidation state so that aluminum-oxygen tetrahedra form centers that are electrically deficient one electron. Thus, zeolite frameworks are typically anionic, and charge-compensating cations populate the pores to maintain electrical neutrality. These cations can participate in ion-exchange processes, and this yields some important properties for zeolites. When charge-compensating cations are "soft" cations such as sodium, zeolites are excellent water softeners because they can pick up the "hard" magnesium and calcium cations in water leaving behind the soft cations. When the zeolitic cations are protons, the zeolite becomes a strong solid acid. Such solid acids form the foundations of zeolite catalysis applications including the important fluidized bed cat-cracking refinery process. Other types of reactive metal cations can also populate the pores to form catalytic materials with unique properties. Thus, zeolites are also commonly used in catalytic operations and catalysis which zeolites is often called "shape-selective catalysis".

3.2 Structure of Zeolite

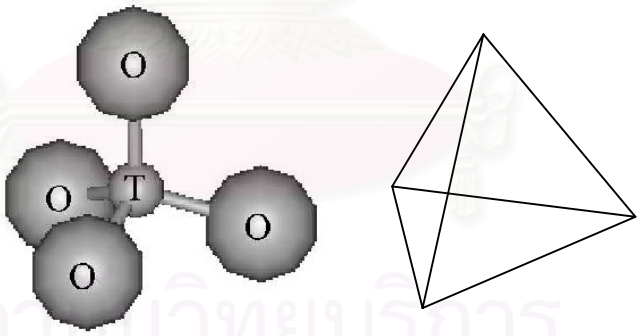

Figure 3.1 TO_4 tetrahedra (T = Si or Al) [24]

Zeolites are porous, crystalline aluminosilicate that develop uniform pore structure having minimum channel diameter of 0.3-0.1 nm. This size depends primarily upon the type of zeolite. Zeolites provide high activity and unusual selectivity in a variety of acid-catalyzed reactions. Most of the reactions are caused by the acidic nature of zeolites.

The structure of zeolite consists of a three-dimensional framework of SiO_4 or AlO_4 tetrahedra, each of which contains a silicon or aluminum atom in the center (Figure 3.1) [24]. The oxygen atoms are shared between adjoining tetrahedra, which can be present in various ratios and arranged in a variety of way. The framework thus obtained contains pores, channels, and cages, or interconnected voids.

A secondary building unit (SBU) consists of selected geometric groupings of those tetrahedral. There are sixteen such building units, which can be used to describe all of known zeolite structures; for example, 4 (S4R), 6 (S6R), and 8 (S8R)-member single ring, 4-4 (D6R), 8-8 (D8R)-member double rings. The topologies of these units are shown in Figure 3.2 [25]. Also listed are the symbols used to describe them. Most zeolite framework can be generated from several different SBU's. Descriptions of known zeolite structures based on their SBU's are listed in Table 3.1 [26]. Both zeolite ZSM-5 and Ferrierite are described by their 5-1 building units. Offertile, Zeolite L, Cancrinite, and Erionite are generated using only single 6-member rings. Some zeolite structures con be described by several building units. The sodalite framework can be built from either the single 6-member ring or the single 4-member ring. Faujasite (type X or type Y) and Zeolite A can be constructed using 4 ring or 6 ring building units. Zeolite A can also be formed using double 4 ring building units, whereas Faujasite cannot.

Zeolite may be represented by the general formula,

$$M_{x/n}[(AlO_2)_x(SiO_2)_y]wH_2O$$

Where the term in brackets is the crystallographic unit cell. The metal cation of valence n is present to produce electrical neutrality since for wash aluminum tetrahedron in the lattice there is an overall charge of –1 [27]. M is a proton, the zeolites becomes a strong Brønsted acid. As catalyst, zeolite becomes a strong Brønsted acid. As catalysts, zeolite are unique in their ability to discriminate between reactant molecular size and shape [28].

Table 3.1 Zeolites and their secondary building units. The nomenclature used is consistent with that presented in Figure 3.2 [26]

ZEOLITE	SECONDARY BUILDING UNITS								
	4	6	8	4-4	6-6	8-8	4-1	5-1	4-4=1
Bikitaite								X	
Li-A (BW)	X	X	X						
Analcime	X	X							
Yagawaralite	X		X						
Episitbite								X	
ZSM-5								X	
ZSM-11								X	
Ferrierite								X	
Dachiardite								X	
Brewsterite	X								
Laumonite		X							
Mordenite								X	
Sodalite	X	X							
Henulandite									X
Stibite									X
Natrolite							X		
Thomsonite							X		
Edingtonite							X		
Cancrinite		X							
Zeolite L		X							
Mazzite	X								
Merlinoite	X		X			X			
Philipsite	X		X						
Zeolite Losod		X							
Erionite	X	X							
Paulingite	X								
Offretite		X							
TMA-E(AB)	X	X							
Gismondine	X		X						
Levyne		X							
ZK-5	X	X	X		X				
Chabazite	X	X			X				
Gmelinite	X	X	X		X				
Rho	X	X	X			X			
Type A	X	X	X	X					
Faujasite	X	X			X				

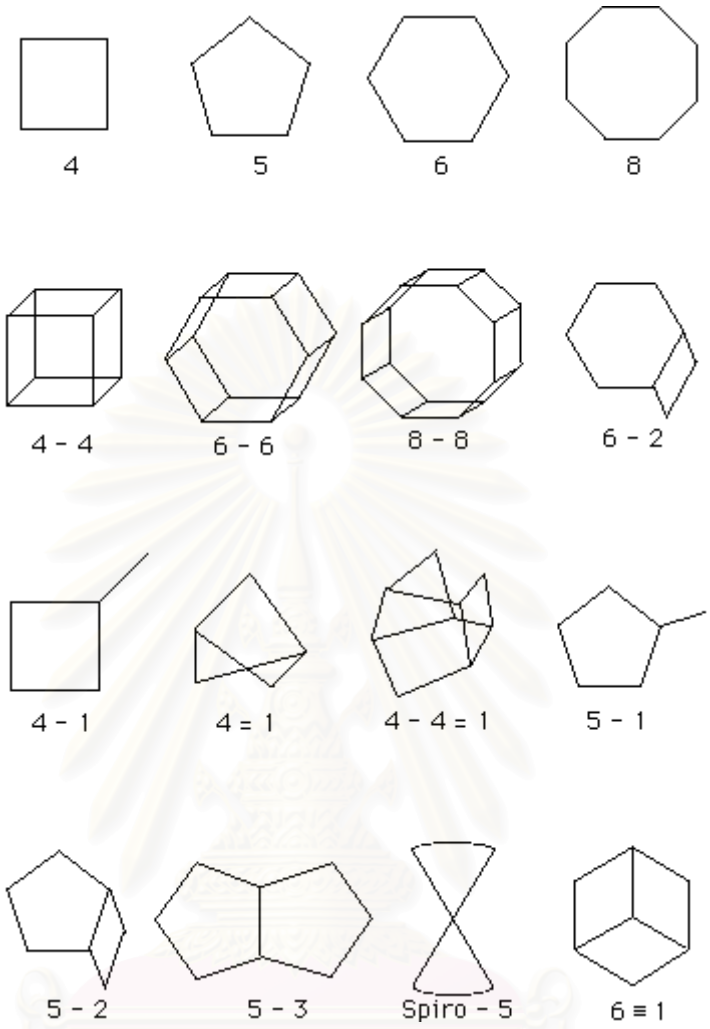

Figure 3.2 Secondary building units (SBU's) found in zeolite structures [25]

3.3 Category of Zeolite

There are over 40 known natural zeolites and more than 150 synthetic zeolites have been reported [29]. The number of synthetic zeolites with new structure morphologies grows rapidly with time. Based on the size of their pore opening, zeolites can be roughly divided into five major categories, namely 8-, 10- and 12-member oxygen ring systems, dual pore systems and mesoporous systems [30]. Their pore structures can be characterized by crystallography, adsorption measurements and/or through diagnostic reactions. One such diagnostic characterization test is the "constraint index" test. The concept of constraint index was defined as the ratio of the

cracking rate constant of *n*-hexane to 3-methylpentane. The constraint index of a typical medium-pore zeolite usually ranges from 3 to 12 and those of the large-pore zeolites are in the range1-3. For materials with an open porous structure, such as amorphorous silica alumina, their constraint indices are normally less than 1. On the contrary, small-pore zeolites normally have a large constraint index; for example, the index for erionite is 38.

A comprehensive bibliography of zeolite structures has been published by the International Zeolite Association [29]. The structural characteristics of assorted zeolites are summarized in Table 3.2.

Zeolites with 10-membered oxygen rings normally possess a high siliceous framework structure. They are of special interest in industrial applications. In fact, they were the first family of zeolites that were synthesized with organic ammonium salts. With pore openings close to the dimensions of many organic molecules, they are particularly useful in shape selective catalysis. The 10-membered oxygen ring zeolites also possess other important characteristic properties including high activity, high tolerance to coking and high hydrothermal stability. Among the family of 10-membered oxygen ring zeolites, the MFI-type (ZSM-5) zeolite (Figure 3.3) is probably the most useful one.

Although the 10-membered oxygen ring zeolites were found to possess remarkable shape selectivity, catalysis of large molecules may require a zeolite catalyst with a large-pore opening. Typical 12-membered oxygen ring zeolites, such as faujasite-type zeolites, normally have pore opening greater than 5.5 Å and hence are more useful in catalytic applications with large molecules, for example in trimethylbenzene (TMB) conversions. Faujasite (X or Y; Figure 3.4) zeolites can be synthesized using inorganic salts and have been widely used in catalytic cracking since the 1960s. The framework structures of zeolite Beta and ZSM-12 are shown in Figure 3.5 and Figure 3.6, respectively.

Table 3.2 Structural characteristics of selected zeolites [31].

Zeolite	Number of rings	Pore opening (Å)	Pore/channel structure	Void volume (ml/g)	D_{Frame}[a] (g/ml)	CI[b]
8-membered oxygen ring						
Erionite	8	3.6×5.1	Intersecting	0.35	1.51	38
10-membered oxygen ring						
ZSM-5	10	5.3×5.6 5.1×5.5	Intersecting	0.29	1.79	8.3
ZSM-11	10	5.3×5.4	Intersecting	0.29	1.79	8.7
ZSM-23	10	4.5×5.2	One-dimensional	-	-	9.1
Dual pore system						
Ferrierite (ZSM-35, FU-9)	10,8	4.2×5.4 3.5×4.8	One-dimensional 10:8 intersecting	0.28	1.76	4.5
MCM-22	12 10	7.1 Elliptical	Capped by 6 rings	-	-	1-3
Mordenite	12 8	6.5×7.0 2.6×5.7	One-dimensional 12:8 intersecting	0.28	1.70	0.5
Omega (ZSM-4)	12	7.4	One-dimensional	-	-	2.3
	8	3.4×5.6	One-dimensional	-	-	0.6
12-membered oxygen ring						
ZSM-12	12	5.5×5.9	One-dimensional	-	-	2.3
Beta	12	7.6×6.4 5.5×5.5	Intersecting	-	-	0.6
Faujasite (X,Y)	12 12	7.4 7.4×6.5	Intersecting 12:12 intersecting	0.48	1.27	0.4
Mesoporous system						
VPI-5	18	12.1	One-dimensional	-	-	-
MCM41-S	-	16-100	One-dimensional	-	-	-

[a]Framework density

[b]Constraint index

Zeolites with a dual pore system normally possess interconnecting pore channels with two different pore opening sizes. Mordenite is a well-known dual pore zeolite having a 12-membered oxygen ring channel with pore opening 6.5×7.0 Å which is interconnected to 8-membered oxygen ring channel with opening 2.6×5.7 Å (Figure 3.7). MCM-22, which was found more than 10 years, also possesses a dual

pore system. Unlike Mordenite, MCM-22 consists of 10- and 12-membered oxygen rings (Figure 3.8) and thus shows prominent potential in future applications.

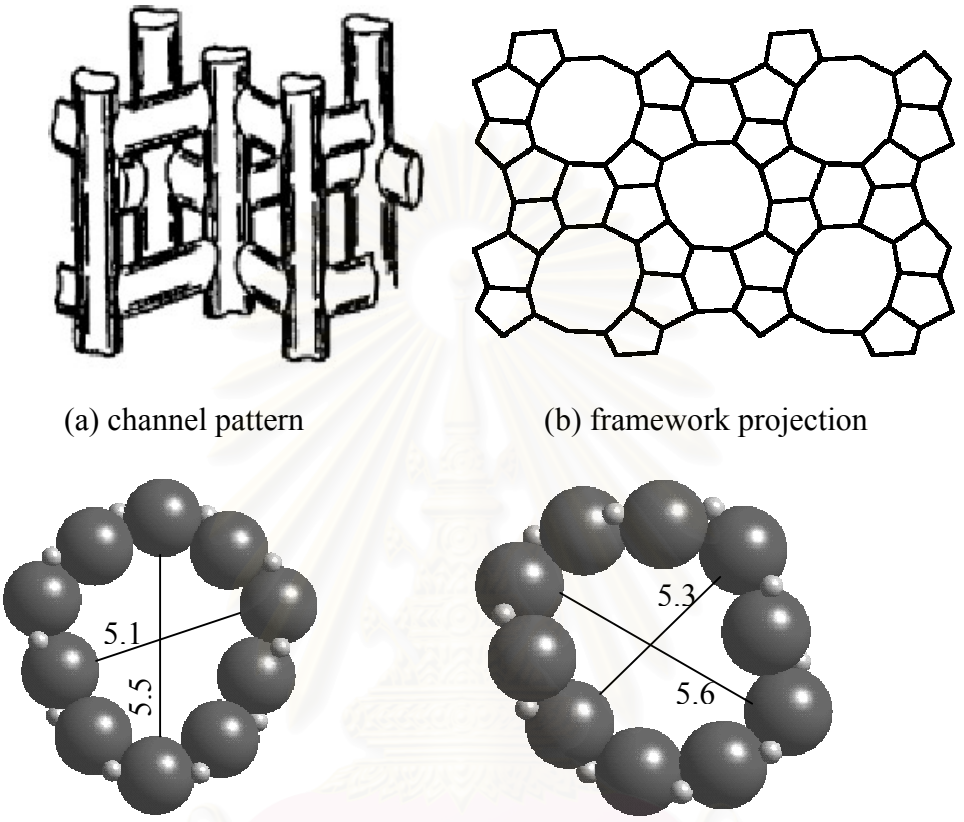

(a) channel pattern (b) framework projection

(c) tortuous channel (d) straight channel

Figure 3.3 Structure of ZSM-5 [29]

In the past decade, many research efforts in synthetic chemistry have been invested in the discovery of large-pore zeolite with pore diameter greater than 12-membered oxygen rings. The recent discovery of mesoporous materials with controllable pore opening (from 12 to more than 100 Å) such as VPI-5, MCM-41S undoubted will shed new light on future catalysis applications.

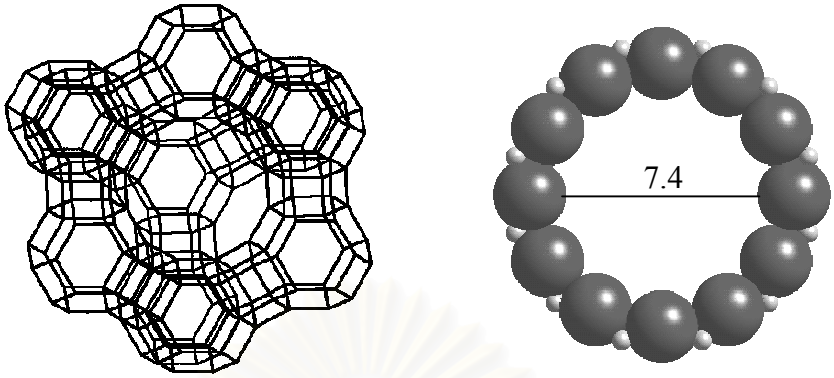

(a) framwork structure (b) pore opening

Figure 3.4 Structure of Faujasite [29]

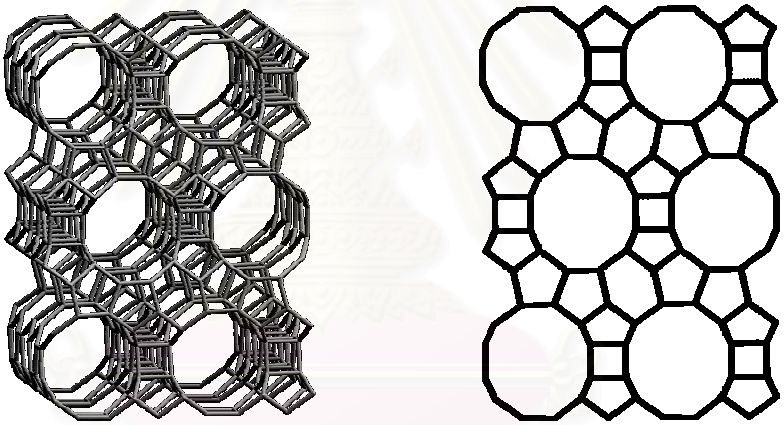

(a) framework structure (b) framework projection

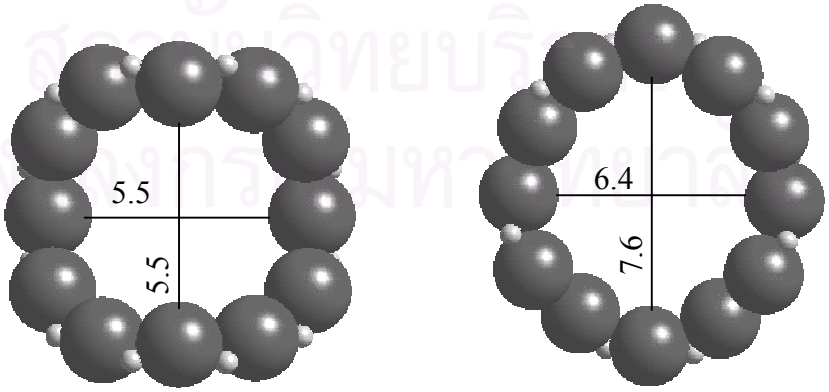

(c) tortuous channel (d) straight channel

Figure 3.5 Structure of Beta zeolite [29]

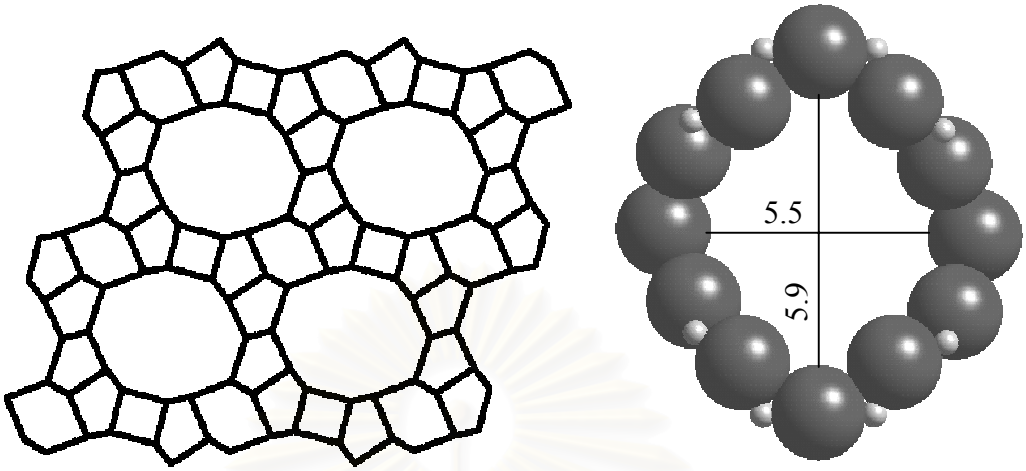

(a) framework projection (b) pore opening

Figure 3.6 Structure of ZSM-12 [29]

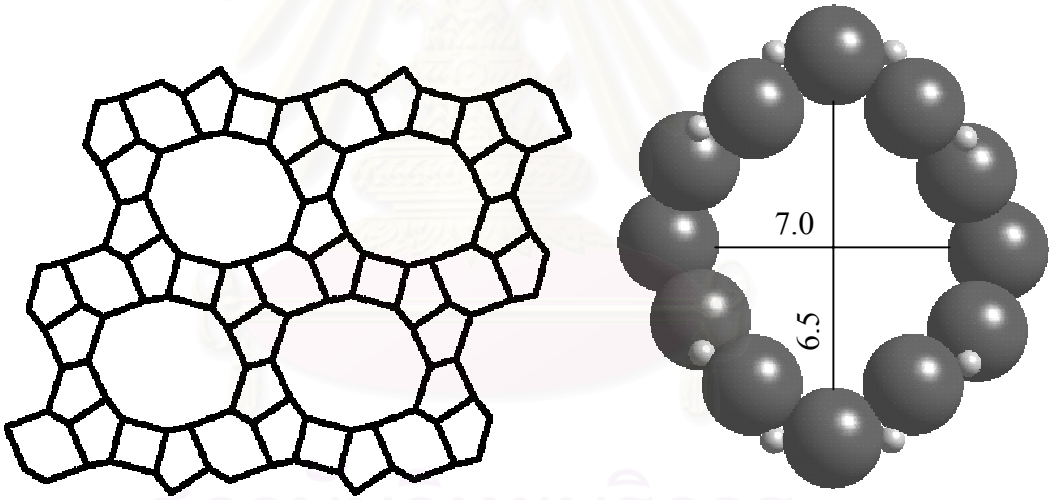

(a) framework projection (b) pore opening

Figure 3.7 Structure of Mordenite [29]

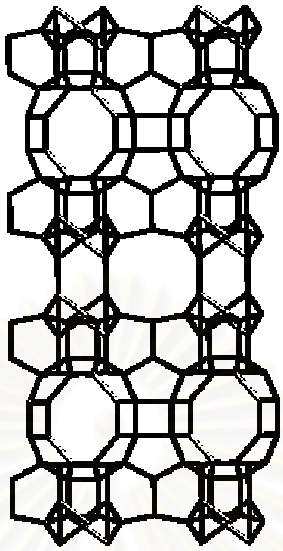

Figure 3.8 Framework structure of MCM-22 [29]

3.4 Zeolite Active Sites

3.4.1 Acid sites

Classical Brønsted and Lewis acid models of acidity have been used to classify the active sites on zeolites. Brønsted acidity is proton donor acidity; a tridiagonally coordinated alumina atom is an electron deficient and can accept an electron pair, therefore behaves as a Lewis acid [28,32].

In general, the increase in Si/Al ratio will increase acidic strength and thermal stability of zeolites [33]. Since the numbers of acidic OH groups depend on the number of aluminum in zeolites framework, decrease in Al content is expected to reduce catalytic activity of zeolite. If the effect of increase in the acidic centers, increase in Al content, shall result in enhancement of catalytic activity.

Based on electrostatic consideration, the charge density at a cation site increases with increasing Si/Al ratio. It was conceived that these phenomena are related to reduction of electrostatic interaction between framework sites, and possibly

to difference in the order of aluminum in zeolite crystal - the location of Al in crystal structure [32].

An improvement in thermal or hydrothermal stability has been ascribed to the lower density of hydroxyl groups, which is parallel to that of Al content [28]. A longer distance between hydroxyl groups decreases the probability of dehydroxylation that generates defects on structure of zeolites.

3.4.2 Generation of Acid Centers

Protonic acid centers of zeolite are generated in various ways. Figure 3.9 depicts the thermal decomposition of ammonium-exchanged zeolites yielding the hydrogen form [26].

The Brønsted acidity due to water ionization on polyvalent cations, described below, is depicted in Figure 3.10 [27].

$$M^{n+} + xH_2O \longrightarrow M(OH)_x^{(n-x)} + xH^+ \qquad (3.1)$$

The exchange of monovalent ions by polyvalent cations could improve the catalytic property. Those highly charged cations create very centers by hydrolysis phenomena. Brønsted acid sites are also generated by the reduction of transition metal cations. The concentration of OH groups of zeolite containing transition metals was note to increase by hydrogen at 250-450^{o}C to increase with the rise of the reduction temperature [27].

$$Cu^{2+} + H_2 \longrightarrow Cu^0 + 2H^+ \qquad (3.2)$$

$$Ag^+ + \tfrac{1}{2}H_2 \longrightarrow Ag^0 + H^+ \qquad (3.3)$$

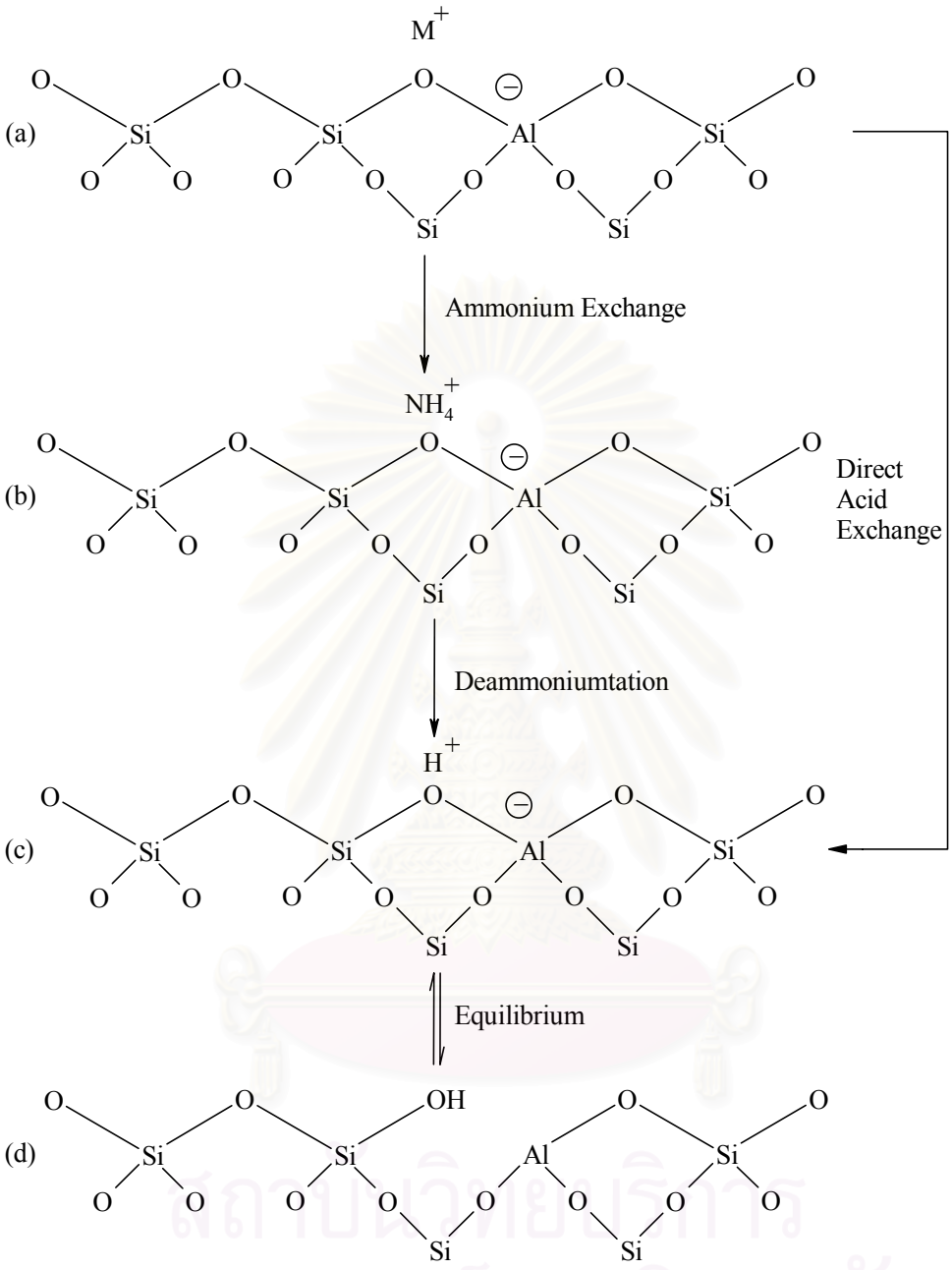

Figure 3.9 Diagram of the surface of a zeolite framework [26].

a) In the as-synthesis form M^+ is either an organic cation or an alkali metal cation.

b) Ammonium in exchange produces the NH_4^+ exchanged form.

c) Thermal treatment is used to remove ammonia, producing the H^+, acid form.

d) The acid form in (c) is in equilibrium with the form shown in (d), where there is a silanol group adjacent to tricoodinate aluminum.

The formation of Lewis acidity from Brønsted acid sites is depicted in Figure 3.11 [27]. The dehydration reaction decreases the number of protons and increases that of Lewis sites. Brønsted (OH) and Lewis (-Al-) sites can be present simultaneously in the structure of zeolite at high temperature. Dehydroxylation is thought to occur in ZSM-5 zeolite above 500°C and calcinations at 800 to 900°C produces irreversible dehydroxylation, which causes defection in crystal structure of zeolite.

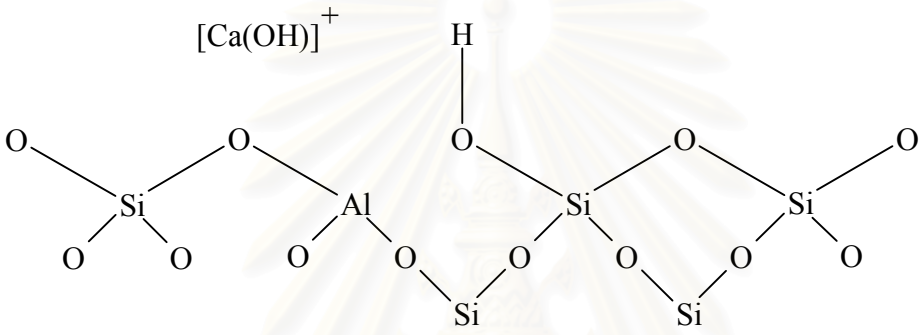

Figure 3.10 Water molecules co-ordinated to polyvalent cation are dissociated by heat treatment yielding Brønsted acidity [27]

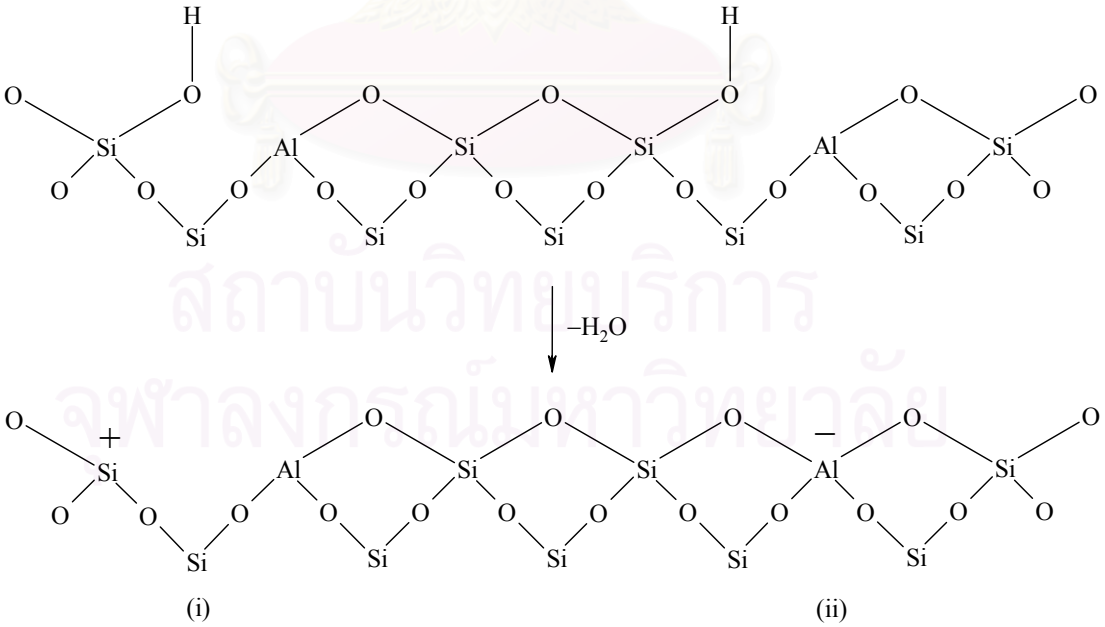

Figure 3.11 Lewis acid site developed by dehydroxylation of Brønsted acid site [27]

Dealumination is believed to occur during dehydroxylation which may result from the steam generation within the sample. The dealumination is indicated by an increase in the surface concentration of aluminum on the crystal. The dealumination process is expressed in Figure 3.12. The extent of dealumination monotonously increases with the partial pressure of steam.

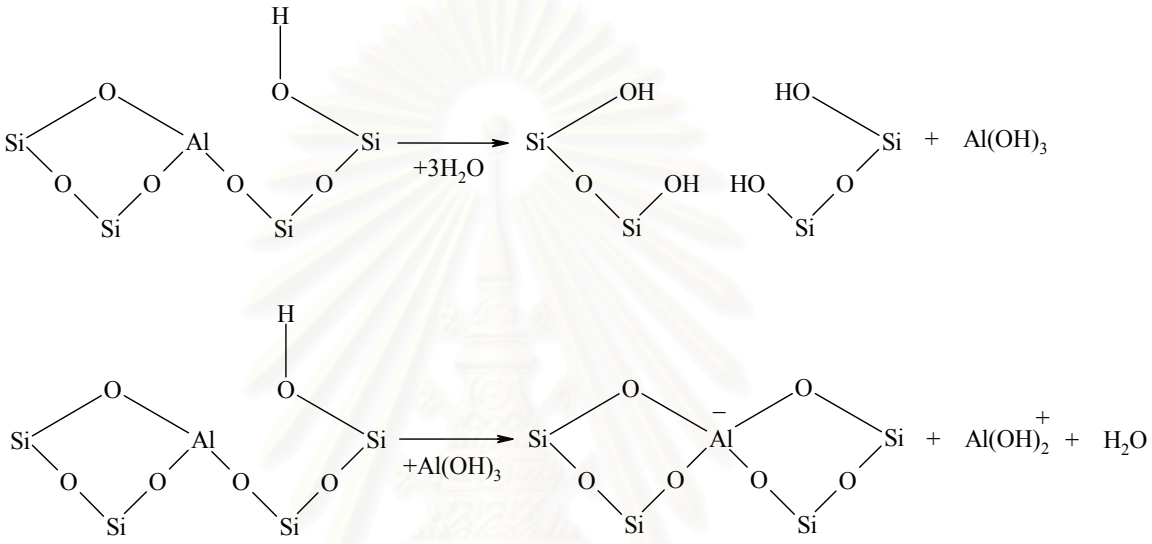

Figure 3.12 Steam dealumination process in zeolite [27]

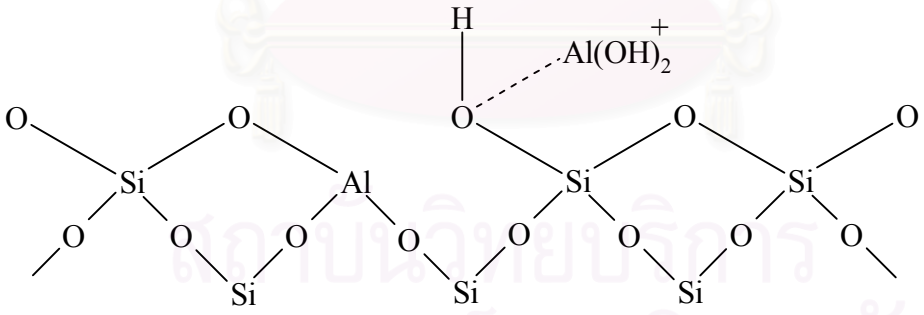

Figure 3.13 The enhancement of the acid strength of OH groups by their interaction with dislodged aluminum species [27]

The enhancement of the acid strength of OH groups is recently proposed to be pertinent to their interaction with those aluminum species sites tentatively expressed in Figure 3.13 [27]. Partial dealumination might therefore yield a catalyst of higher activity while severe steaming reduces the catalytic activity.

3.4.3 Basic Sites

In certain instances reactions have been shown to be catalyzed at basic (cation) site in zeolite without any influences from acid sites. The best-characterized example of this is that K-Y which splits n-hexane isomers at 500^{o}C. The potassium cation has been shown to control the unimolecular cracking (β-scission). Free radical mechanisms also contribute to surface catalytic reactions in these studies.

3.5 Shape Selective

Many reactions involving carbonium intermediates are catalyzed by acidic zeolites. With respect to a chemical standpoint the reaction mechanisms are not fundamentally different with zeolites or with any other acidic oxides. What zeolite add is shape selectivity effect. The shape selective characteristics of zeolites influence their catalytic phenomena by three modes; reactants shape selectivity, products shape selectivity and transition states shape selectivity. These types of selectivity are illustrated in Figure 3.14 [26].

Reactants of charge selectivity results from the limited diffusibility of some of the reactants, which cannot effectively enter and diffuse inside crystal pore structures of the zeolites. Product shape selectivity occurs as slowly diffusing product molecules cannot escape from the crystal and undergo secondary reactions. This reaction path is established by monitoring changes in product distribution as a function of varying contact time.

Restricted transition state shape selectivity is a kinetic effect arising from local environment around the active site, the rate constant for a certain reaction mechanism is reduced of the space required for formation of necessary transition state is restricted.

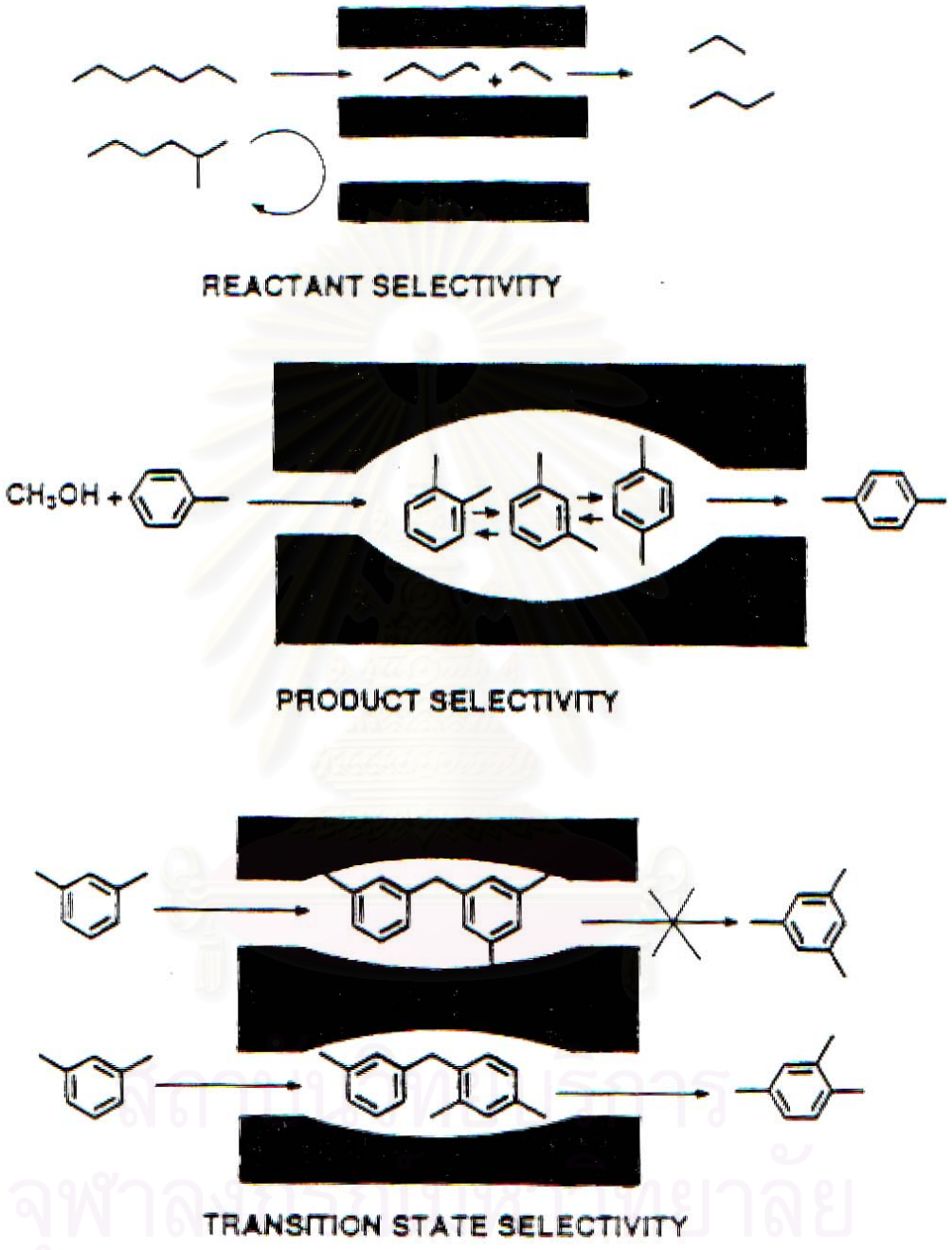

Figure 3.14 Diagram depicting the three type of selectivity [26]

The critical diameter (as opposed to the length) of the molecules and the pore channel diameter of zeolites are important in predicting shape selective effects. However, molecules are deformable and can pass through openings, which are smaller than their critical diameters. Hence, not only size but also the dynamics and structure of the molecules must be taken into account.

3.6 ZSM-5 Zeolite

ZSM-5 zeolite has two types of channel systems of similar size, one with a straight channel of pore opening 5.3×5.6 Å and the other with a tortuous channel of pore opening 5.1×5.5 Å. Those intersecting channels are perpendicular to each other, generating a three-dimensional framework. ZSM-5 zeolites with a wide range of SiO_2/Al_2O_3 ratio can easily be synthesized. High siliceous ZSM-5 zeolites are more hydrophobic and hydrothermally stable compared to many other zeolites. Although the first synthetic ZSM-5 zeolite was discovered more than two decades ago (1972) new interesting applications are still emerging to this day. For example, its recent application in NO_x reduction, especially in the exhaust of lean-burn engine, has drawn much attention. Among various zeolite catalysts, ZSM-5 zeolite has the greatest number of industrial applications, covering from petrochemical production and refinery processing to environmental treatment.

3.7 The aromatizasion mechanism

The aromatization of n-heptane on modified H-ZSM-5 has the reaction pathway comprised numerous successive steps. The reaction mechanism with possible pathways of reactant molecules has been proposed which is shown in Figure 3.15 [34].

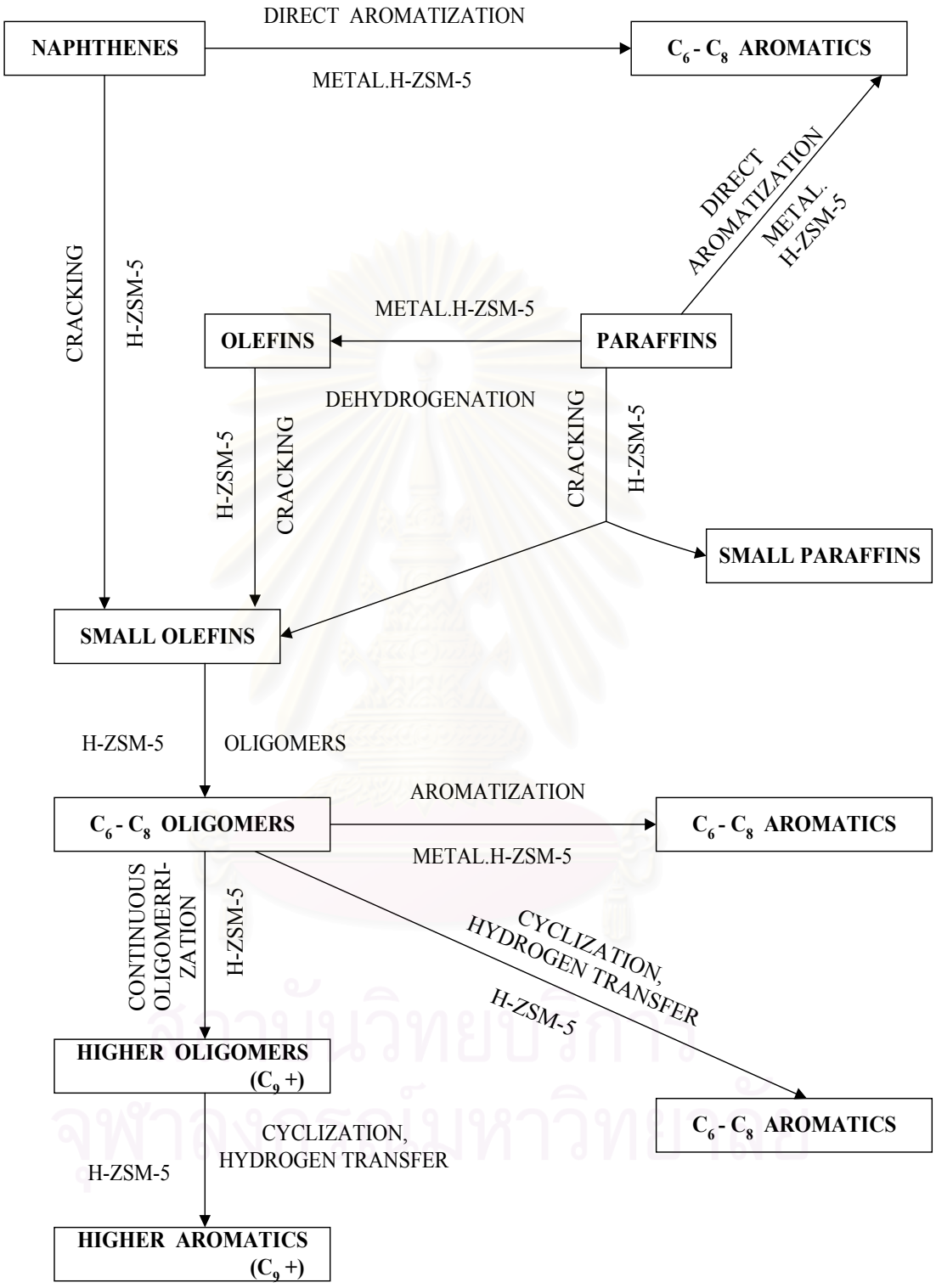

Figure 3.15 Reaction pathways for aromatization on paraffins [34]

Reaction in the figure 3.15 indicate the pathway over acid sites and metal sites and the reaction possible are two cases. For the first case, the main reaction consist cracking, dehydrogenation, oligomerization and aromatization. And the second case, it possible occurred direct dehydrocyclization of hydrocarbons.

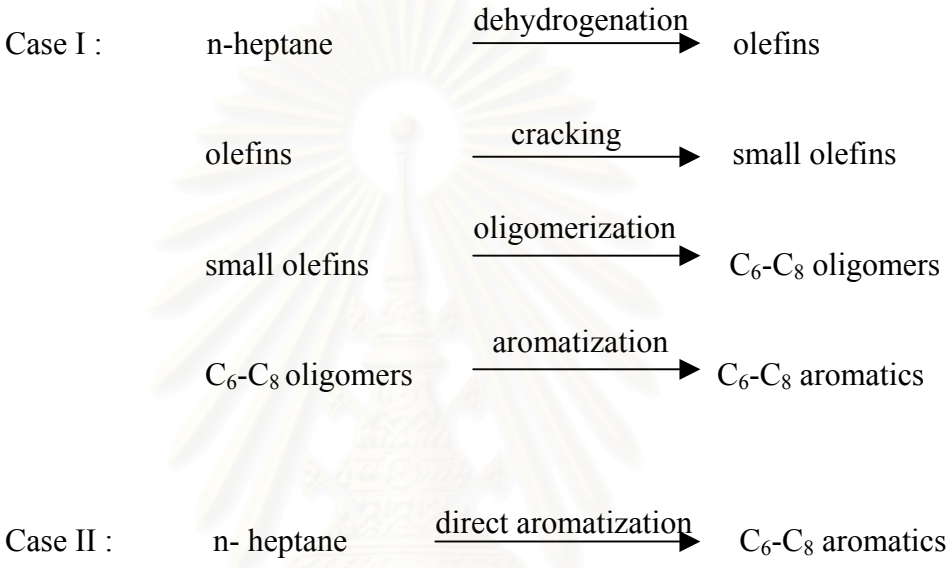

CHAPTER IV
EXPERIMENTS

The catalyst study for aromatization of n-heptane over metal containing MFI – type zeolite catalysts was explained in the following section.

4.1 Catalyst Preparation

ZSM-5 , Ga.Al-silicate , and Zn.Al-silicate catalyst having various metal contents were prepare. The $AlCl_3$ was replaced by $Ga_2(SO_4)_3$ or $Zn(NO_3)_2.6H_2O$ at the stage of gel formation and TPABr (Tetra-n-Propyl Ammonium Bromide) $[(CH_3CH_2CH_2)_4N)Br]$ was used as organic template in the rapid crystallization method for H-ZSM-5 synthsesis [35]. The preparation procedures and the reagents use are shown in Figure 4.1 and Table 4.1, respectively. (For calculation see Appendix A-1).

4.1.1 Preparation of Gel Precipitation and Decantation Solution

The source of metal was $AlCl_3$. TPABr (Tetra-n-Propyl Ammonium Bromide) $[(CH_3CH_2CH_2)_4N)Br]$ was used as organic template. The atomic ratio of silicon/Aluminium was set at 40. The Preparation of supernatant liquid was separated from that of gel, which was important to prepare the uniform crystals. The detailed procedures were as follows: Firstly, a gel mixture was prepared by adding G1-solution and G2-solution into G3-solution while stirring with a magnetic stirrer (figure 4.2) at room temperature. G1-solution and G2-solution was added from burette by the manual control to keep the pH of the mixed solution in the range of 9-11, since it is expected that this pH value is suitable for precipitation. The gel mixture was separated from the supernatant liquid by centrifuge. The precipitated gel mixture was milled for totally 1 hr. by powder miller (Yamato-Notto,UT-22) as shown in Figure 4.3.The milling procedure was follows: milled 20 min. → centrifuge (to remove the liquid out) → milled 20 min. → Centrifuge → milled 20 min.

Milling the gel mixture before the hydrothermal treatment was essential to obtain the uniform and find crystals. The gel precipitate was kept for mixing with the supernatant solution. On the other hand, another decantation solution was prepared by adding S1-solution and S2-solution into S3-solution. The method and condition of mixing were similar to the preparation of gel mixture. Upon the complete mixing the precipitating gel was then removed from the supernatant solution by the centrifuge and the supernatant solution was mixed altogether with the milled gel mixture, expecting that before mixing adjust the pH of solution between 9-11 with H_2SO_4 (conc.) or 1 M NaOH solution.

Table 4.1 Reagents used for the catalysts preparation

Reagents for the gel preparation		**Reagents for decant solution preparation**	
Solution G1		**Solution S1**	
$AlCl_3$ (g)	1.0911	$AlCl_3$ (g)	1.0911
$Ga_2(SO_4)_3$ and / or $Zn(NO_3)_2.6H_2O$ (g)	x	$Ga_2(SO_4)_3$ and / or $Zn(NO_3)_2.6H_2O$ (g)	x
TPABr (g)	5.72	TPABr (g)	7.53
NaCl	11.95	Distilled water (ml)	60
Distilled water (ml)	60	H_2SO_4 (conc.) (g)	3.40
H_2SO_4 (conc.) (g)	3.4		
Solution G2		**Solution S2**	
Distilled water (ml)	45	Distilled water (ml)	45
Water glass (g)	69	Water glass (g)	69
Solution G3		**Solution S3**	
TPABr (g)	2.61	NaCl (g)	26.27
NaCl (g)	40.59	Distilled water (ml)	104
NaOH (g)	2.39		
Distilled water (ml)	208		
H_2SO_4 (conc.) (g)	1.55		

X based on Si/Ga and / or Si/Zn charge ratio

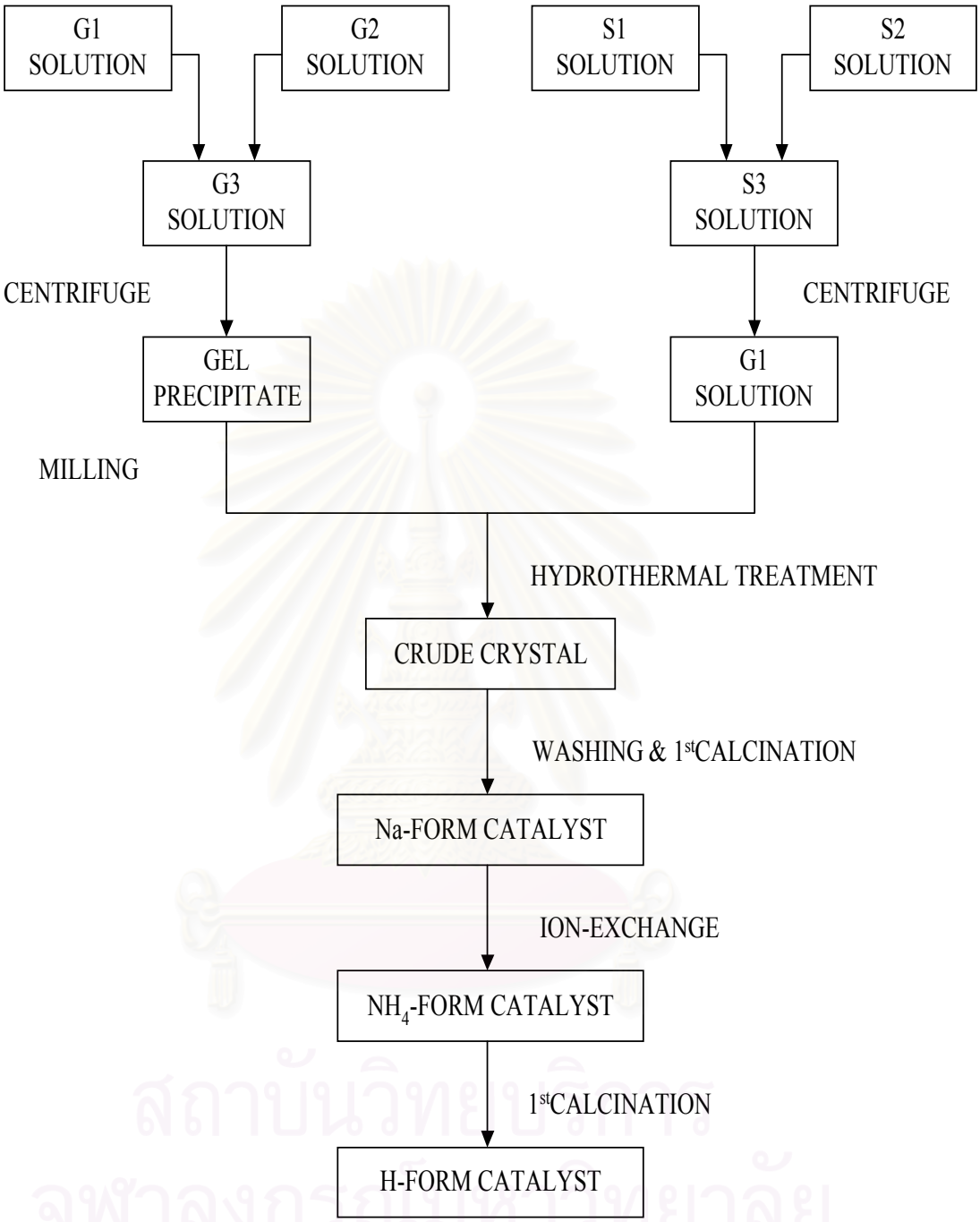

Figure 4.1 Preparation procedure of MFI catalysts by rapid crystallization

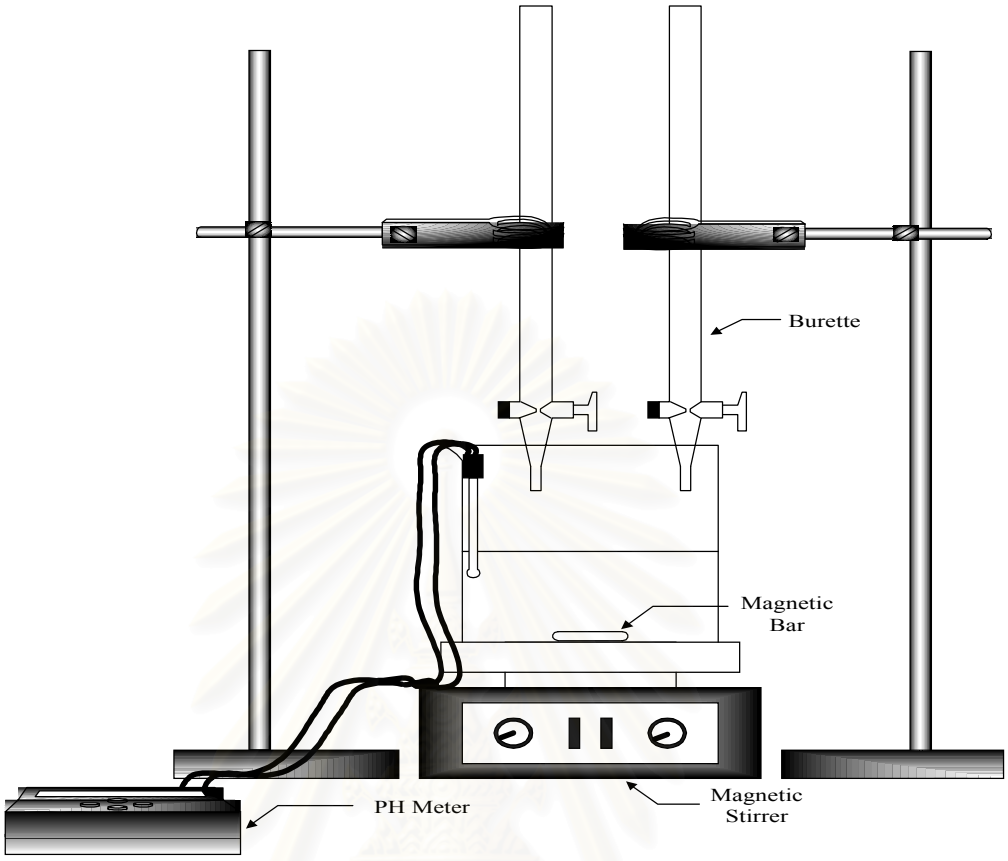

Figure 4.2 A set of apparatus used for preparation of supernatant solution and gel precipitation as providing for the rapid crystallization.

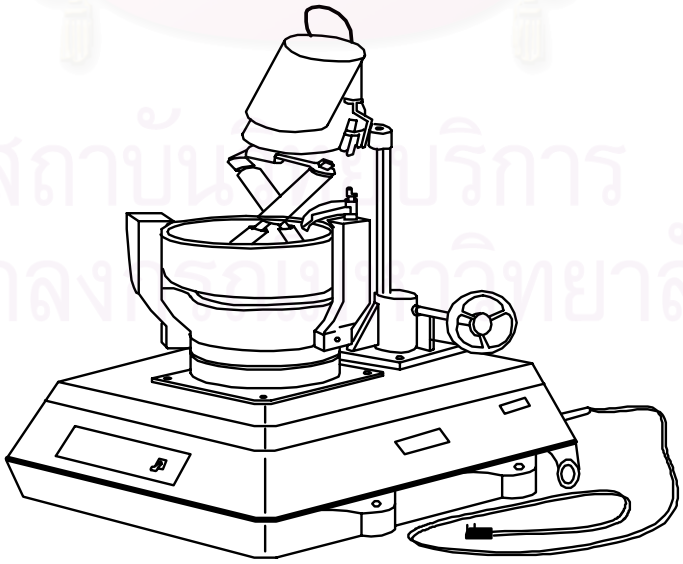

Figure 4.3 A power miller (Yamato-Nitto, UT-22)

4.1.2 Crystallization

The mixture of milling precipitate and the supernatant of decant solution was charged in an one litre stainless steel autoclave. The atmosphere in the autoclave was replaced by nitrogen gas and pressurized up to 3 kg/cm^2 gauge. Then the mixture in the autoclave was heated from room temperature to 160 ^oC in 90 min. and then up to 210 ^oC in 4.2 hr. while being stirred at 60 rpm, followed by cooling down the hot mixture to room temperature in the autoclave overnight. The temperature was programmed under the hydrothermal treatment to minimize the time which was necessary for the crystallization. The produced crystals were washed with distilled water, to remove Cl^- out of the crystals, about 8 times by using the centrifugal separator (about 10 min. for each time) and dried in an oven at 110 ^oC for at least 3 hr.
.

4.1.3 First Calcination

The dry catalysts in a porcelain was heated in a furnace under an air ambient from room temperature to 540 ^oC in 60 min. and then kept at this temperature for 3.5 hr.

At this step, The organic template (TPABr) was burned out and left the cavities and channels in the crystals. The calcined crystal was cooled to room temperature in a desiccator. After this step the crystals formed were called “Na-form catalyst”.

4.1.4 Ammonium Ion-exchange of Na-form Crystal

The ion-exchange step was carried out by mixing 3 g. of Na-form catalyst with 90 ml of 1 M NH_4NO_3 and heated on a stirring hot plate at 80 ^oC for 40 min. After that, the mixture was cooled down to room temperature and washed with distilled water about 3 times by using the centrifugal separator (about 10 min. for each time). The ion-exchange step was repeated about 3 times. Then, the ion-exchanged crystal

was dried at 110 ^{o}C for at least 3 hr. in an oven. The Na-form crystal was thus changed to "NH_4-form catalyst".

4.1.5 Second Calcination

The NH_4-form crystal was calcined in a furnace by heating from room temperature to 540 ^{o}C in 60 min and then kept at this temperature for 3.5 hr. After this step the crystal thus obtained was called "H-form catalyst".

4.2 Metal Loading by Ion-Exchange

Abount 2 g. of catalyst was immersed in 60 ml of metal salt aqueous solution at 100 ^{O}C for 3 hr. It was washed with distilled water about 5 times, about 10 min. for each time (as shown in Figure 4.4). The sample was dried overnight at 110 ^{o}C. Finally, dry crystal was heated in air with the constant heating rate of 10 ^{o}C/min up to 350 ^{o}C and maintained for 2 hr.

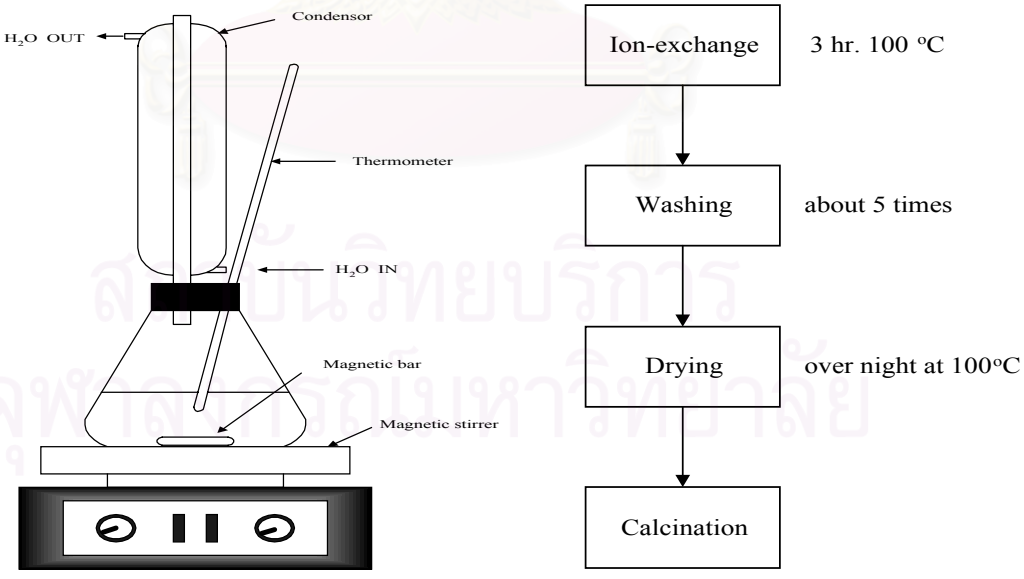

(a) (b)

Figure 4.4 (a) A set of apparatus used for preparation of metal ion-exchanged on catalyst (b) A diagram for metal ion-exchanged on catalyst

The catalysts were tableted by a tablet machine. After that, the catalysts were crushed and sieved to range of 8-16 mesh to provide the same diffusion rate and the reaction.

4.3 Aromatization of n-Heptane

4.3.1 Chemicals and Reagents

n-Heptane available from CARLO ERBA Reagent 99.7%

4.3.2 Instruments and apparatus

4.3.2.1 Reactor: The reactor is a conventional microreactor made from quartz tube with 6 mm inside diameter, so it can be operated at high temperature. The reaction was carried out under ordinary gas flow and atmospheric pressure.

4.3.2.2 Automation Temperature Controller: This consists of magnetic switch connected to a variable voltage and a RKC temperature controller connected to a thermocouple attached to the catalyst bed in a reactor. A dial setting establishes a set point at any temperature within the range between 0 ^{o}C to 600 ^{o}C.

4.3.2.3 Electrical furnace: This supplies the required heat to the reactor for reactor. The reactor can be operated from room temperature up to 700 ^{o}C at maximum voltage of 220 vol.

4.3.2.4 Gas Controlling System: nitrogen is equipped with a pressure regulator (0-120 psig), an on-off valve and a needle valve were used to adjust flow rate of gas.

4.3.2.5 Gas Chromatographs: flame ionization dectector-type gas chromatographs, Shimadzu GC-14A and Shimadzu GC-14B were used to analyze feed and effluent gas composition. Operating conditions used are shown in Table 4.2.

Table 4.2 Operating conditions for gas chromatograph

Gas chromatograph	Shimadzu GC 14A	Shimadzu GC 14B
Detector	FID	FID
Column	Capillary	VZ-10
Carrier gas	N_2 (99.999 %)	N_2 (99.999 %)
Carrier gas flow	25 ml/min	25 ml/min
Column temperature		
- Initial	40	70
- Final	140	70
Detector temperature	150	150
Injector temperature	100	100
Analyzed gas	Hydrocarbon	Hydrocarbon C1-C4

4.3.3 Reaction Method

The aromatization of n-heptane reaction was carried out by using a conventional flow apparatus shown in Figure 4.5. A 0.25 g. of the catalyst was packed in a quartz tubular reactor. Aromatization of n-heptane was carried out under the following conditions: atmospheric pressure; gas hourly space velocity (GSHV), 2000 – 6000 h^{-1}, reaction temperature, 450-600 ^oC.

The procedure used to operate this reactor is as follows:

(1) Adjust the outlet pressure of nitrogen to 1 kg/cm^2 and allow the gas to flow through a rotameter (See Appendix A-3), measure the outlet gas flow rate by using a bubble flowmeter.

(2) Heat up the reactor (under N_2 flow) by raising the temperature from room temperature to 300 ^oC in 30 min. and then hold at that temperature for 30 min. for preheat catalyst. Then the temperature was raising from 300 ^oC to

the required temperature and wait until the required temperature becomes constant.

(3) Put heptane 10 ml in saturator and set the partial vapor pressure of n-heptane to the requirement by adjust the temperature of water bath.

(4) Start to run the reaction by adjusting two three-way valves to allow nitrogen gas to pass through n-heptane inside the saturator set in the water bath, and at that time the reaction time is taken as zero.

(4) Take sample to analyze at 1 hr. on stream. The reaction products were analyzed by FID-type gas chromatographs (For calculation see Appendix A-5).

4.4 Characterization of the catalysts

5.4.1 X-ray Diffraction Patterns

X-ray diffraction (XRD) patterns of the catalysts were performed with SIEMENS XRD D5000, accurately measured in the 5-40^{o} 2θ angular region, at petrochemical Engineering Reasearch Laboratory, Chulalongkorn University.

4.4.2 Morphology

The shape and the distribution of size of the crystals were observed by JEOL Scanning Electron Microscope (SEM) at the Scientific and Technological Research Equipment Center, Chulalongkorn University (STREC).

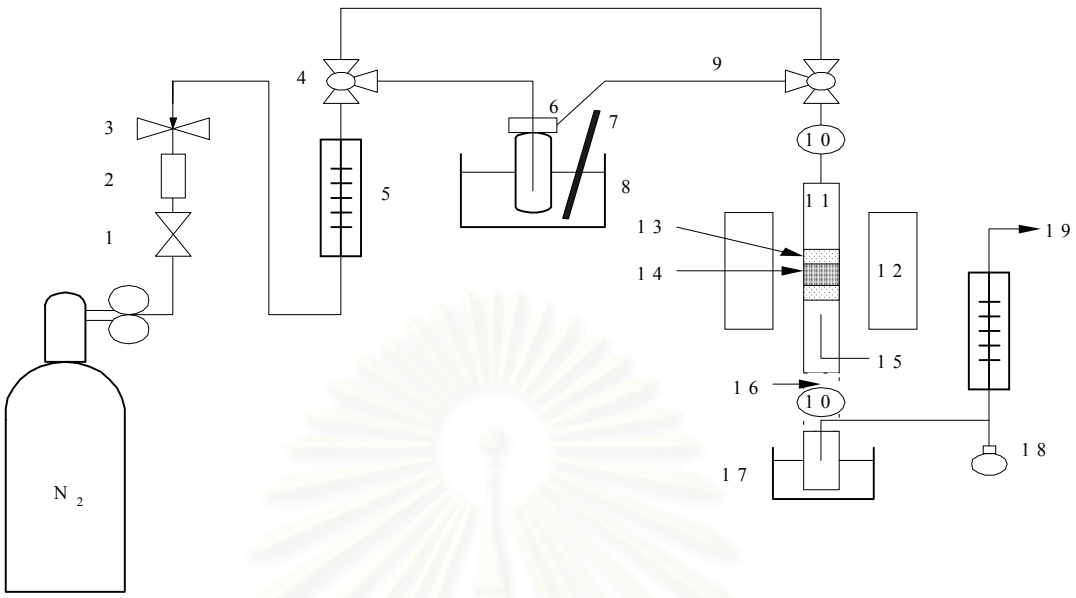

1. On-off valve	2. Gas filter	3. Needle valve	4. Three-way valve
5. Flow meter	6. Saturator	7. Thermocouple	8. Water bath
9. Heating line	10. Sampling port	11. Tubular reactor	12. Electric furnace
13. Quartz wool	14.Catalyst	15. Thermocouple	16. Heating tape
17. Trap	18. Soap-film flowmeter		19. Purge

Figure 4.5 Schematic diagram of the reaction apparatus for the aromatization of n-heptane

4.4.3 BET Surface Area Measurement

Surface areas of the catalysts were measured by the BET method, with nitrogen as the adsorbate using a micrometritics model ASAP 2000 at liquid-nitrogen boiling point temperature at the Analysis Center of Department of Chemical Engineering, Faculty of Engineering, Chulalongkorn University.

4.4.4 Chemical Analysis

Percentage of metals was analyzed by X-ray fluorescence spectrometer (XRF) technique. The silicon, aluminum, gallium and zinc content of the prepared catalyst

was analyzed by X-ray fluorescence spectrometer (XRF) at the department of science service, Ministry of Science, Technology and Environment.

4.4.5 Acidity Measurement

Infrared spectroscopy and temperature programmed desorption of pyridine have been used to investigate the acidic properties of MFI-type zeolites. The flow diagram of in situ FT-IR apparatus is depicted in Figure 4.6 All gas lines, valves and fitting in this apparatus are made of pyrex glass except for IR gas cell and sample dish holder which are of quartz glass in order to avoid the adsorption of any gas species which may remain on the inner surface of glass tube while the system was evacuated. A Nicolet model impact 400 FT-IR equipped with deuterated triglycine sulfate (DYGS) detector and connected to a personal computer with Omnic version 1.2a on Windows software (to fully control the functions of the IR analyzer) were applied to this study. The analyzer was place on a movable table for conveniently adjustment.

About 0.06 g. of catalyst powder was pressed into self-supporting dish form with about 1 cm. diameter by using a stainless steel press apparatus. The sample dish was placed into quartz in situ IR gas cell. The cell was attached with two KBr windows at both ends. Prior to adsorption, the sample was heated at 300^{o}C and evacuated to about 10^{-4} torr for 1 hr. After that the sample was cooled down to room temperature and pyridine was introduced into the IR cell by self-vaporizing in vacuum condition and was circulated through the system by electromagnetic pump. After 2 hr of adsorption, the excess and weakly adsorped and physisorbed pyridine was removed by evacuating at 150^{o}C for 30 min. Desorption was then carried out by evacuation at progressively higher temperature, every 50^{o}C, and IR spectra were recorded at the various stages of desorption. Each spectrum was completed by 500 scan at a resolution of 4 cm^{-1}. Background spectrums, i.e., prior to adsorption, were subtracted from all spectra so that the effects of adsorption and thermal treatments could be more clearly seen.

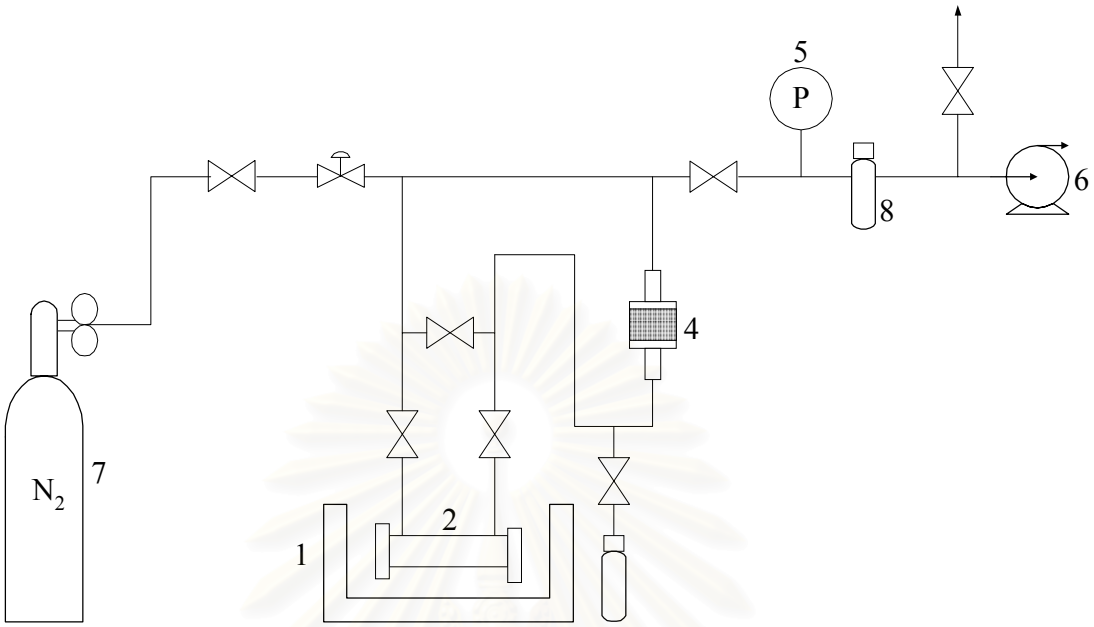

1. FT-IR Analyzer 2. IR quartz gas cell 3. Pyridine tube
4. Electromagnetic circulating pump 5. Digital pressure indicator
6. Vacuum pump 7. Nitrogen gas cylinder 8. Solvent trap

Figure 4.6 Flow diagram of instrument used for pyridine adsorption experiment

CHAPTER V
Results and Discussion

In this chapter, the results and discussion are divided to two sections. First, characterizations of catalyst are presented in section 5.1. The techniques are XRD, SEM, BET, XRF and FTIR pyridine adsorption. Second, catalytic behavior of catalyst on the aromatization of n-heptane is explained in section 5.2.

5.1 Catalyst Characterization

5.1.1 X-ray Diffraction Pattern

The X-ray diffraction patterns for the prepared catalysts are shown in Figure 5.1. All the XRD patterns of catalyst correspond well with those report in the literature [36]. While other non-zeolite phases such as oxide phases of Ga and oxide phases of Zn were not detected. This indicates that all the catalysts have the same pentasil pore-opening structure as ZSM-5 and a little amount of metal loaded did not change the main structure of MFI-type zeolite catalyst.

5.1.2 Morphology

Scanning electron microscope (SEM) photographs of the prepared catalyst are shown in Figure 5.2. As shown, the morphology of the whole samples were composed of tiny rectangular unit crystallites agglomerated to substantially spherical particle in shape. The crystal sizes of ZSM-5 modified with Ga or Zn were somewhat larger or smaller than the unmodified ZSM-5; however, the crystal sizes of all the samples were approximately varied during 1-3 μm.

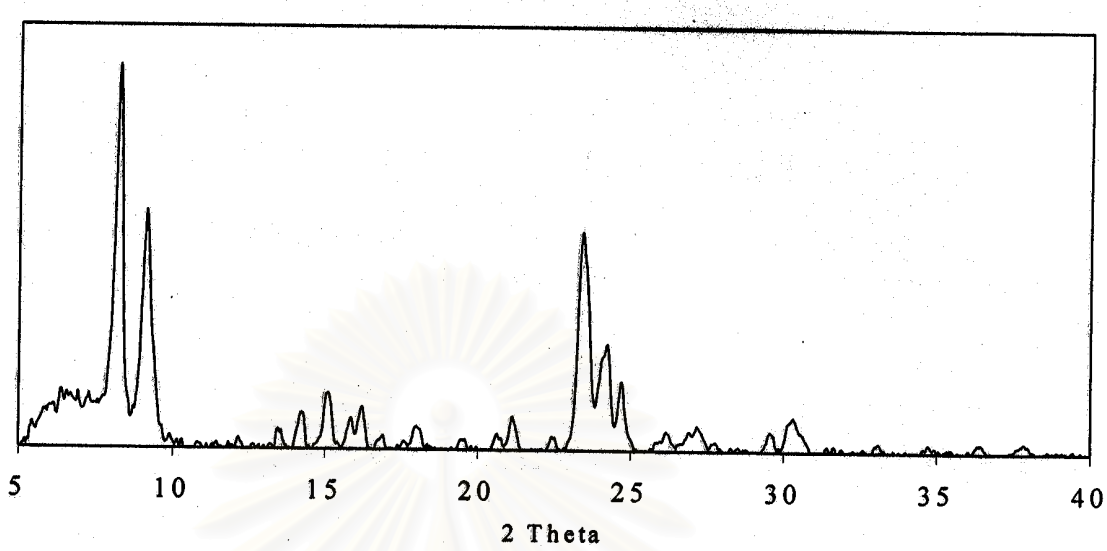

(a) Na-ZSM-5

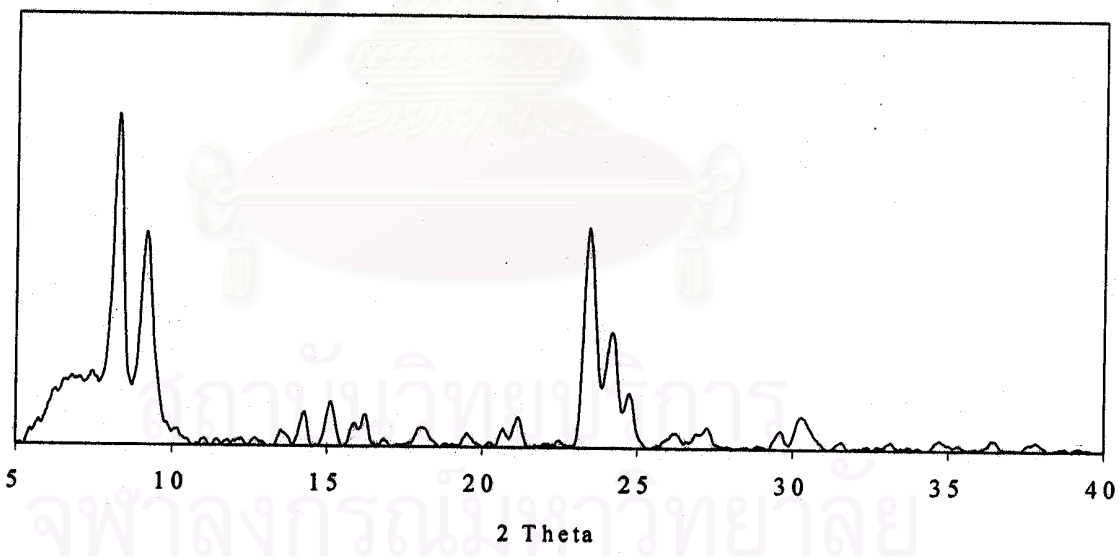

(b) H-ZSM-5

Figure 5.1 X-ray diffraction of the prepared catalysts

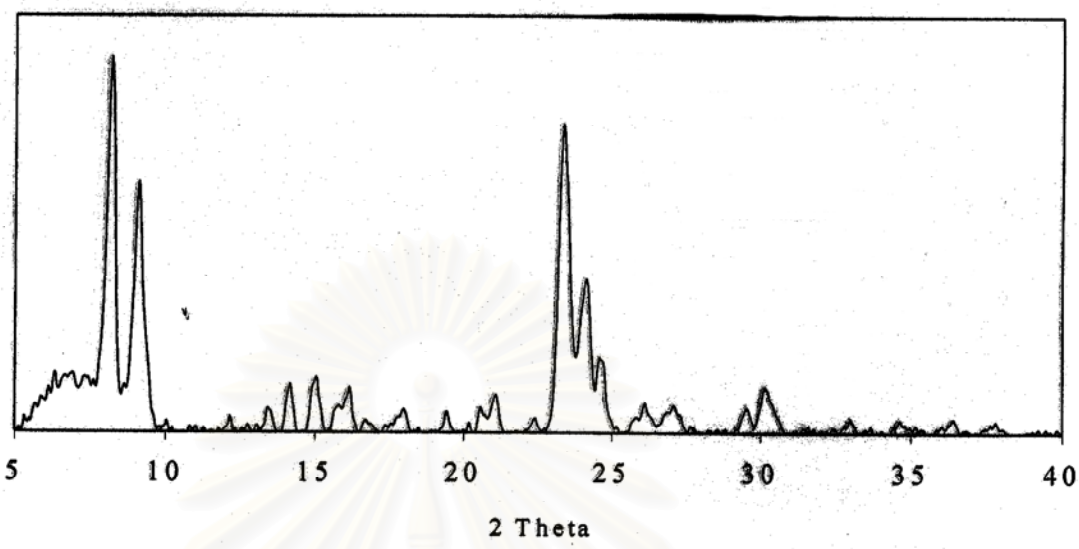

(c) H-Ga.Al-silicate (Si/Ga loading ratio of 40)

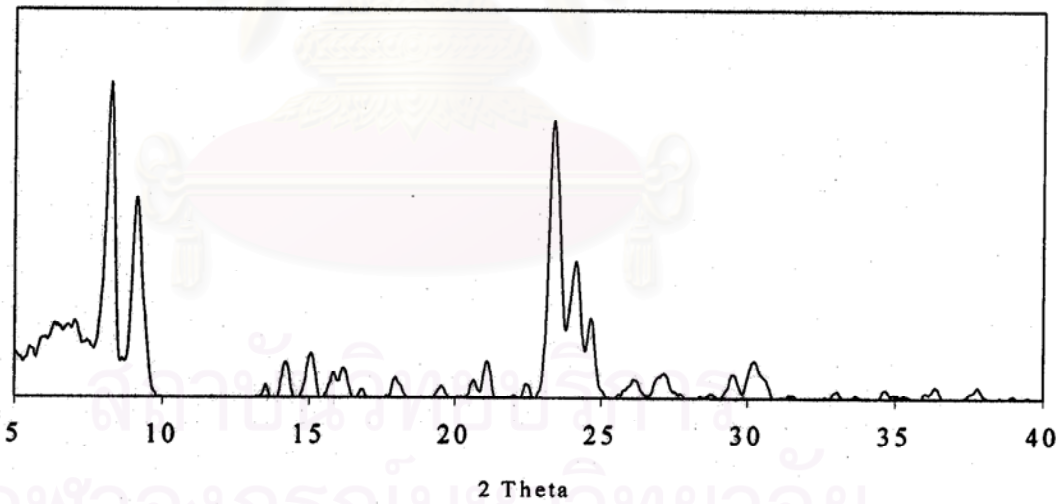

(d) H-Ga.Al-silicate (Si/Ga loading ratio of 100)

Figure 5.1 X-ray diffraction of the prepared catalysts (continued)

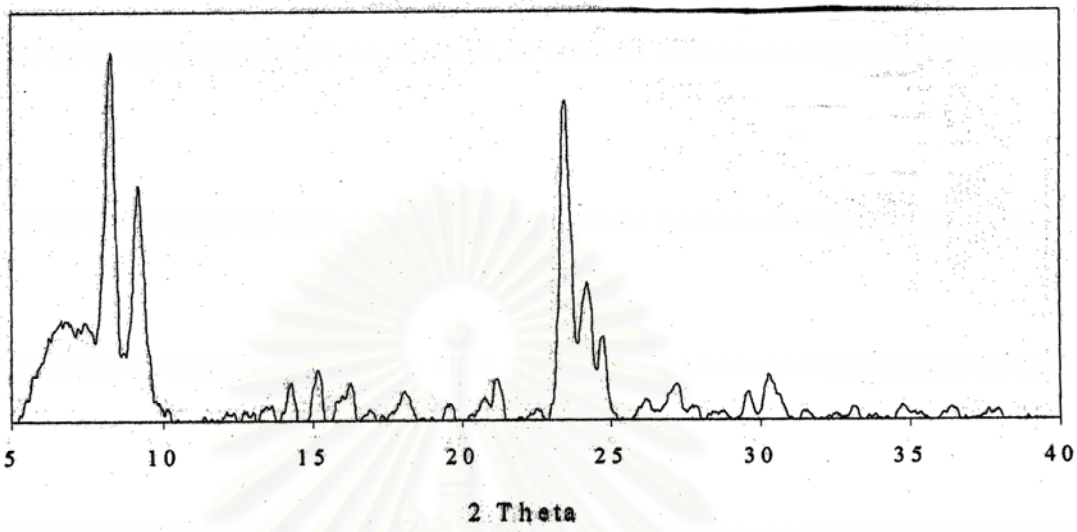

(e) H-Ga.Al-silicate (Si/Ga loading ratio of 155)

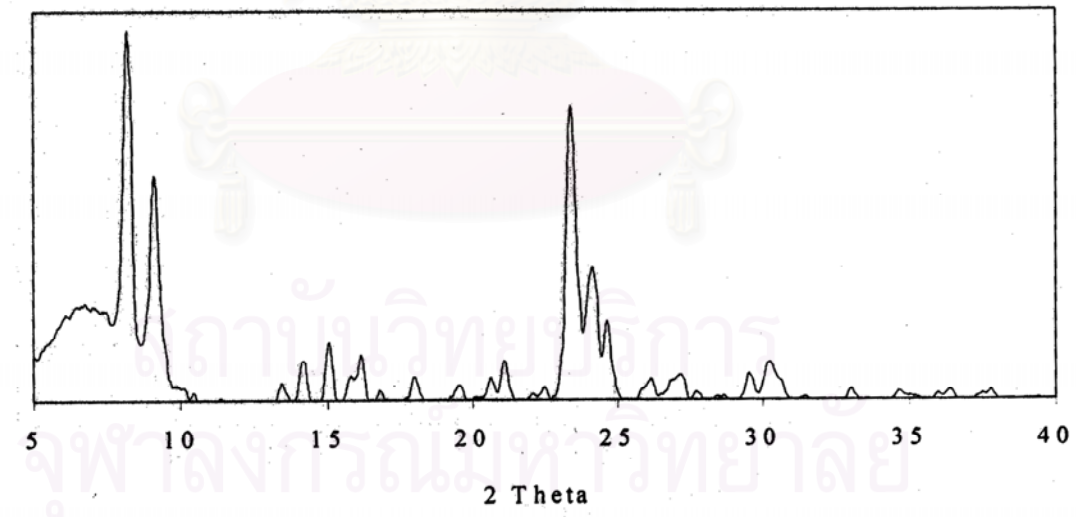

(f) H-Ga.Al-silicate (Si/Ga loading ratio of 310)

Figure 5.1 X-ray diffraction of the prepared catalysts (continued)

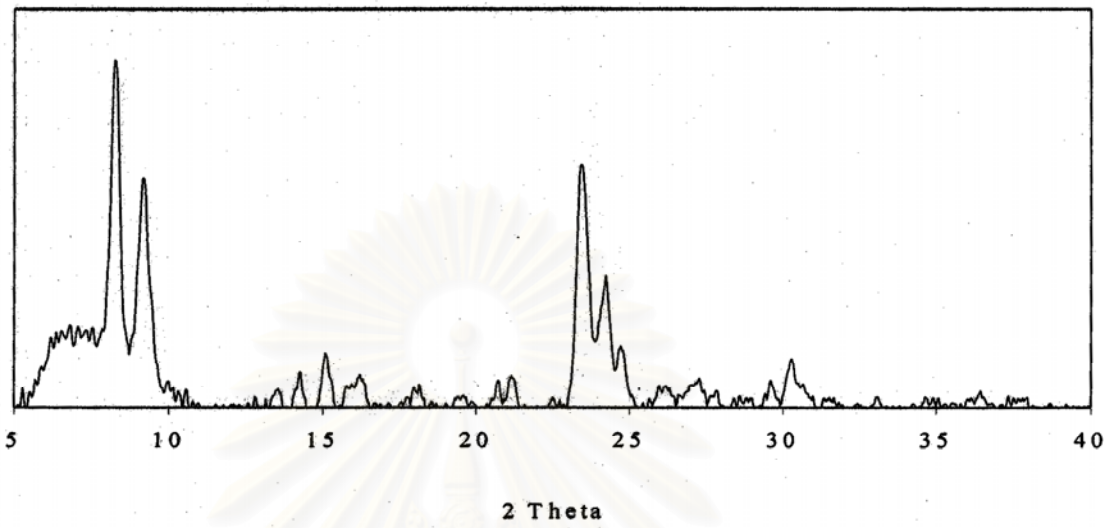

(g) Ga (2.0 wt% loading) / H-ZSM-5

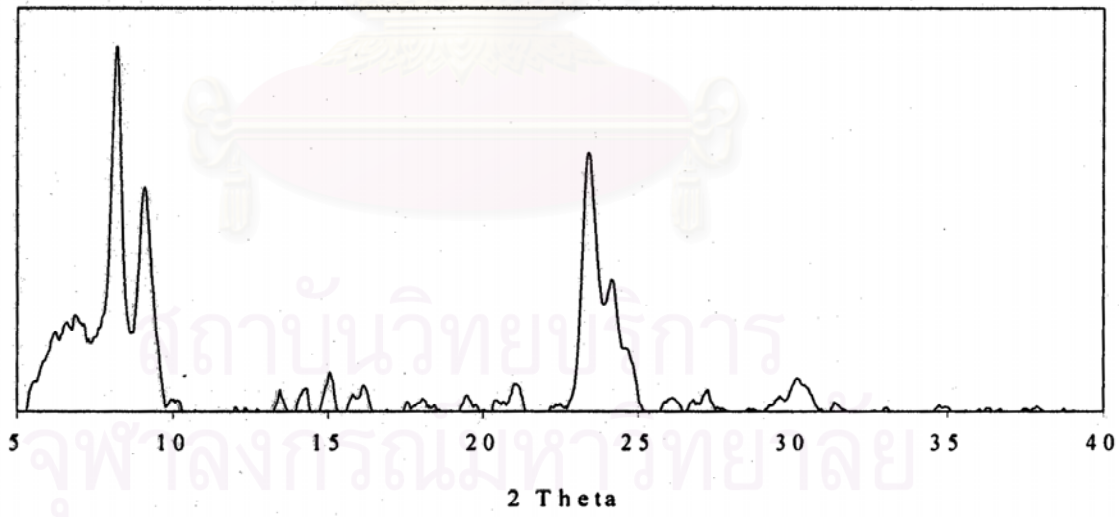

(h) H-Zn.Al-silicate (Si/Zn loading ratio of 40)

Figure 5.1 X-ray diffraction of the prepared catalysts (continued)

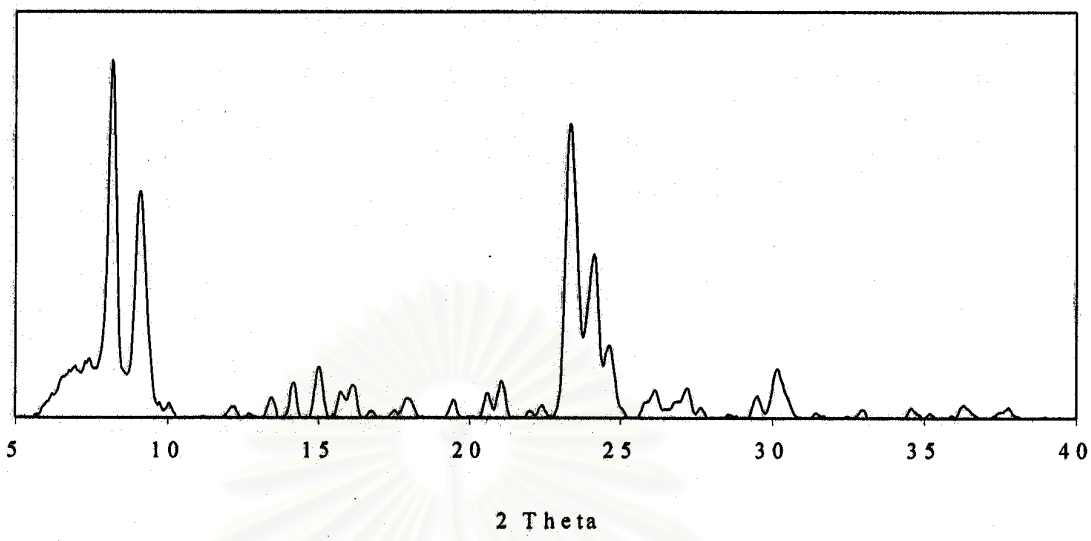

(i) H-Zn.Al-silicate (Si/Zn loading ratio of 100)

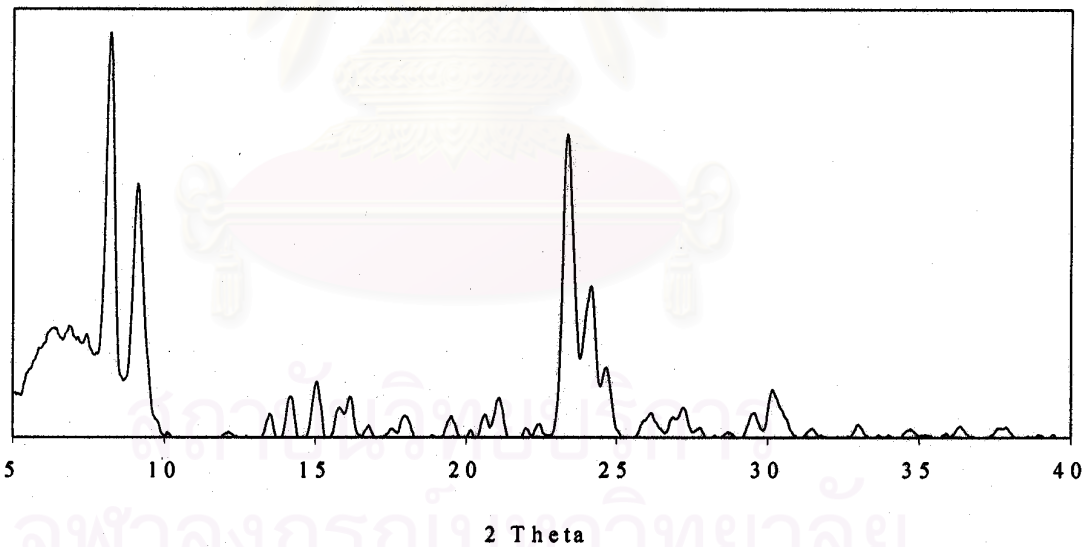

(j) H-Zn.Al-silicate (Si/Zn loading ratio of 150)

Figure 5.1 X-ray diffraction of the prepared catalysts (continued)

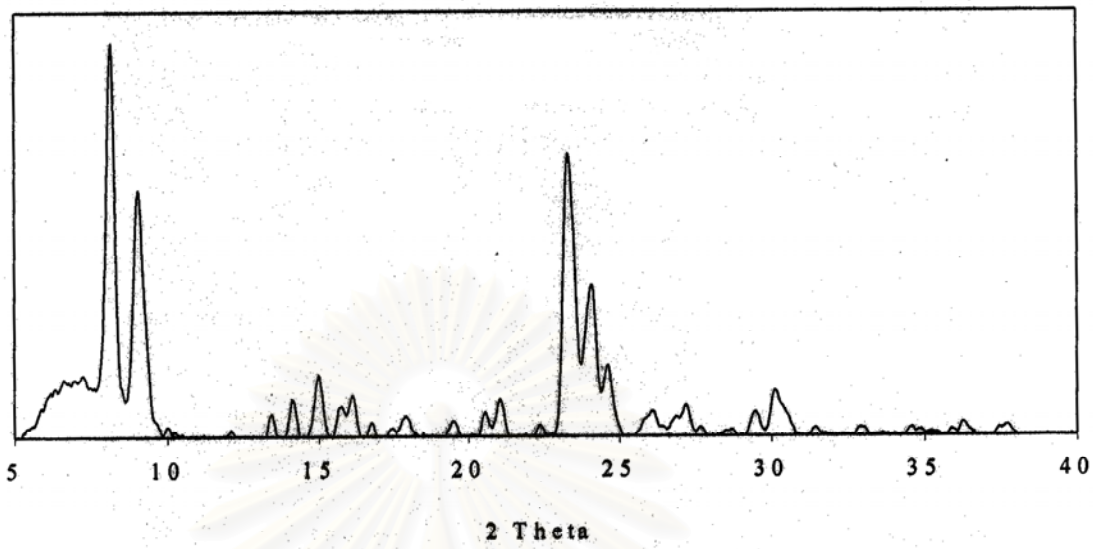

(k) H-Zn.Al-silicate (Si/Zn loading ratio of 270)

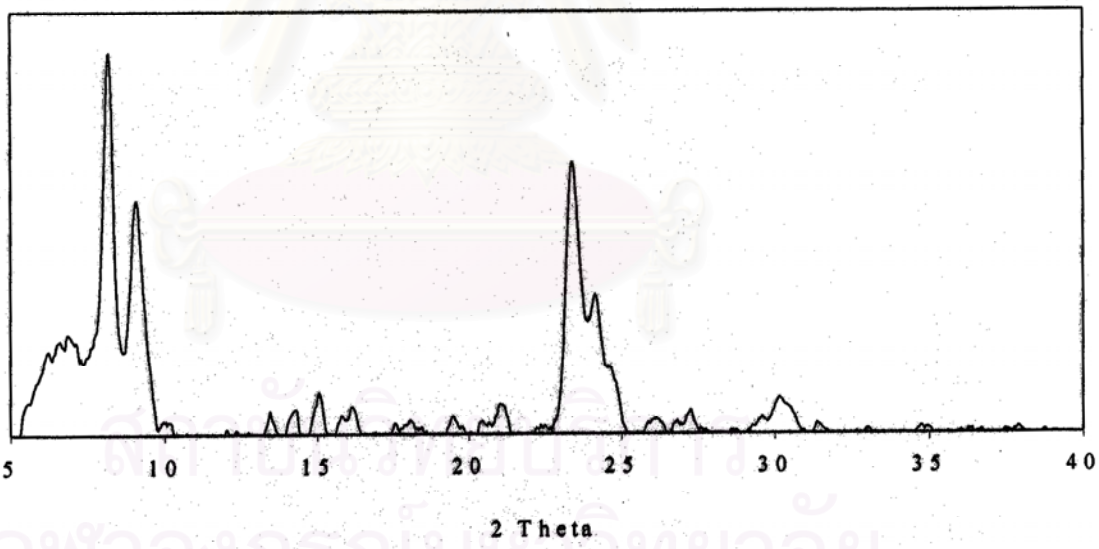

(l) Zn (1.9 wt% loading) / H-ZSM-5

Figure 5.1 X-ray diffraction of the prepared catalysts (continued)

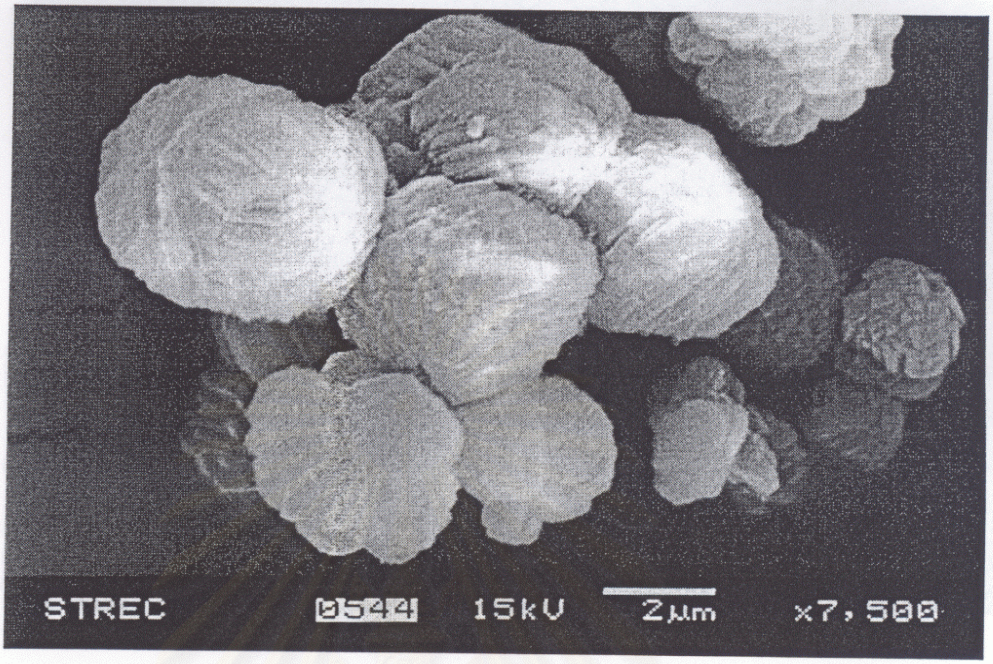

(a) Na-ZSM-5

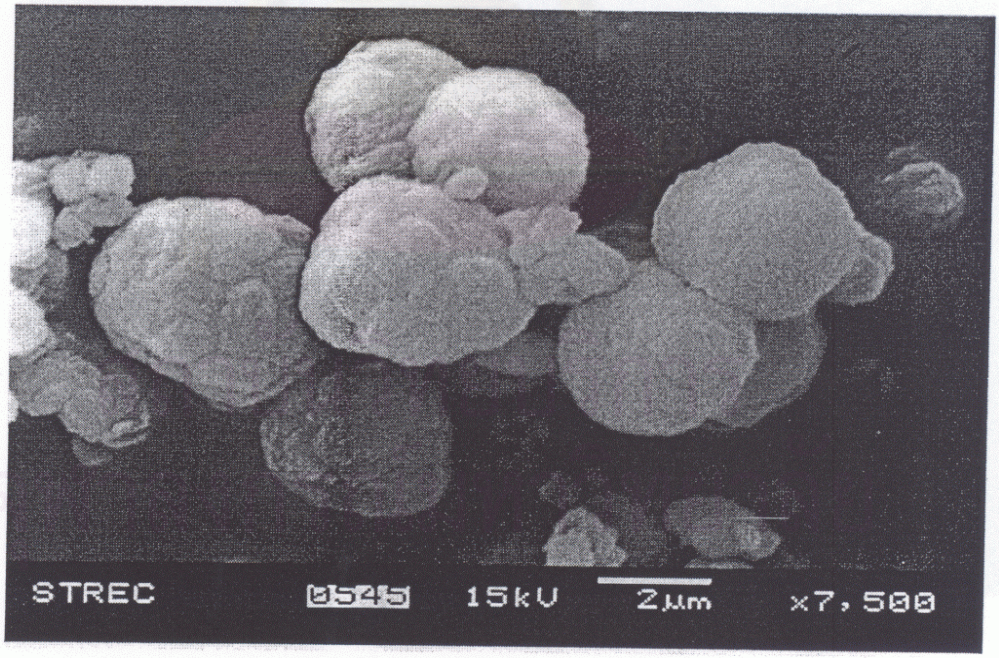

(b) H-ZSM-5

Figure 5.2 SEM photographs of the prepared catalysts

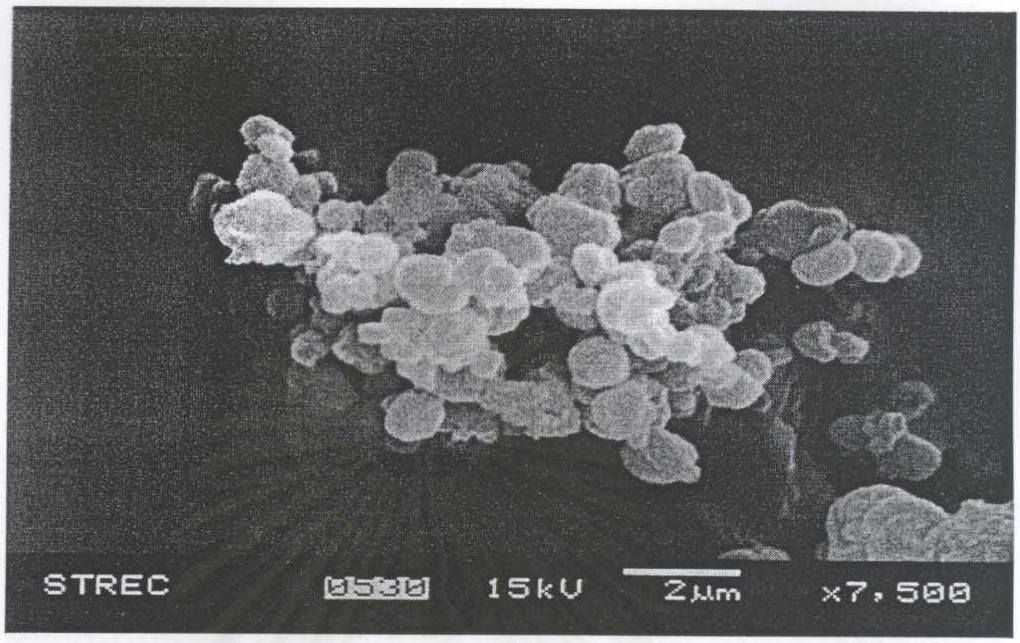

(c) H-Ga.Al-silicate (Si/Ga loading ratio of 40)

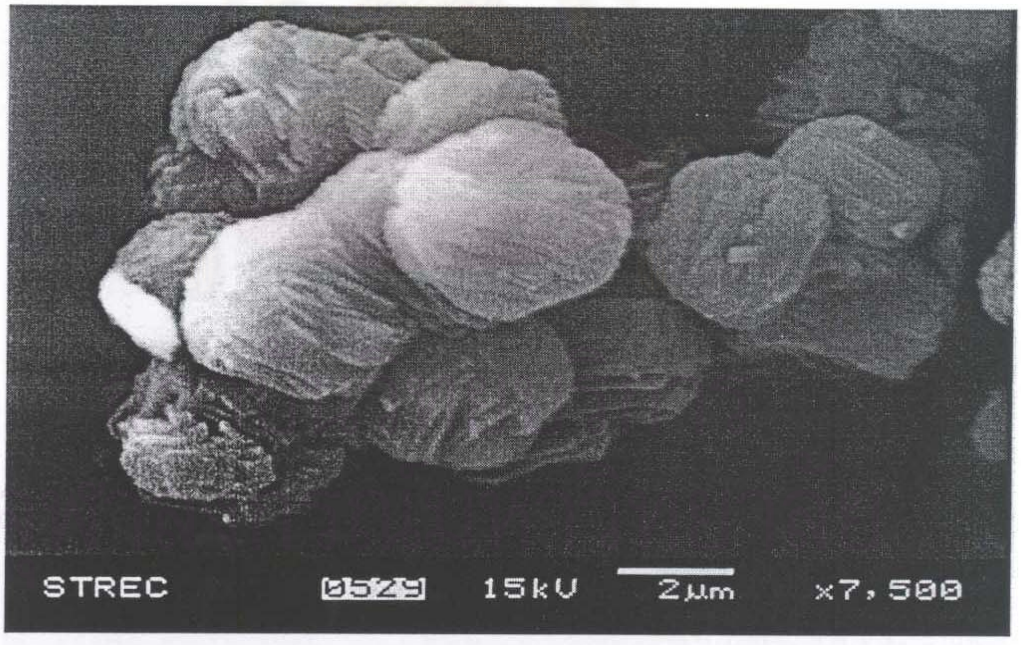

(d) H-Ga.Al-silicate (Si/Ga loading ratio of 100)

Figure 5.2 SEM photographs of the prepared catalysts (continued)

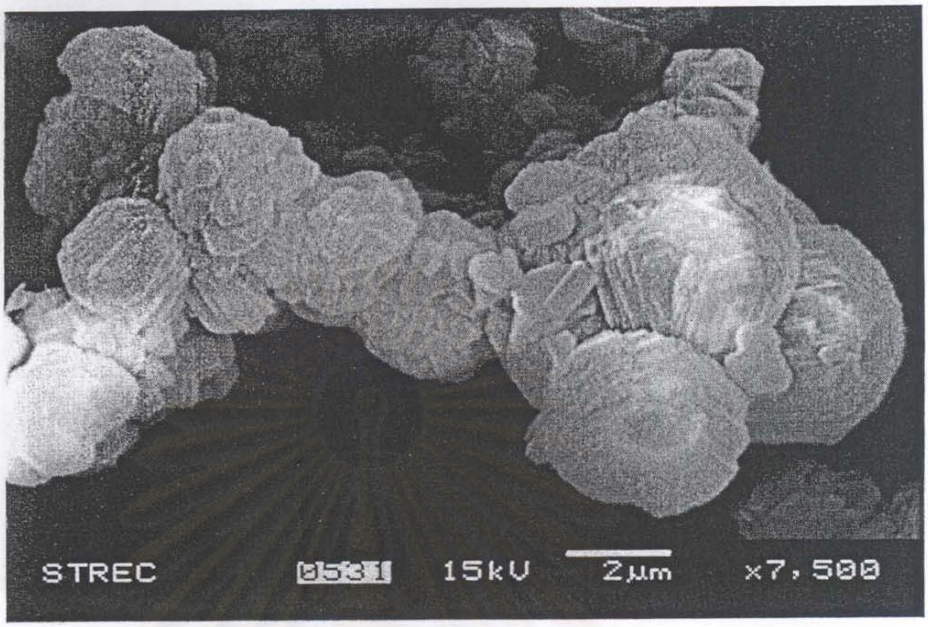

(e) H-Ga.Al-silicate (Si/Ga loading ratio of 155)

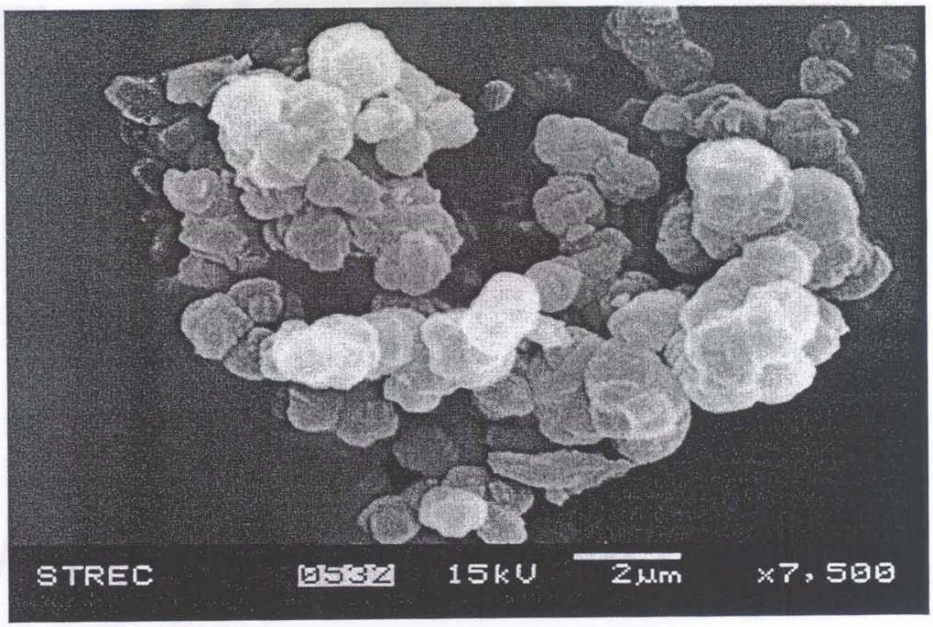

(f) H-Ga.Al-silicate (Si/Ga loading ratio of 310)

Figure 5.2 SEM photographs of the prepared catalysts (continued)

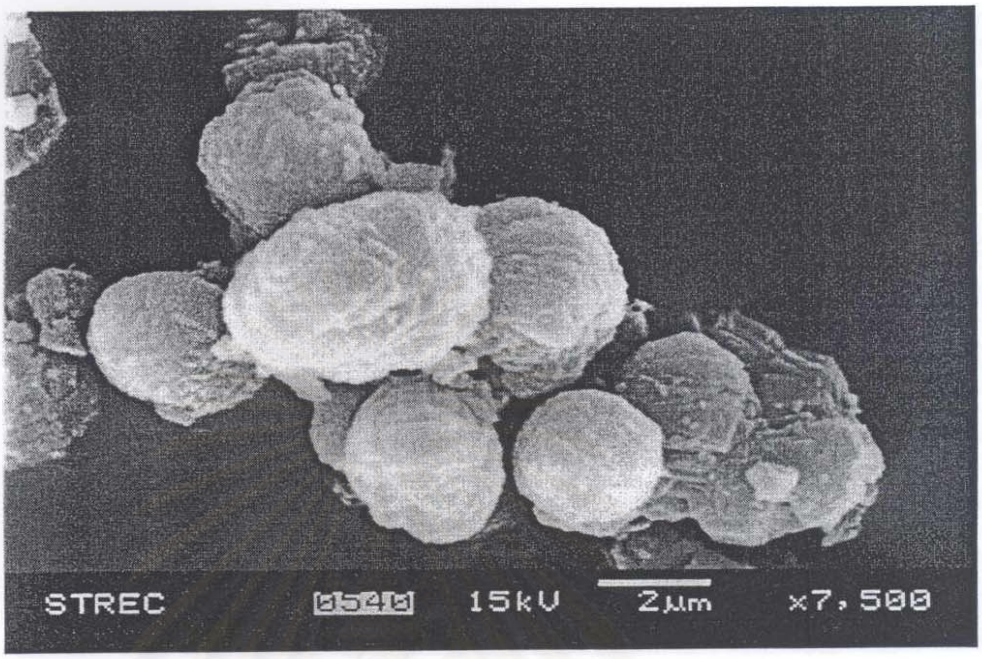

(g) Ga (2.0 wt% loading) / H-ZSM-5

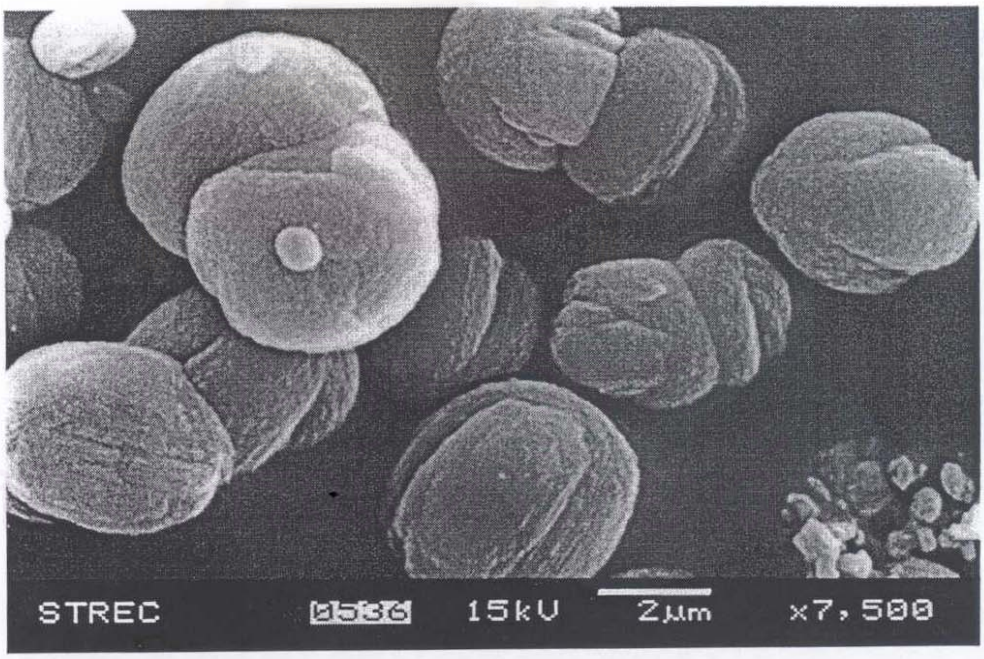

(h) H-Zn.Al-silicate (Si/Zn loading ratio of 40)

Figure 5.2 SEM photographs of the prepared catalysts (continued)

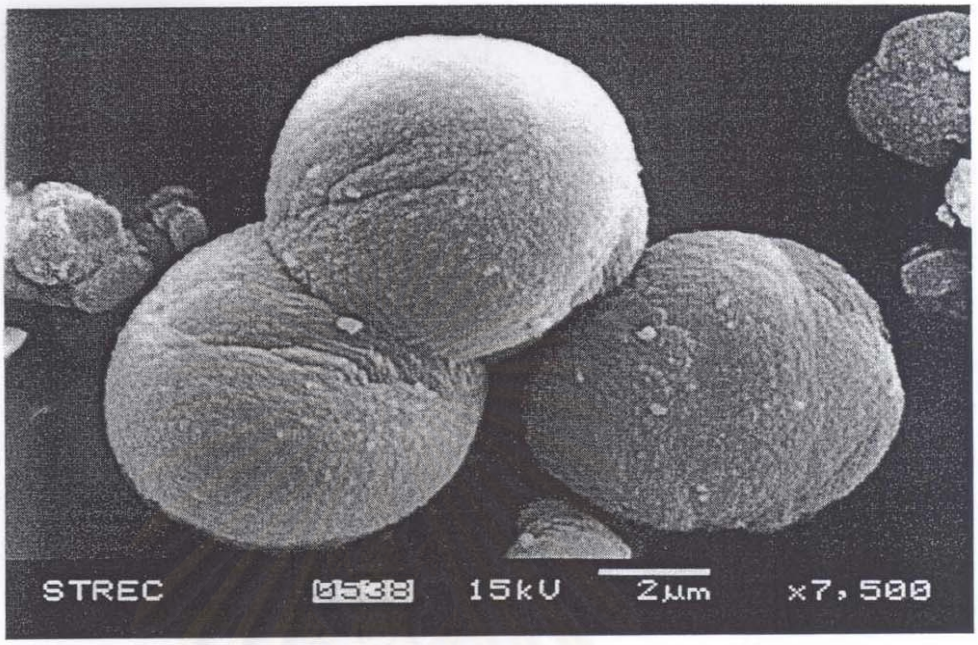

(i) H-Zn.Al-silicate (Si/Zn loading ratio of 100)

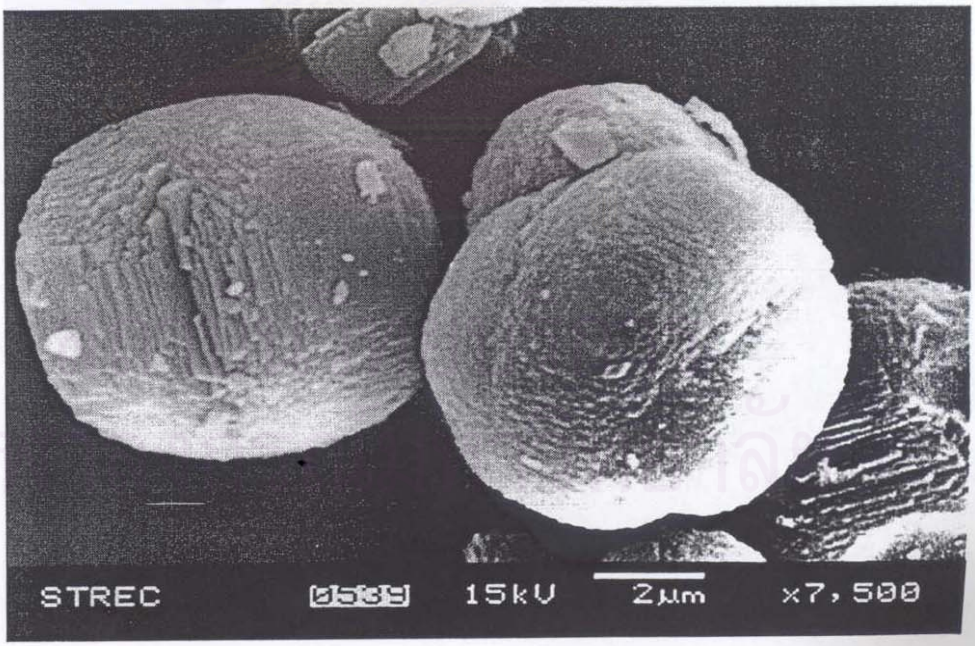

(j) H-Zn.Al-silicate (Si/Zn loading ratio of 150)

Figure 5.2 SEM photographs of the prepared catalysts (continued)

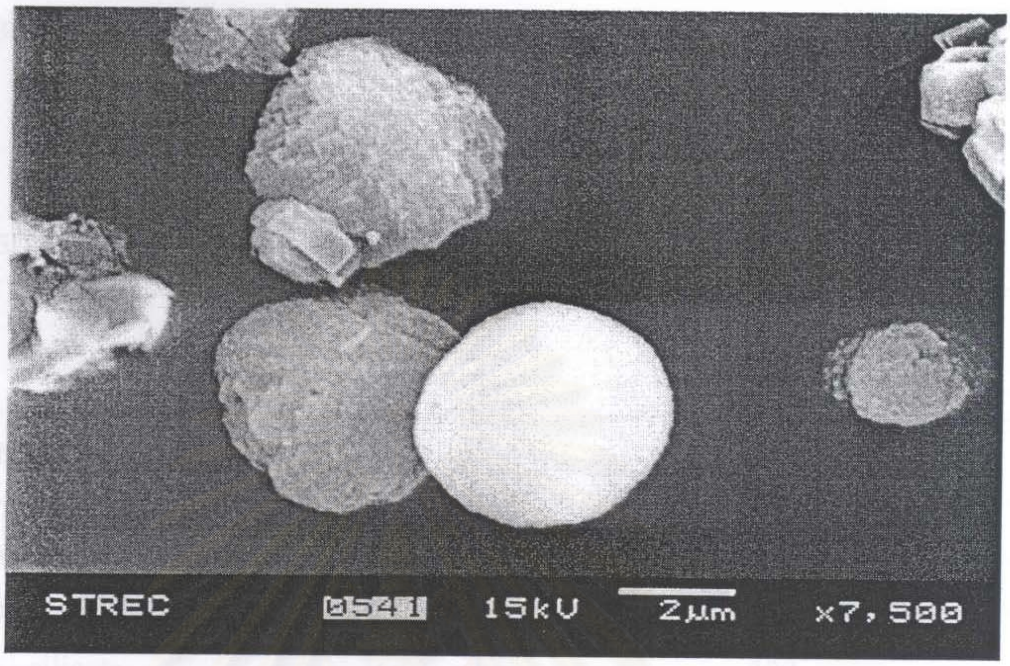

(k) H-Zn.Al-silicate (Si/Zn loading ratio of 270)

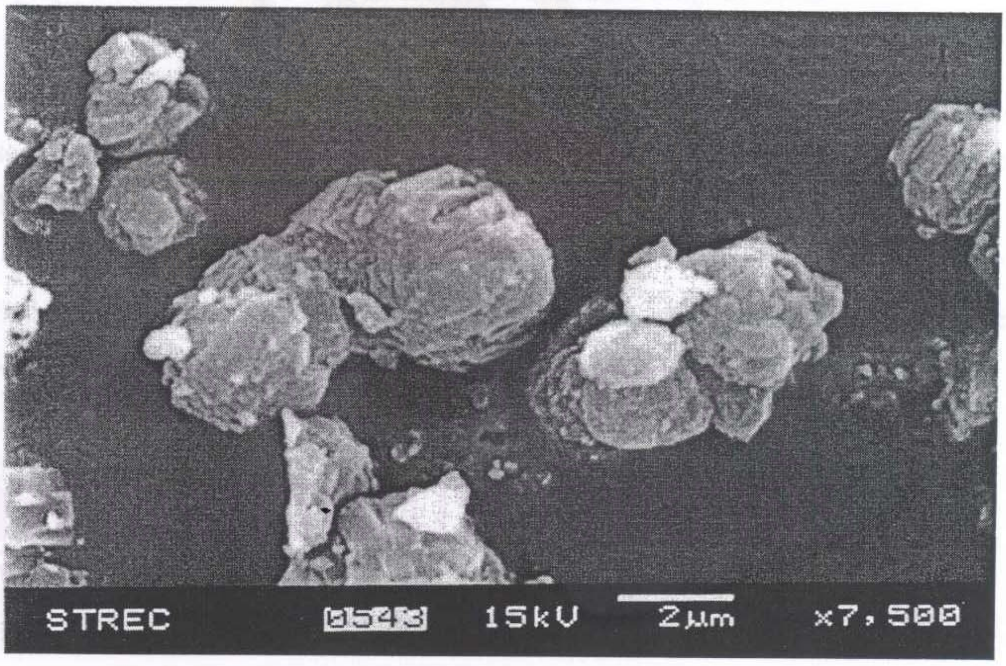

(l) Zn (1.9 wt% loading) / H-ZSM-5

Figure 5.2 SEM photographs of the prepared catalysts (continued)

5.1.3 BET surface Area

BET surface areas of the prepared catalysts are shown in Table 5.1.

Table 5.1 BET surface areas of the prepared catalysts

Catalyst	BET surface areas (m^2/g of catalysts)
Na-ZSM-5	389
H-ZSM-5	418
H-Ga.Al-silicate	390
Ga (2.91 wt%) / H-ZSM-5	407
H-Zn.Al-silicate	388
Zn (1.99 wt%) / H-ZSM-5	407

***All the prepared catalysts have bulk Si/Al atomic ratio in the range of 33-40**

From Table 5.1, the BET surface area after metal loading was slightly decreased. This introduces the channel occupation of a small amount of metal or pore mouth blockage.

Hence, it may be said that their BET surface area were the same range as commonly found between 340-423 in MFI-type catalyst [16].

5.1.4 Chemical Composition

The results of quantitative analysis of silica, aluminum, and metal in the synthesized crystals are shown in Table 5.2. and Table 5.3, respectively.

Table 5.2 Ga or Zn Contents in Metalloaluminosilicate

(a) H-Ga.Al-silicate

Si/Ga loaded	Si/Ga observed	Si/Al observed
40	45.5	35.1
100	115.8	39.9
155	164.5	38.2
310	378.7	38.5

(b) H-Zn.Al-silicate

Si/Zn loaded	Si/Zn observed	Si/Al observed
40	30.4	35.0
100	97.5	33.5
150	117.4	34.9
270	226.9	35.4

* **All the prepared catalysts have bulk Si/Al atomic ratio in loading 40**

Table 5.2 shows the loaded and observed ratio of Si to metals. It has been found that Si/Ga observed ratio was higher than Si/Ga loaded ratio while Si/Zn observed ratio was lower than Si/Zn loaded ratio. This should be ascribed to the less incorperation of Ga into the framework hindered by the fact that Ga has atomic radius higher than that of Zn.

5.1.5 FTIR Pyridine Adsorption

From the previous studies [37, 38], the bands at about 1540 cm^{-1} and 1450 cm^{-1} were assigned to pyridine adsorbed on Brønsted and Lewis acid sites, respectively. Thus, the bands in the region between 1600-1400 cm^{-1} were interested. The relevant regions of IR spectra after exposure to pyridine as a function of temperature of evacuation for the prepared catalyst are shown in Figure 5.3.

As shown, the intensity of the pyridine adsorbed on both at Brønsted and Lewis acid site of each zeolite sample decreased with the increasing temperature during 150 ^{o}C and 500 ^{o}C.

Figures 5.4-5.9 illustrate amount of pyridine desorbed from Lewis and Brønsted acid sites during the range of 150 ^{o}C - 500 ^{o}C. It has been found that the integral amount of pyridine desorbed was greatly affected by the type of metal. Gallium-modified catalyst had a higher amount of Brønsted acid site than unmodified one. On the other hand, zinc-modified catalyst had more amount of Lewis acid site than unmodified one.

These results show that gallium promoted Brønsted acid site and zinc promoted Lewis acid site.

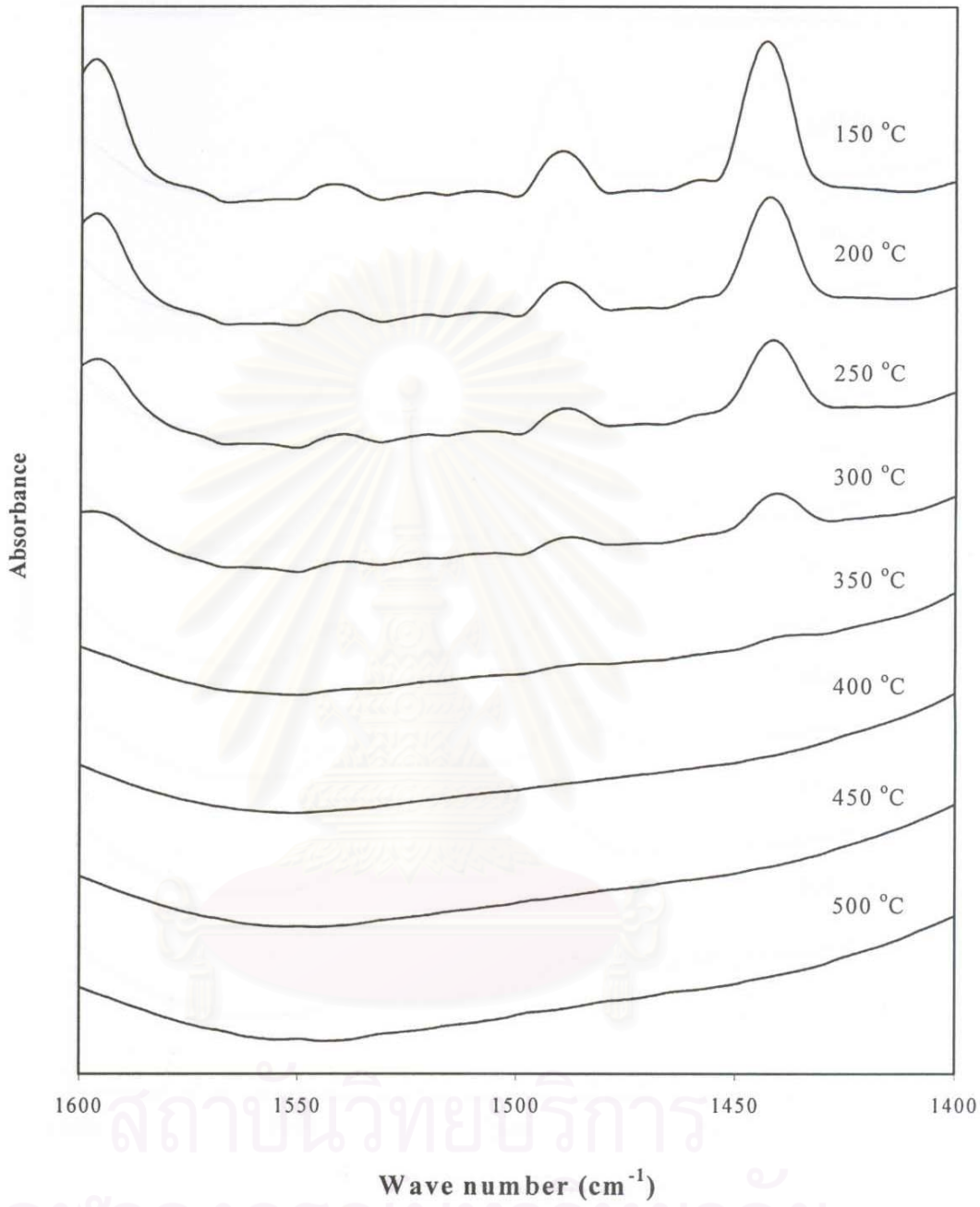

(a) Na-ZSM-5

Figure 5.3 FTIR spectra of pyridine adsorbed prepared catalyst

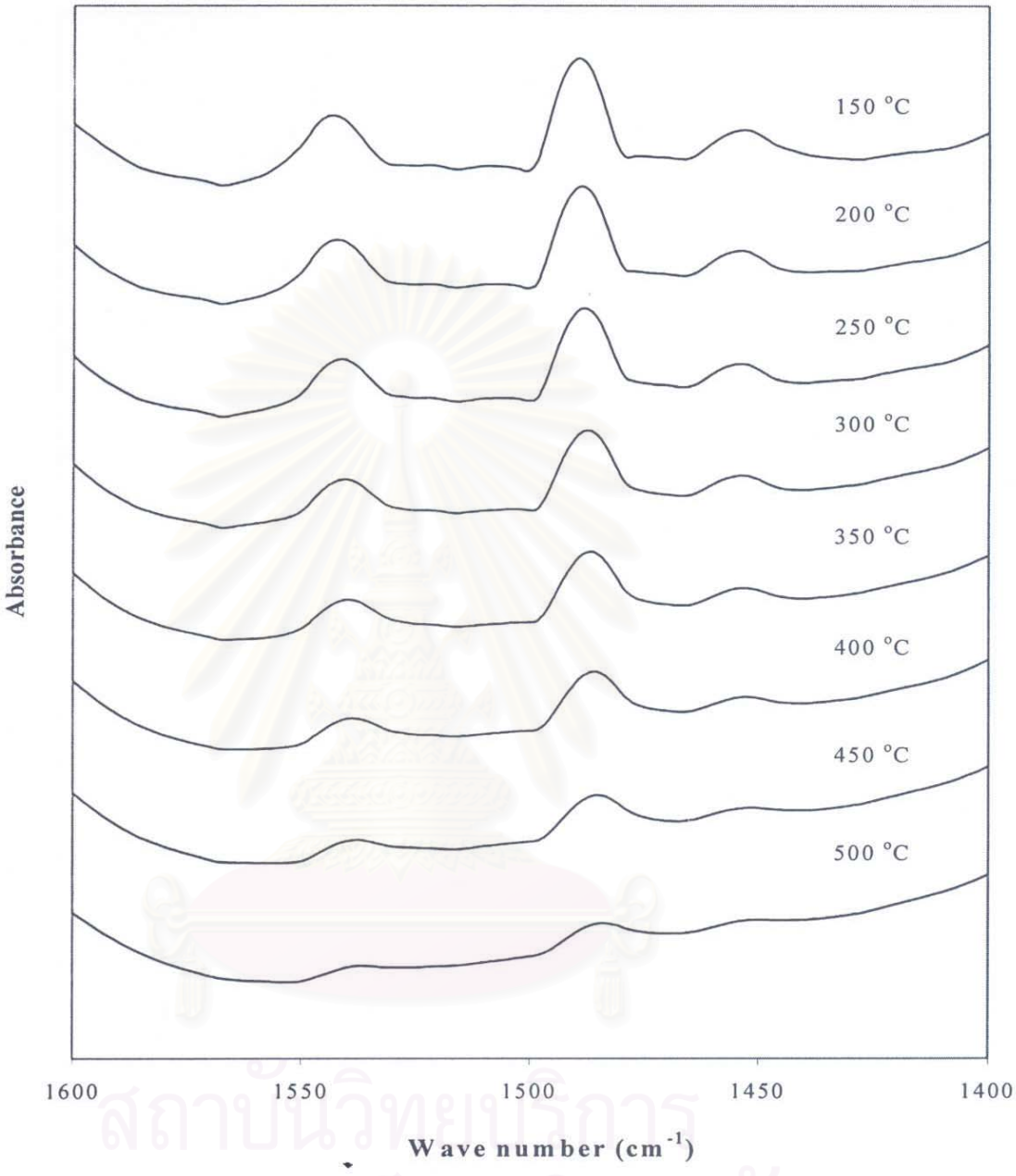

(b) H-ZSM-5

Figure 5.3 FTIR spectra of pyridine adsorbed prepared catalyst (continued)

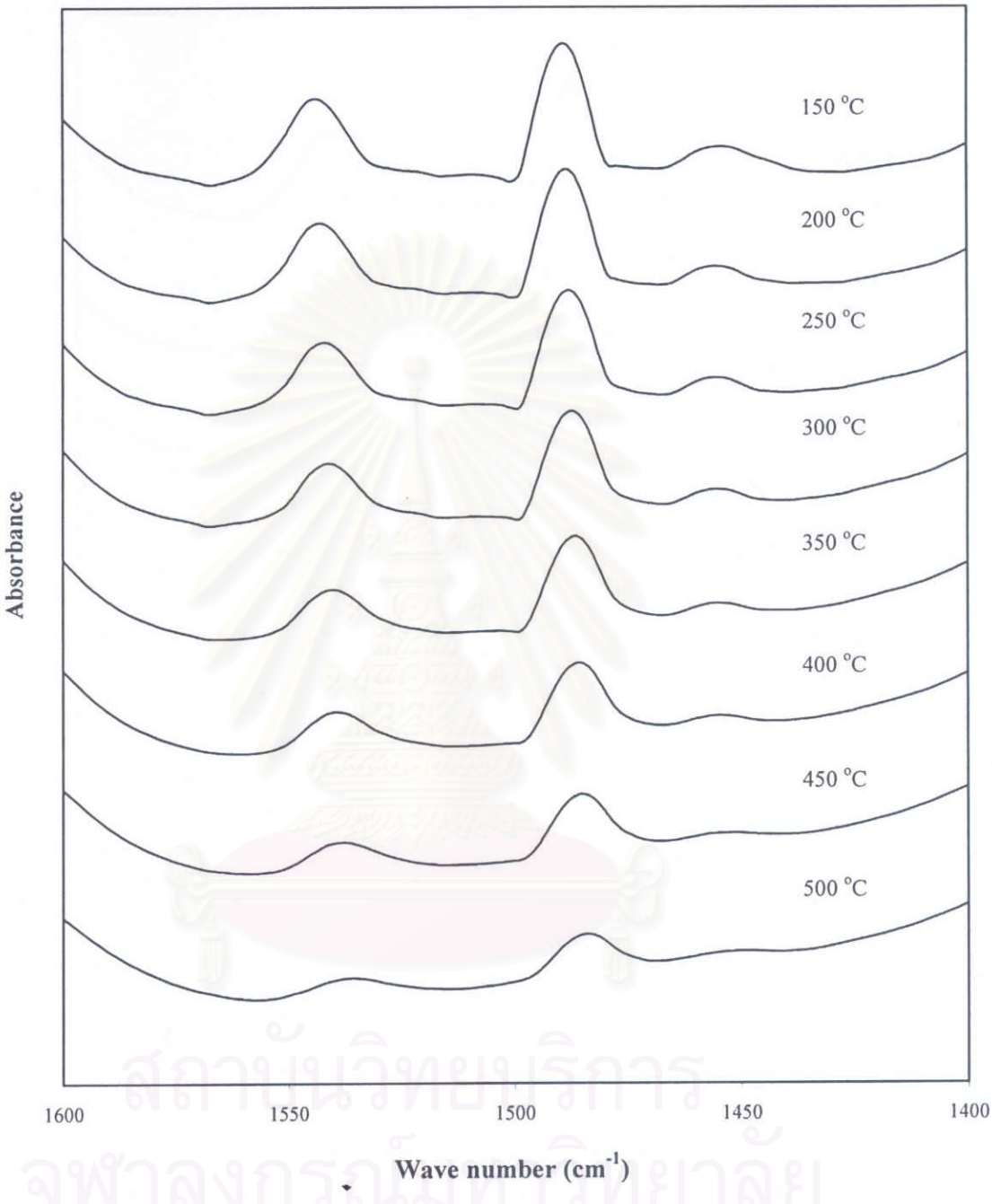

(c) H-Ga.Al-silicate (Si/Ga loading ratio of 100)

Figure 5.3 FTIR spectra of pyridine adsorbed prepared catalyst (continued)

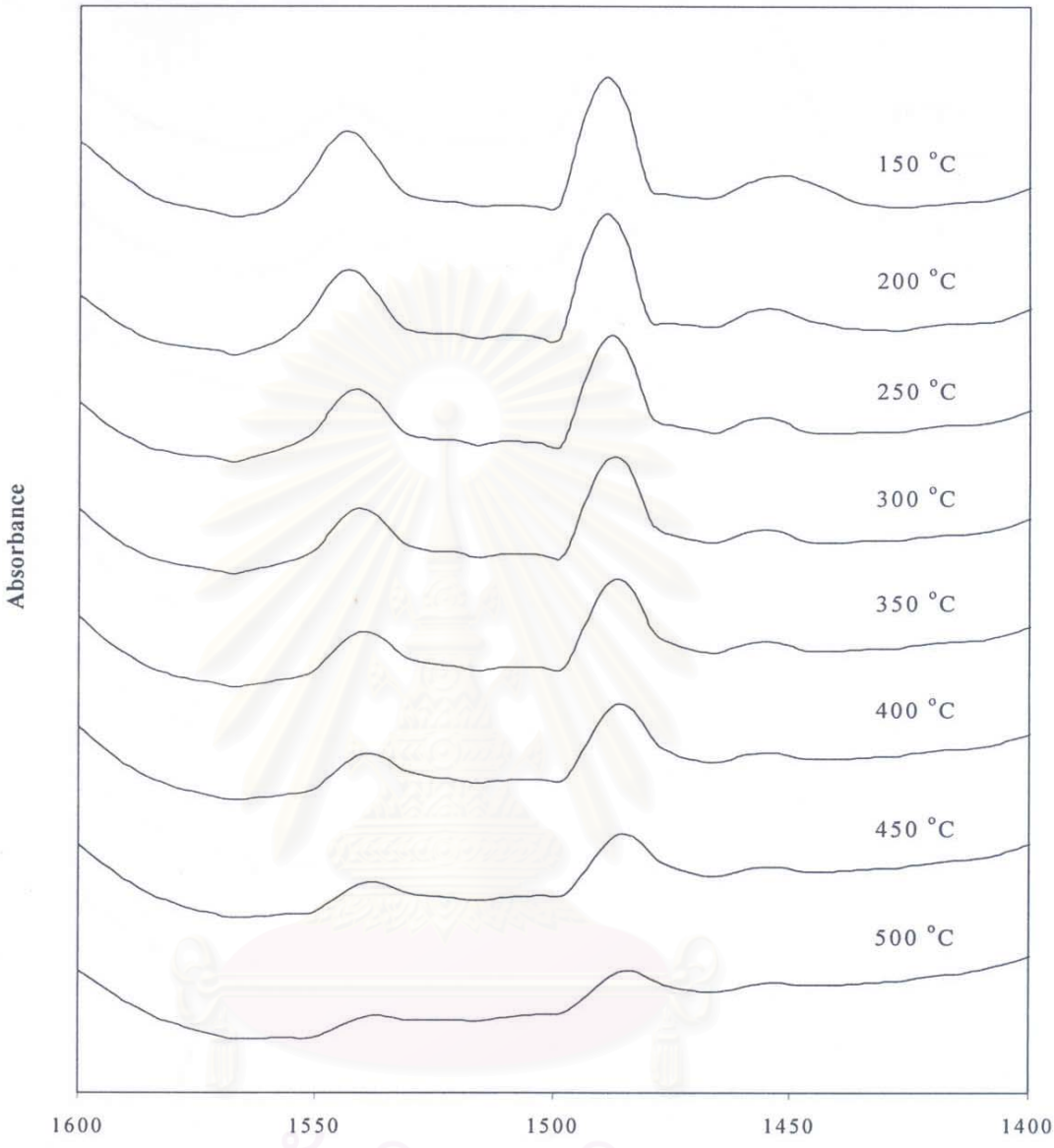

(d) Ga (2.0 wt% loading) / H-ZSM-5

Figure 5.3 FTIR spectra of pyridine adsorbed prepared catalyst (continued)

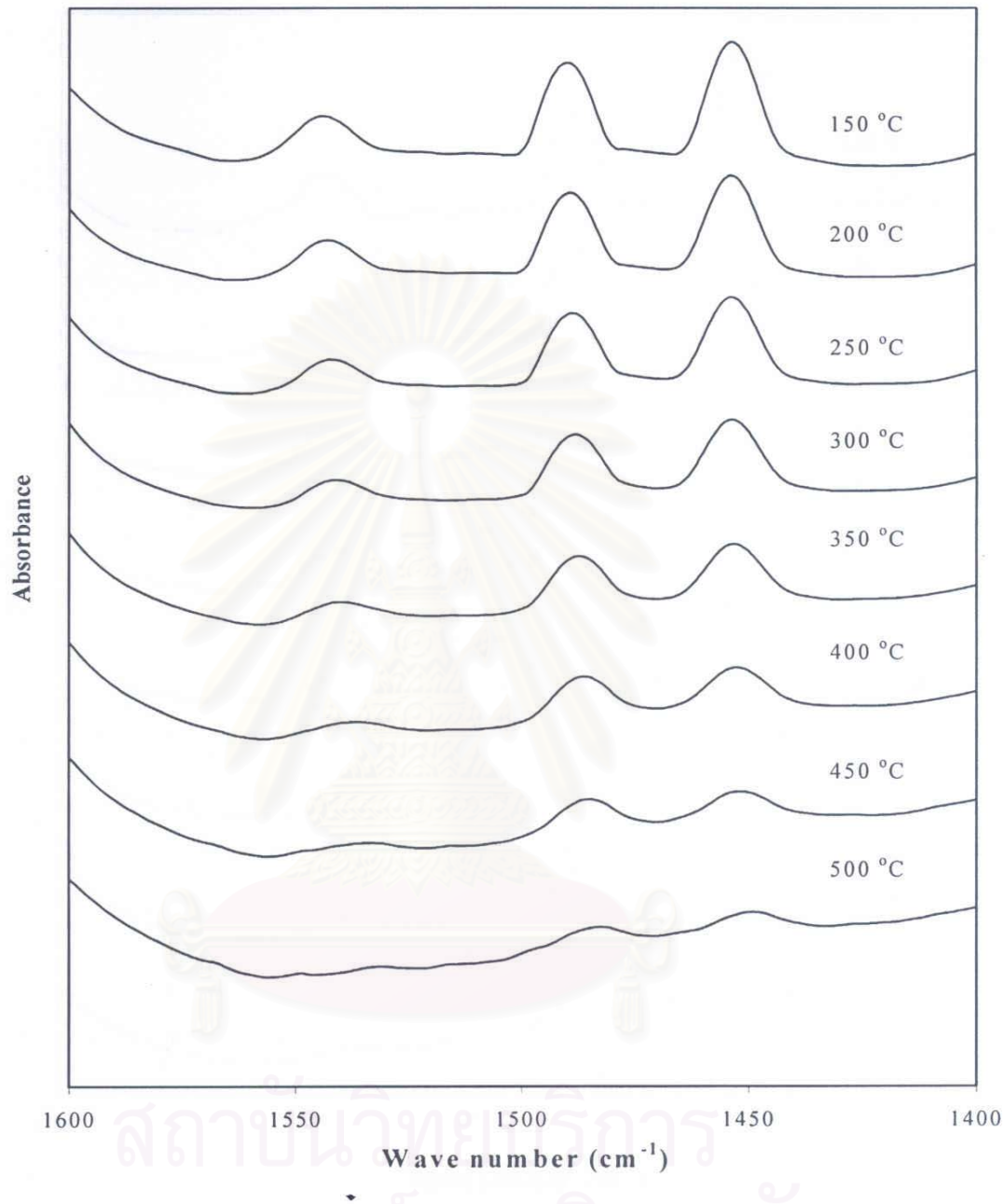

(e) H-Zn.Al-silicate (Si/Zn loading ratio of 150)

Figure 5.3 FTIR spectra of pyridine adsorbed prepared catalyst (continued)

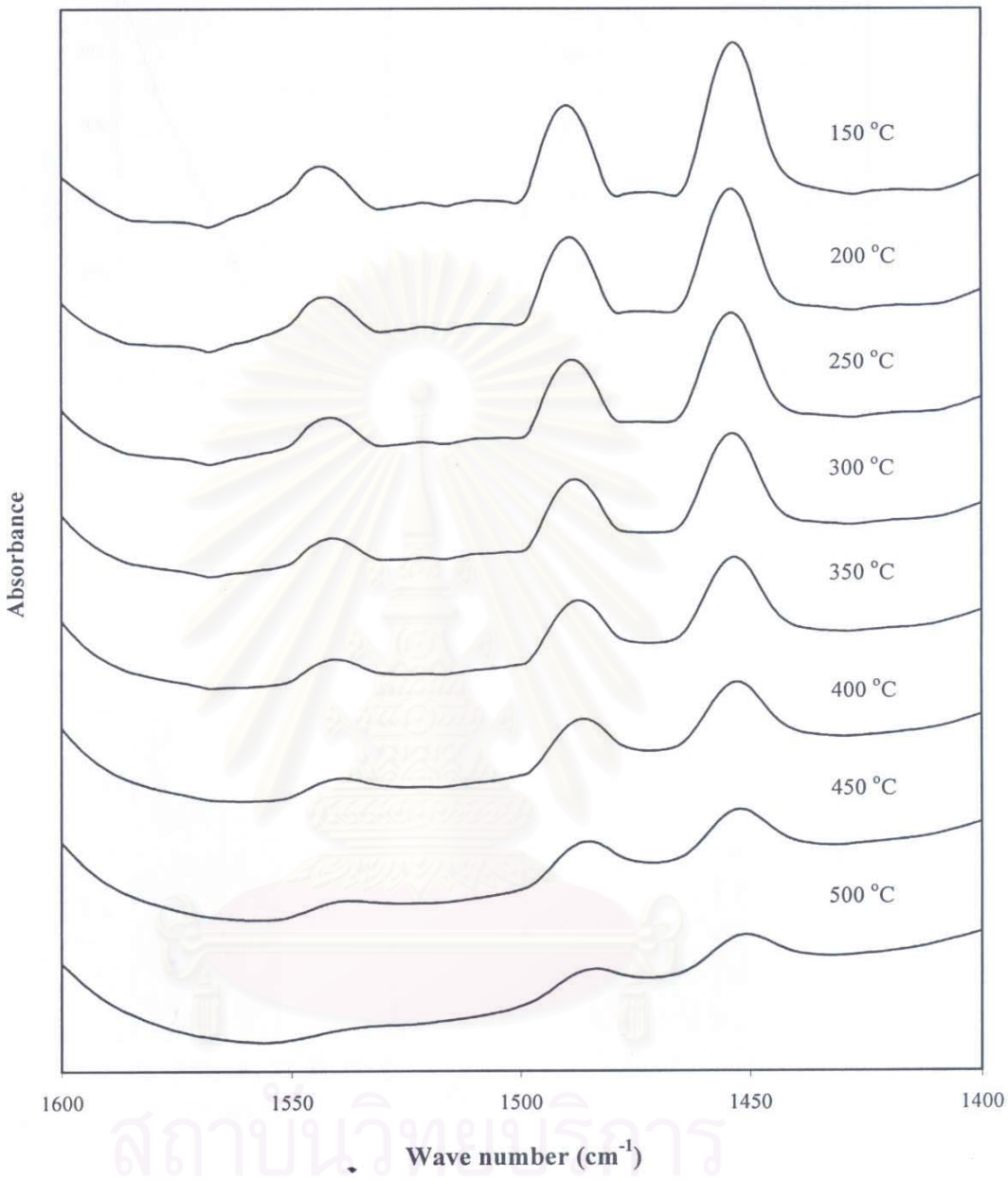

(f) Zn (1.9 wt% loading) / H-ZSM-5

Figure 5.3 FTIR spectra of pyridine adsorbed prepared catalyst (continued)

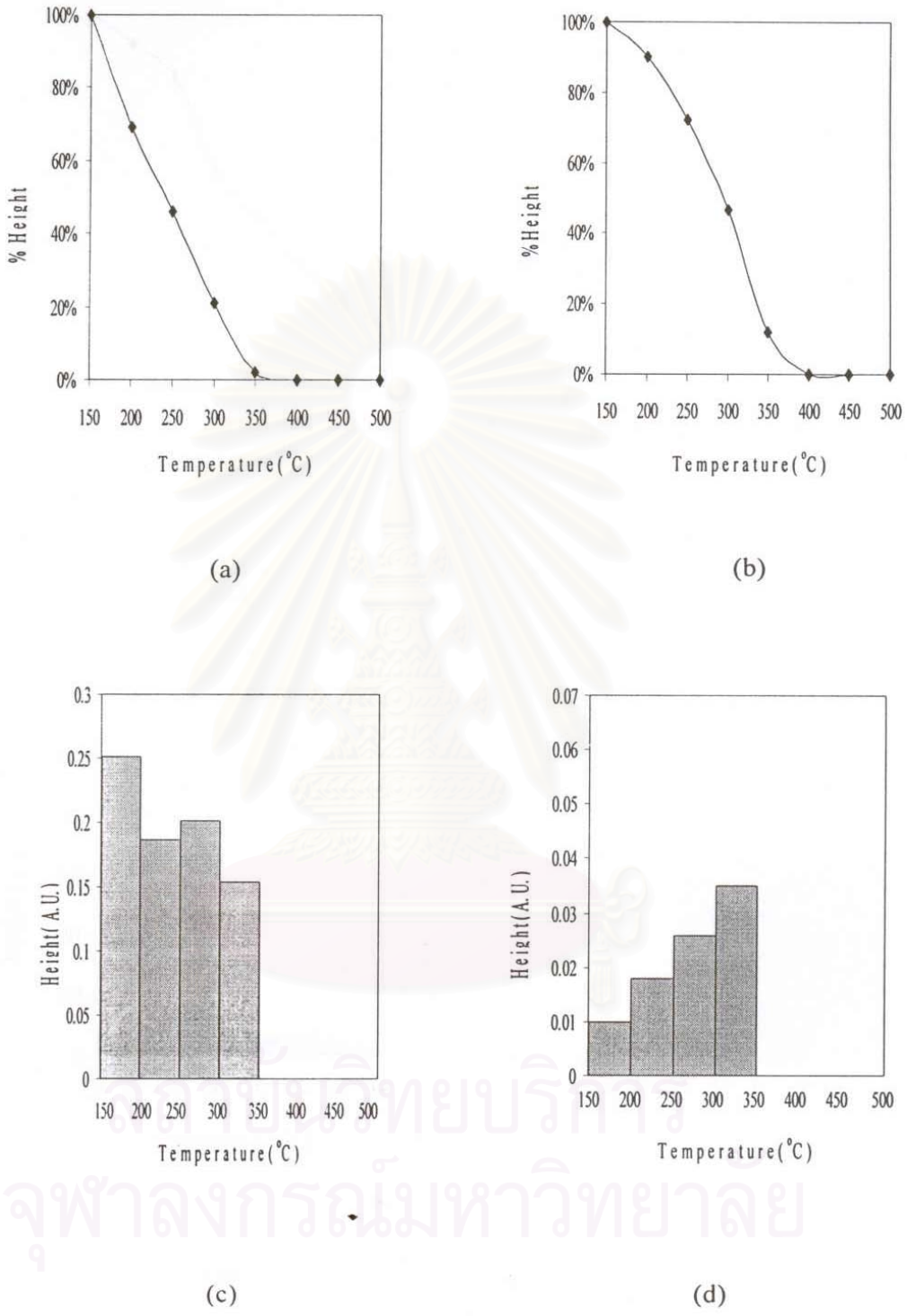

Figure 5.4 The percentage of the band height of pyridine adsorbed on : (a) Lewis and (b) Brønsted acid site. The amount of pyridine desorbed on : (c) Lewis and (d) Brønsted acid site on Na-ZSM-5

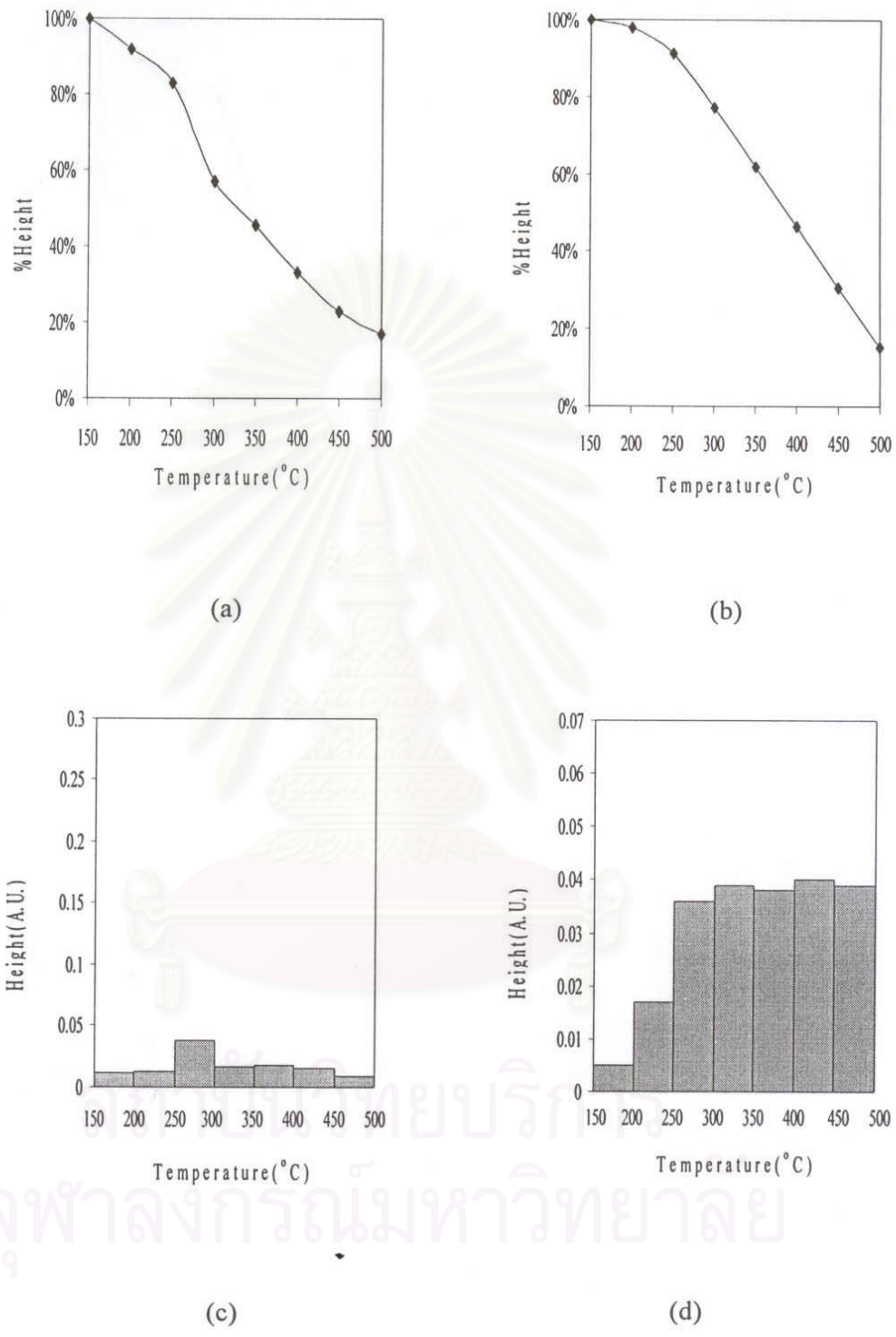

Figure 5.5 The percentage of the band height of pyridine adsorbed on : (a) Lewis and (b) Brønsted acid site. The amount of pyridine desorbed on (c) Lewis and (d) Brønsted acid site on H-ZSM-5

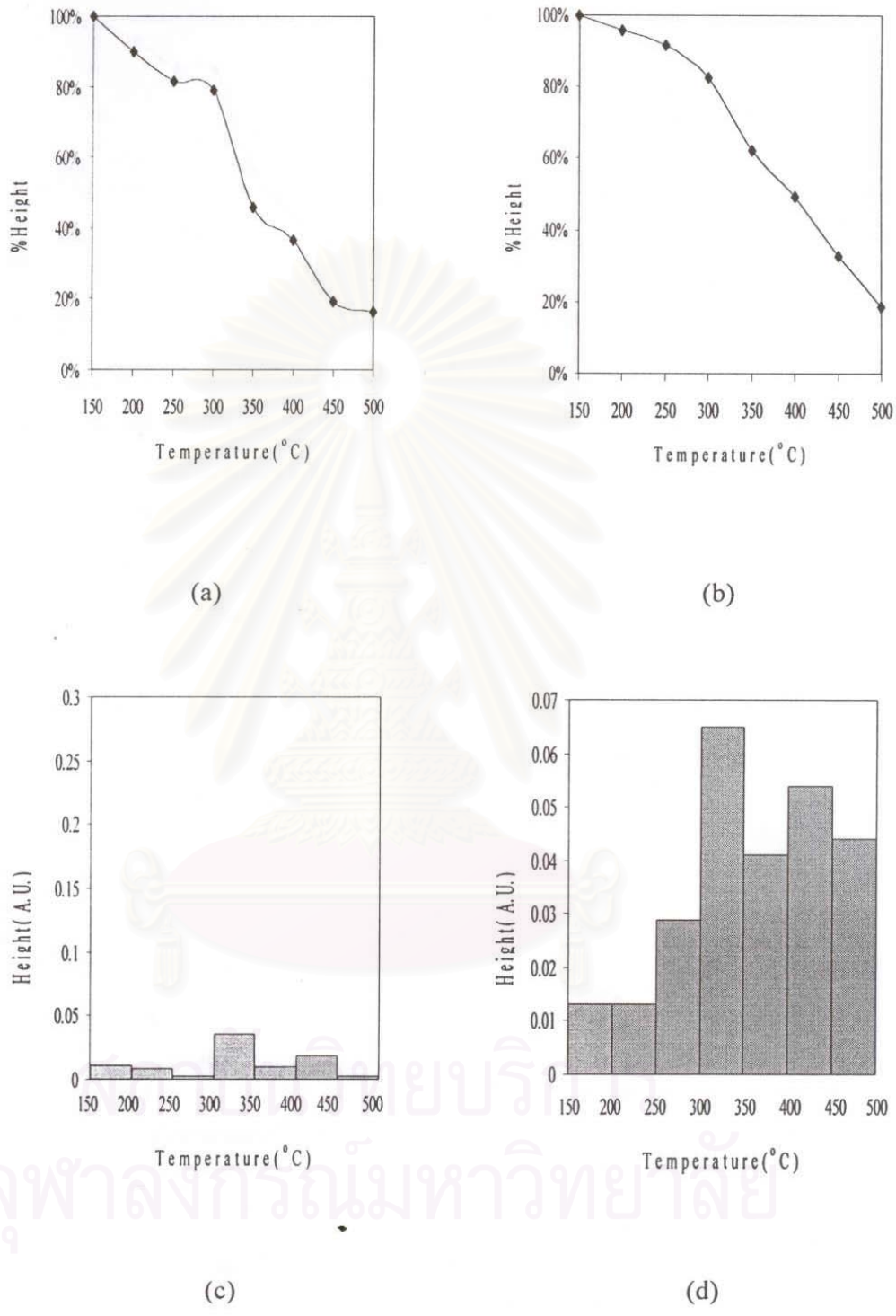

Figure 5.6 The percentage of the band height of pyridine adsorbed on : (a) Lewis and (b) Brønsted acid site. The amount of pyridine desorbed on : (c) Lewis and (d) Brønsted acid site on H-Ga.Al-silicate (Si/Ga loading ratio of 100)

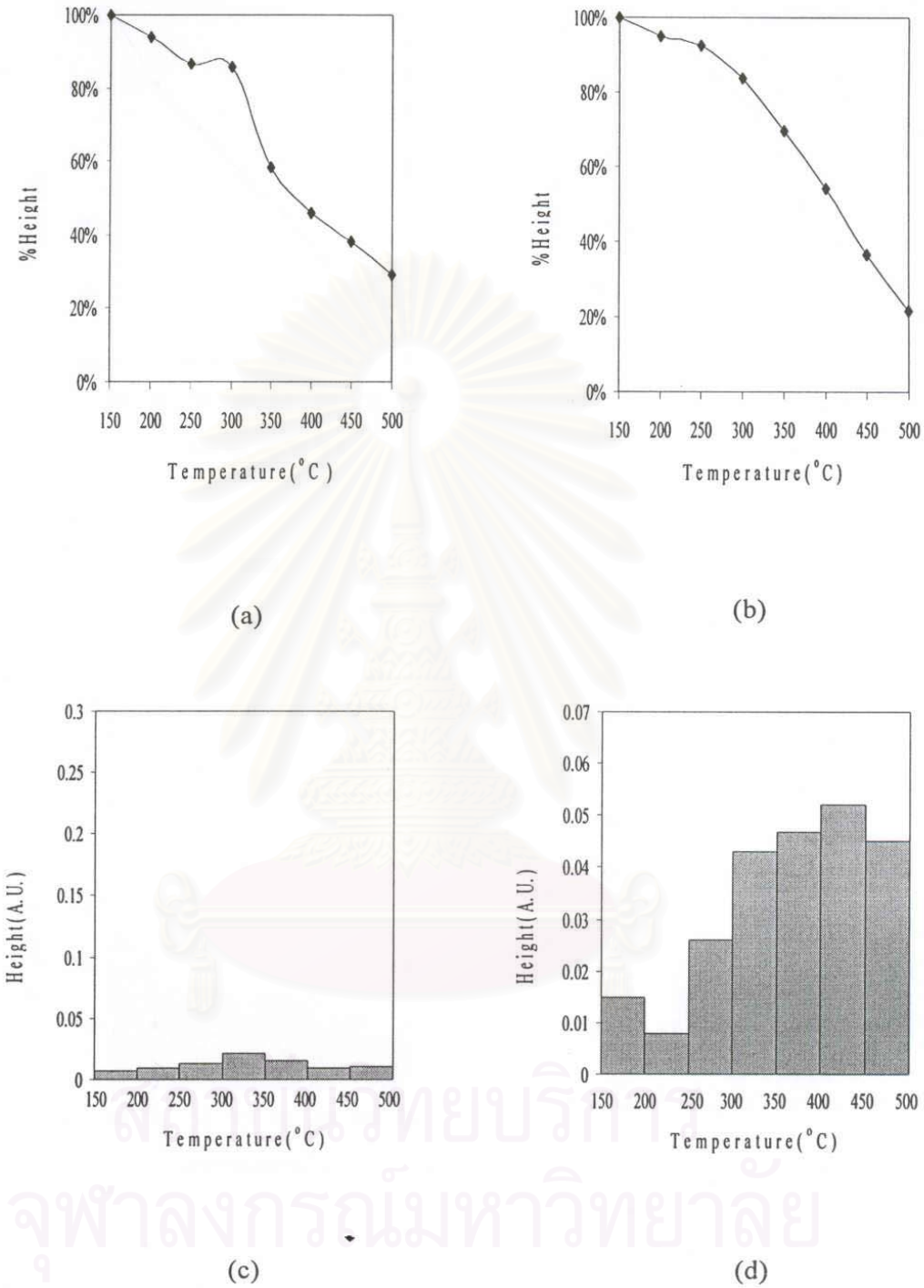

Figure 5.7 The percentage of the band height of pyridine adsorbed on : (a) Lewis and (b) Brønsted acid site. The amount of pyridine desorbed on : (c) Lewis and (d) Brønsted acid site on Ga (2.0 wt% loading) / H-ZSM-5

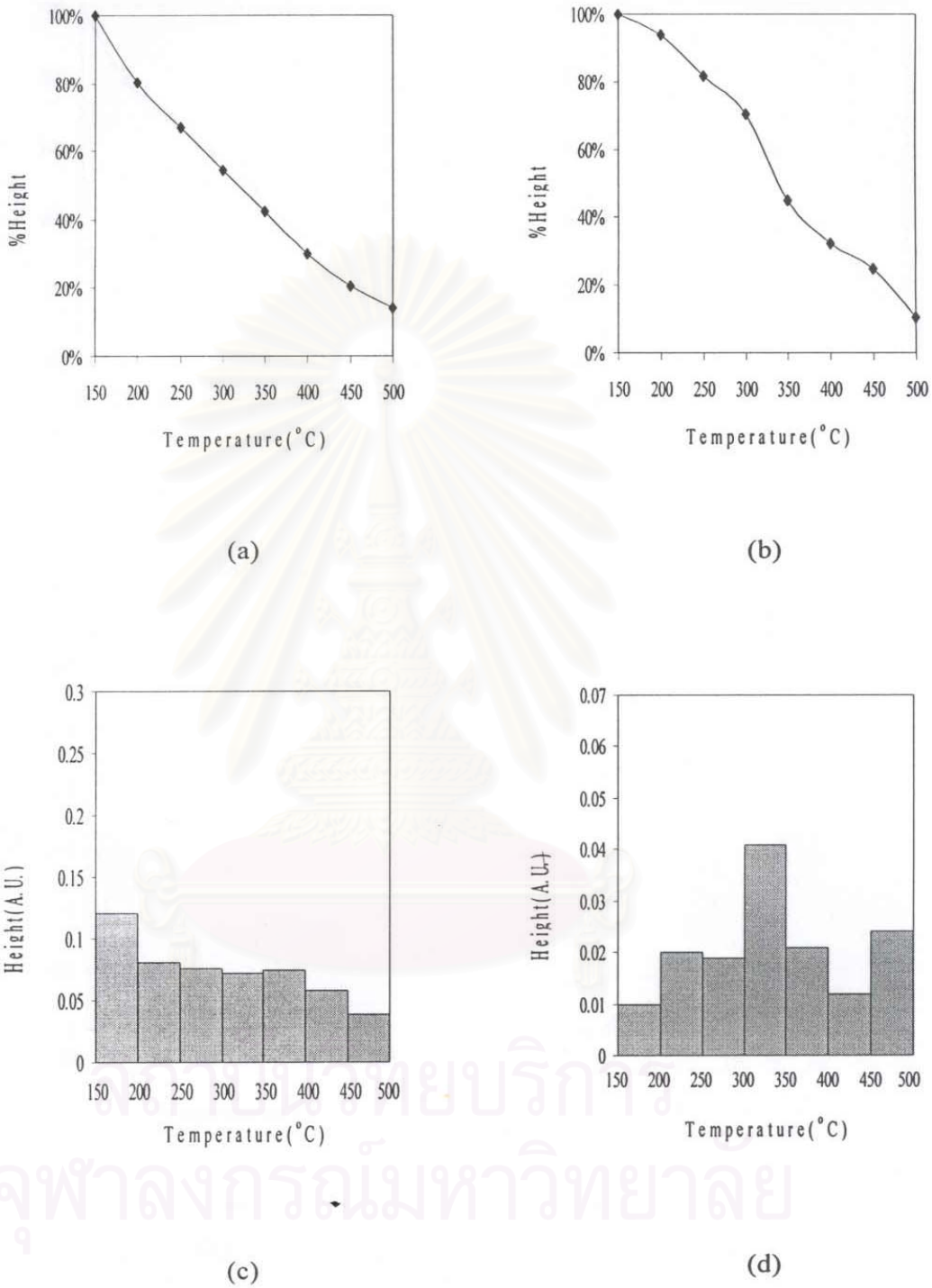

Figure 5.8 The percentage of the band height of pyridine adsorbed on : (a) Lewis and (b) Brønsted acid site. The amount of pyridine desorbed on (c) Lewis and (d) Brønsted acid site on H-Zn.Al-silicate (Si/Zn loading ratio of 150)

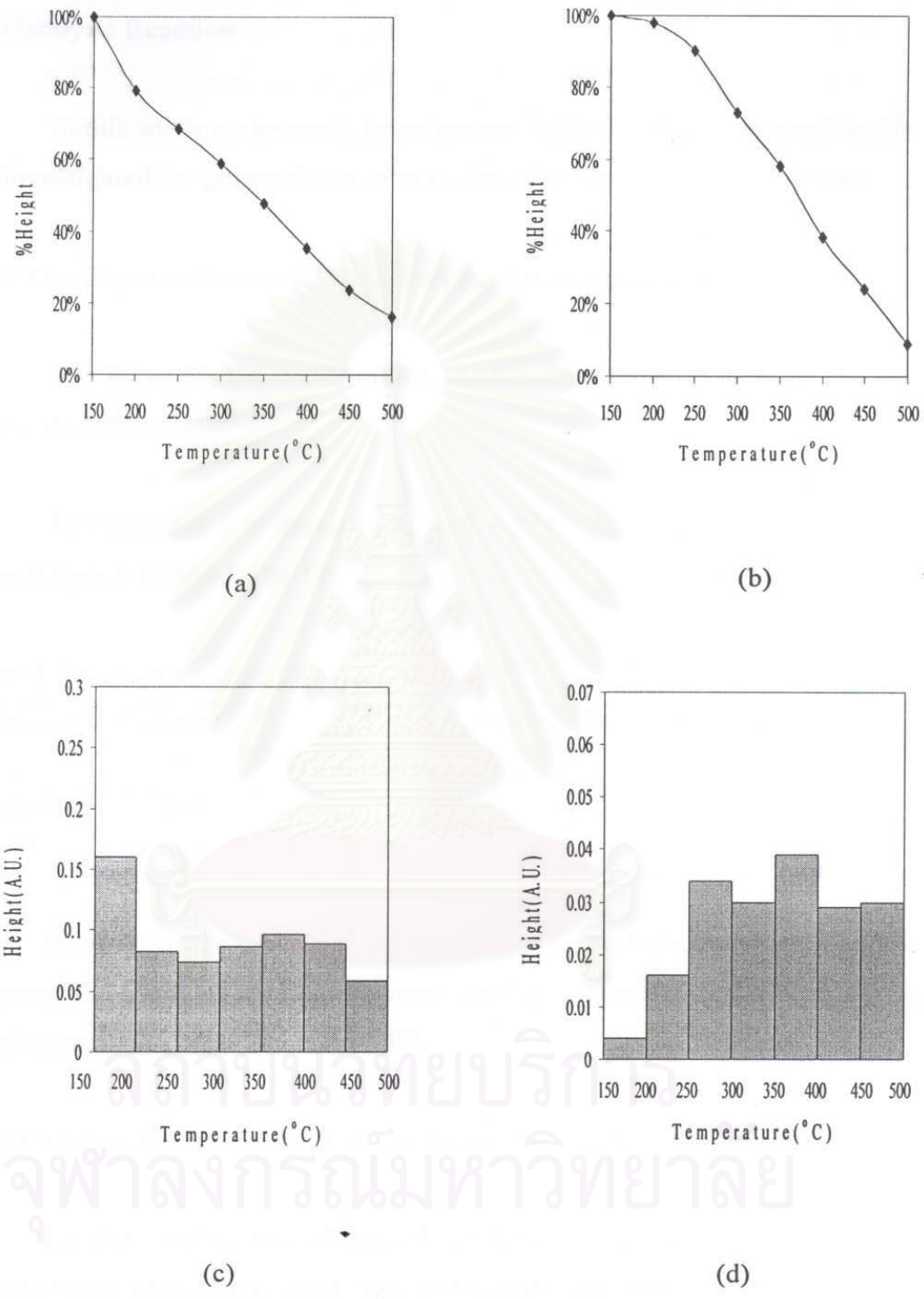

Figure 5.9 The percentage of the band height of pyridine adsorbed on : (a) Lewis and (b) Brønsted acid site. The amount of pyridine desorbed on : (c) Lewis and (d) Brønstedacid site on Zn (1.9 wt% loading) / H-ZSM-5

5.2 Catalytic Reaction

In this section, the catalytic properties of the catalysts prepared in this research are investigated by testing the aromatization of n-heptane (6% n-heptane).

5.2.1 The Effect of Form of Catalyst on the Aromatization of n-heptane

The hydrocarbon distributions produced in different form of the catalysts are shown in Table 5.3.

The reaction was carried out with ZSM-5 having Si/Al atomic ratio of 40 at the reaction temperature of 550 ^{o}C, GHSV of 2000 h^{-1} and 1 hour time on stream.

Table 5.3 n-Heptane aromatization on Na-ZSM-5 and H-ZSM-5.

Catalyst	Conversion (%)	Production Distribution (C- wt %)							
		C1	C2	C2 =	C3	C3 =	C4 +	BTX	A9+
Na-ZSM-5	34.5	2.9	5.4	16.2	7.6	32.7	31.5	3.7	-
H-ZSM-5	100	6.1	9.3	26.4	12.6	17.7	2.5	25.0	0.4

From Table 5.3, H-ZSM-5 showed higher performance than Na-ZSM-5. This suggests that the reaction requires more acidity because H-ZSM-5 has higher amount of strong acid site than Na-ZSM-5 [8].

5.2.2 Catalytic Performance of H-Ga.Al-silicate Catalyst

In this study, the effect of gallium in zeolite framework prepared by incorporation was investigated from Si/Ga ratio 310 to 40. The reaction was carried out at 550 ^{o}C, GHSV of 2000 h^{-1} and 1 hour time on stream.

Table 5.4 n-Heptane aromatization on H-Ga.Al-silicate.

Si/Ga loading ratio	Conversion (%)	Production Distribution (C- wt %)							
		C1	C2	C2 =	C3	C3 =	C4 +	BTX	A9+
40	100	10.7	6.1	6.7	4.5	2.1	0.1	64.8	5.0
100	100	5.6	4.7	6.3	4.0	2.1	0.4	63.4	13.5
155	100	9.6	9.2	27.9	3.5	11.0	2.3	35.6	0.9
310	99.5	6.8	10.4	22.3	11.6	12.1	3.6	32.3	0.9

Table 5.4. shows the catalytic performance on n-heptane aromatization of H-Ga.Al-silicate. The activity and selectivity for aromatic increased with the higher amount of gallium (or decreasing Si/Ga ratio), but H-Ga.Al-silicate with Si/Ga loading ratio of 40 and 100 exhibited the similar selectivity though Si/Ga loading ratio of 40 had much more gallium loading content. Thus, H-Ga.Al-silicate with Si/Ga loading ratio of 100 was selected with economic concern (63.4% of BTX).

The best performance of H-Ga.Al-silicate owing to gallium has been attributed to their ability to dehydrogenate alkanes and enhance the activity for aromatization of the olefin [39].

5.2.3 Catalyst Performance of H-Zn.Al-silicate Catalyst

In this study, H-Zn.Al-silicate was prepared by incorporation of zinc in zeolite framework. The catalytic performances on n-heptane aromatization of H-Zn.Al-silicate with various Si/Zn ratios are shown in Table 5.5. The reaction was carried out under the same conditions at 550 ^{o}C, GHSV of 2000 h^{-1}, TOS of 1 hour. Zinc amount was varied from Si/Zn ratio 270 to 40.

Table 5.5 n-Heptane aromatization on H-Zn.Al-silicate.

Si/Zn loading ratio	Conversion (%)	Production Distribution (C- wt %)							
		C1	C2	C2 =	C3	C3 =	C4 +	BTX	A9+
40	100	12.7	14.0	6.6	4.3	4.8	1.4	54.3	1.9
100	98.6	11.2	12.1	6.7	4.9	4.7	0.4	58.0	2.0
150	100	6.1	5.4	9.5	5.3	7.0	2.1	60.3	4.3
270	99.0	5.2	7.5	18.0	9.2	11.3	3.7	44.9	0.2

When the amount of zinc was increased (or decreasing Si/Zn ratio), the aromatics selectivity increased and H-Zn.Al-silicate with Si/Zn loading ratio of 150 exerted as high as 60.3% of BTX. Further increase of zinc incorporation (Si/Zn loading ratio of 40) did not enhance the catalyst selectivity. This should be due to crowdedness of aromatization process in an interconnected channel area due to high Zn loading, which could cause steric hindrance towards formation of aromatics [40]. Thus Si/Zn loading ratio of 150 was considered to be optimum.

These results suggest that the presence of zinc facilitates the formation of the olefinic fragments (precursors for aromatics) which ultimately improves the aromatics production [34].

5.2.4 Effect of Metal Introduction by Incorporation and Ion-exchange Method

The n-heptane aromatization on catalyst modified with metal incorporation and/or ion-exchange was conducted at 550 ^{o}C, GHSV of 2000 h^{-1} and 1 hour time on stream.

H-Ga.Al-silicate with Si/Ga loading ratio of 100, which was equivalent to approximately 2.0 wt% gallium and Ga/H-ZSM-5 with Ga-loading content of 2.9 wt% are shown in Table 5.6. It has been found that H-Ga.Al-Silicate gave similar selectivity to Ga/H-ZSM-5.

Table 5.6 n-Heptane aromatization on H-Ga.Al-silicate (Si/Ga loading ratio of 100) and Ga (2.03 wt% loading) / H-ZSM-5.

Catalyst	Conversion (%)	Production Distribution (C- wt %)							
		C1	C2	C2 =	C3	C3 =	C4 +	BTX	A9+
H-Ga.Al-silicate	100	5.6	4.7	6.3	4.0	2.1	0.4	63.4	13.5
Ga/H-ZSM-5	100	8.9	9.5	6.2	3.1	1.6	-	61.1	9.6

For zinc modification, H-Zn.Al-silicate with Si/Zn loading ratio of 150 which was equivalent to approximately 1.9 wt% zinc and 2.0 wt% Zn-exchange H-ZSM-5 were compared. The result is shown in Table 5.7. H-Zn.Al-silicate exhibited similar selectivity to Zn/H-ZSM-5.

Table 5.7 n-Heptane aromatization on H-Zn.Al-silicate (Si/Zn loading ratio of 150) and Zn (1.88 wt% loading) / H-ZSM-5.

Catalyst	Conversion (%)	Production Distribution (C- wt %)							
		C1	C2	C2 =	C3	C3 =	C4 +	BTX	A9+
H-Zn.Al-silicate	100	6.1	5.4	9.5	5.3	7.0	2.1	60.3	4.3
Zn/H-ZSM-5	100	11.7	12.6	4.8	3.1	2.8	0.5	59.5	5.0

The above results show that catalysts prepared using the two modified methods behave almost similar activity, selectivity and product distribution (Tables 5.6 and 5.7), however, it is clear that the incorporation method is advantageous to the ion-exchange method in reducing the catalyst preparation procedures (one-step crystallization), saving time and energy.

5.2.5 Factors Affecting The catalyst Activity and Selectivity for Aromatics

The catalyst performances on n-heptane aromatization were extensively investigated by using the unmodified catalyst and the suitably modified one that are shown in Table 5.8. The reaction was carried out at 550 ^{o}C, GHSV of 2000 h^{-1}, and 1 hour time on stream.

Table 5.8 Performance in different catalysts for n-heptane aromatization.

Catalyst	Conversion (%)	Production Distribution (C- wt %)							
		C1	C2	C2 =	C3	C3 =	C4 +	BTX	A9+
Na-ZSM-5	34.5	2.9	5.5	16.2	7.6	32.7	31.5	3.7	-
H-ZSM-5	100	6.1	9.3	26.4	12.6	17.7	2.5	25.0	0.4
H-Ga.Al-silicate	100	5.6	4.7	6.3	4.0	2.1	0.4	63.4	13.5
Ga/H-ZSM-5	100	8.9	9.5	6.2	3.1	1.6	-	61.1	9.6
H-Zn.Al-silicate	100	6.1	5.4	9.5	5.3	7.0	2.1	60.3	4.3
Zn/H-ZSM-5	100	11.7	12.6	4.8	3.1	2.8	0.5	59.5	5.0

As shown in table 5.8, for the Na-ZSM-5 and H-ZSM-5 catalysts, the activity and aromatic selectivity of H-ZSM-5 are higher than Na-ZSM-5. From figures 5.4, 5.5, (in section 5.1.5), it was found that Na-ZSM-5 had large amount of total acidity which are almost lewis acid site whereas H-ZSM-5 had less amount of total acidity but are almost brønsted acid site. This results that brønsted acid site enhance activity and selectivity for aromatic far better than lewis acid site.

In case of gallium modification, from figures 5.5 to 5.7, it was found that the acidity of H-Ga.Al-silicate was comparable to H-ZSM-5 but exhibited higher aromatic selectivity than H-ZSM-5. This should be due to the metal effect. Other investigations [41-43], found that the enhanced aromatic yields obtained over these catalysts was attributed to the participation of the metal in the paraffin and naphthene dehydrogenation step.

As for zinc modification, it was found that the acidity of zinc loading catalyst (figures 5.8, 5.9) was approximately comparable to Na-ZSM-5 (figure 5.4) but exhibited higher activity and aromatic selectivity than Na-ZSM-5. The presence of metal in catalyst, should be responsible for the increase in aromatic yield that is similar to the case of gallium modification.

The above results show that a better performance in the n-heptane aromatization should be due to the participation between the brønsted acid site and metal species in the zeolite channel.

5.2.6 Effect of Reaction Temperature on Product Distribution of n-heptane Aromatization

The reaction temperature for n-heptane conversion was varied ranging from 500 to 600 ^{o}C. The reaction was carried out at GSHV of 2000 h^{-1}, by using feed gas of n-heptane for 1 hour time on stream.

The product distribution of n-heptane aromatization over the H-Ga.Al-silicate (Si/Ga loading ratio of 100) and the H-Zn.Al-Silicate (Si/Zn loading ratio of 150) at various reaction temperatures are shown in Table 5.9. and 5.10, respectively.

Table 5.9 n-Heptane aromatization on H-Ga.Al-silicate catalyst (Si/Ga loading ratio of 100) at various reaction temperature.

Temperature	Conversion	Production Distribution (C- wt %)							
(^{o}C)	(%)	C1	C2	C2 =	C3	C3 =	C4 +	BTX	A9+
500	100	7.4	6.9	7.1	16.2	3.7	3.5	52.9	2.2
550	100	5.6	4.7	6.3	4.0	2.1	0.4	63.4	13.5
600	100	11.7	8.1	8.5	0.7	1.4	0.8	59.1	9.7

Table 5.10 n-Heptane aromatization on H-Zn.Al-silicate catalyst (Si/Zn loading ratio of 150) at various reaction temperature.

Temperature	Conversion	Production Distribution (C- wt %)							
(^{o}C)	(%)	C1	C2	C2 =	C3	C3 =	C4 +	BTX	A9+
500	100	4.8	5.5	11.0	10.1	11.9	8.4	47.9	0.4
550	100	6.1	5.4	9.5	5.3	7.0	2.1	60.3	4.3
600	100	12.6	8.0	12.5	2.0	4.7	1.4	54.8	4.0

For both catalysts, n-heptane conversion did not change with the increasing temperatures. The selectivity of aromatic increased with increasing temperature and passed through a maximum at the temperature of 550 ^{o}C. While the temperature increased, the olefin selectivity decreased and passed through a minimum at the temperature of 550 ^{o}C. This indicates olefin can not aromatize well under the low

temperature. It was understood that the reaction temperature range of 550-600 ^{o}C was required to achieve considerably high aromatization of n-heptane.

5.2.7 Effect of GHSV on Product Distribution of n-heptane Aromatization

Table 5.11 and 5.12 show that the product distribution of n-heptane aromatization over the H-Ga.Al-silicate (Si/Ga loading ratio of 100) and the H-Zn.Al-Silicate (Si/Zn loading ratio of 150), respectively. The space velocities for n-heptane conversion werevaried ranging from 2000 to 6000 h^{-1}. The reaction was carried out at temperature of 550 ^{o}C for 1 hour time on stream.

Table 5.11 n-Heptane aromatization on H-Ga.Al-silicate catalyst (Si/Ga loading ratio of 100) at various GHSV.

GHSV (h^{-1})	Conversion (%)	Production Distribution (C- wt %)							
		C1	C2	C2 =	C3	C3 =	C4 +	BTX	A9+
2000	100	5.6	4.7	6.3	4.0	2.1	0.4	63.4	13.5
4000	100	7.0	6.4	13.3	11.7	6.4	1.6	52.2	1.4
6000	100	6.1	5.3	14.1	11.2	8.3	3.2	50.2	1.6

Table 5.12 n-Heptane aromatization on H-Zn.Al-silicate catalyst (Si/Zn loading ratio of 150) at various GHSV.

GHSV (h^{-1})	Conversion (%)	Production Distribution (C- wt %)							
		C1	C2	C2 =	C3	C3 =	C4 +	BTX	A9+
2000	100	6.1	5.4	9.5	5.3	7.0	2.1	60.3	4.3
4000	100	5.9	5.8	12.2	7.1	9.8	4.3	53.9	1.0
6000	100	4.8	5.0	12.8	7.0	13.3	6.9	49.8	0.4

For both catalysts, the light olefin fraction such as ethylene and propylene gradually increased with the increasing GHSV and thus aromatic selectivity decreased. This should be ascribed to the fact that at high GHSV, the contact time between heptane and catalyst was shortened [40].

5.2.8 Effect of Time on Stream on Product distribution of the Optimum Catalyst

The stabilities of the H-Ga.Al-silicate (Si/Ga = 100, Si/Al = 40) and the H-Zn.Al-silicate (Si/Zn = 150, Si/Al = 40) on n-heptane aromatization carried out at 550 ^{o}C, GHSV 2000 h^{-1}, for 1-19 hours are shown in Table 5.13 and 5.14, respectively.

Table 5.13 n-Heptane aromatization on H-Ga.Al-silicate catalyst (Si/Ga loading ratio of 100) at various time on stream.

TOS	Conversion	Production Distribution (C- wt %)							
(h)	(%)	C1	C2	C2 =	C3	C3 =	C4 +	BTX	A9+
1	100	9.3	7.0	7.3	4.8	2.2	0.9	62.5	6.0
3	100	10.3	8.4	8.9	5.8	2.7	0.1	59.4	4.4
5	100	8.6	7.6	10.0	6.8	3.5	0.9	56.9	5.7
7	100	8.7	8.4	10.7	9.1	4.4	1.1	54.4	3.2
9	100	8.5	8.4	12.6	10.0	5.8	1.7	50.3	2.7
11	100	8.4	8.4	13.7	10.2	6.7	1.7	48.8	2.1
13	100	6.5	7.6	14.9	12.1	9.3	3.0	45.2	1.4
15	100	6.3	6.7	16.1	10.2	11.2	4.3	43.1	2.1
17	100	6.3	7.4	15.6	11.9	10.7	3.6	41.6	2.9
19	100	6.9	7.0	18.4	9.7	12.8	4.8	38.7	1.7
regeneration	100	11.7	7.3	6.4	2.6	1.6	-	62.2	8.2

Table 5.13 shows the prolonged operation of the H-Ga.Al-silicate (Si/Ga =100, Si/Al = 40). The n-heptane conversion did not decrease with time. The selectivity for aromatic hydrocarbons decreased and the selectivity for olefin, the reaction intermediates to aromatic hydrocarbons, increased with time. It indicates that the strong acid sites, which are responsible for aromatization of light olefins, are selectively decreased by being covered with the deposited coke [12].

After 19 hours, H-Ga.Al-silicate was regenerated by burning the deposited coke with air at 550 ^{o}C for 2 hours, in Table 5.13, the same activity and selectivity of regenerated H-Ga.Al-silicate as those of the fresh one was obtained. This result

suggested the good stability of this catalyst and the activity and selectivity for the aromatic of n-heptane were higher than H-Zn.Al-silicate (Table 5.14).

Table 5.14 n-Heptane aromatization on H-Zn.Al-silicate catalyst (Si/Zn loading ratio of 150) at various time on stream.

TOS	Conversion	Production Distribution (C- wt %)							
(h)	(%)	C1	C2	C2 =	C3	C3 =	C4 +	BTX	A9+
1	100	7.4	7.1	10.1	6.9	6.8	2.8	57.3	1.6
3	100	6.8	7.2	12.0	8.1	9.3	3.5	52.2	0.9
5	100	6.6	7.0	12.1	7.9	9.6	3.6	51.8	1.4
7	100	6.7	6.9	12.8	8.0	11.6	4.2	48.5	1.3
9	99.8	6.6	6.6	14.0	7.7	12.2	5.5	46.3	1.1
11	99.5	6.6	6.2	14.2	7.0	12.6	5.5	46.4	1.5
13	99.6	7.3	6.3	15.4	6.3	13.1	5.4	44.8	1.4
15	99.6	7.5	6.5	16.8	6.4	14.8	6.3	41.2	0.5
17	99.2	7.6	6.5	17.9	6.4	16.4	7.2	37.7	0.3
19	99.0	6.7	5.8	17.1	5.9	17.0	8.0	38.7	0.8
regeneration	99.9	8.3	7.7	13.5	6.3	7.4	2.0	53.5	1.3

For H-Zn.Al-silicate, the catalyst deactivation occurred rapidly comparing with that of H-Ga.Al-silicate. In the section 5.2.3 when the amount of zinc loading increased ethylene hydrogenation to ethane increased too. This result indicates that hydrogen on the catalyst surface was consumed for ethylene hydrogenation, before being used for the combustion of deposited coke. The disadvantageous role of zinc on accelerating the coke formation caused the shorter catalyst life of H-Zn.Al-silicate than H-Ga.Al-silicate. This is consistent with the discussion of Kanai and Kawata [44,17] suggesting that gallium species in galloaluminosilicate has a lower hydrogenation or hydrogenolysis activity than zinc species in ZnO/H-ZSM-5. The yield of aromatic markedly decreased and the yield of ethylene and propylene increased indicating that the strong acid sites, which are responsible for aromatization of light olefins, are selectively decreased by being covered with the deposited coke.

Because of the catalyst deactivation, regeneration of decayed catalyst is necessary for the prolonged operation. As shown in Table 5.14, the activity of the

regenerated H-Zn.Al-silicate changed slightly when compared with fresh H-Zn.Al-silicate. It is suggested that H-Zn.Al-silicate shows good stability.

CHAPTER VI
CONCLUSIONS AND RECOMMENDATIONS

6.1 CONCLUSIONS

This thesis dealt with studies on catalytic conversion of n-heptane to aromatic hydrocarbons using metal-containing MFI-type zeolite catalysts. The following conclusions of this study were drawn:

1. Metalloaluminosilicate such as Ga.Al-silicate, Zn.Al-silicate and metal (Ga, Zn) ion-exchanged ZSM-5 gave the same XRD patterns of MFI structure. This indicates that both methods of metal introduction to ZSM-5 render the same crystalline structure, the pentasil pore opening structure, as ZSM-5.

2. Ga modification contributed to the increase in Brønsted acid site and zinc modification did for Lewis acid site.

3. The presence of metal in ZSM-5 contributed significantly for higher activity and selectivity for n-heptane conversion to aromatic than ZSM-5 without metal addition.

4. The aromatic formation required brønsted acid sites and metal sites.

5. H-Ga.Al-silicate catalyst with Si/Ga loading ratio of 100 exhibited the highest activity and selectivity for n-heptane aromatization.

6. H-Zn.Al-silicate catalyst with Si/Zn loading ratio of 150 was the optimum composition of zinc containing MFI-type zeolite catalyst for n-heptane aromatization.

7. The introduction of metal by incorporation exerted the same selectivity as metal ion-exchange and can be prepared in only one-step crystallization.

8. The metalloaluminosilicate had a good stability especially H-Ga.Al-silicate.

9. The optimum reaction condition for n-heptane aromatization at atmospheric pressure was: temperature 550 ^{o}C, GHSV of 2000 h^{-1} and TOS of 1 hr.

6.2 RECOMMENDATIONS

From this research, the recommendation for future study are as follows:

1. Study in more details on state of Ga or Zn species in ZSM-5.
2. Develop the stability of H-Zn.Al-silicate to be able to compete with H-Ga.Al-silicate.
3. Study the performance of these catalysts for aromatic production from other ranges of hydrocarbon feed such as n-hexane and n-octane.

REFERENCES

1. L. F. Hatch, S. Mater, Hydrocarbon Process. 58 (1) (1979): 189.
2. H. A. Wittcoff, The Chemical Industry: Technology and Concepts, Chem. System Inc., Union Chem. Lab, Ind. Tech. Res. Inst., Hsin Chu, Taiwan, 12-13 March, 1992.
3. D. Greenaway, Pep Report 182, Stanford Res Inst., Menlopark, CA, 1987.
4. R.J. Arganger and G.R. Londolt, US Patent 3702866, 1972.
5. Anunziata, O. A. and Pierella, L. B., Catal. Lett., 16 (1992): 437.
6. V. R. Choudhary, A. K. Kinage and T. V. Choudhary, Appl. Catal. A, 162 (1997): 239-248.
7. M. Guisnet and N. S. Gnep, Appl. Catal. A, 89 (1992): 1-30.
8. Vasant R. Choudhary, Kshudiram Mantri and Chinta Sivadinarayana, Microporous and Mesoporous Mater., 37 (2000)
9. Zaihui Fu, Dulin Yin, Yashu Yaing, Xiexian Guo, Appl. Catal. A, 124 (1995): 59-71.
10. S. Hpiro, E. S., Shevchenko, D. P., Dmitriev, R.V., Tkachenko, O. R., and Minachev, Kh. M., Appl. Catal. A, 107 (1994): 165.
11. N. Kumar, R. Byggningsbacka and L.-E. Lindfors, React. Kinet. Catal. Lett. 61 (2) (1997): 297-305.
12. N. Kumar and L.-E. Lindfors, Catal Lett., 38 (1996): 239-244.
13. Fukase, S., Kumagai, H., and Suzuka, T., Appl. Catal. A, 93 (1992): 35.
14. A. Sripusippo, Aromatization of liquefied petrolium gas over metal containing MFI-type zeolite catalysts, A Thesis Submitted in Partial Fulfillment of the Requirements for the Degree of Master of Engineering, Department of Chemical Engineering, Chulalongkorn University, 1996
15. Hu zeshan, Shi Yonggang, Luang Chuanghui, Chen Songyang, Dong Jingxiu, Lu Xeuding and Peng Shaoyi, Microporous and Mesoporous Mater., 25 (1998): 201-206.
16. D. Bhattacharya and S. Sivasanker, Appl. Catal. A., 141 (1996): 105-115.
17. Kanai, J. and Kawata, N., Appl. Catal. A, 55 (1989): 115-122.

18. H. D. Lanh, V.A. Tuan, H. Kosslick, B. Parlitz, R. Fricke and J. Volter, Appl. Catal. A, 103 (1993): 205-222.

19. Lee, M.-D. and Chang, C.-S., Appl. Catal. A, 123 (1995): 7-21.

20. Chau-Shang Chang and Min-Dar Lee, React. Kinet. Catal. Lett. (1) (1995): 115-120.

21. A. R. Pradhan, N. Viswanadham, S. Suresh, O. P. gupta, N.Ray, G. Muralidhar Uma Shanker and T. S. R. Prasada Rao, Catal. Lett., 28 (1994): 231-239.

22. Kanai, J. and Kawata, N., Appl. Catal. A, 62 (1990): 141.

23. N. Viswanadham, A.R. Pradhan, N. Ray, S. C. Visknoi, Uma Shanker and T. S. R. Prasada Rado, Appl. Catal. A, 137 (1996): 225-233.

24. Halgeri, A. B. and Don, Appl. Catal. A, 181 (1999): 347-354.

25. Bekkum, H. V., flanigen, E. M. and Jansen, J. C., Stud. Surf. Sci. Catal.(1991): 578

26. Szoztak, R., Molecular Sieve Principles of Synthesis and Identification. pp.1-50, New York: Van Nostrand Reingold, 1989.

27. Tamake, K., Misona, M., Ona, Y. and Hattori, H.,"New Solid Acids and Base" (Delmon, B. and Yates, J. T. et al.), Stud. Surf. Sci. Catal., p. 51, Tokyo: Elesvier, 1989.

28. Barthoment, D. " Acidic catalysts with Zeolites", Zeolites Science and Technology (Rebeira, F. R. et al.), Matinus Nijhoff Publishers, The Hemge, 1984.

29. Meier, W. M. and Olson, D. H., Atlan of Zeolite Structure Types, 3rd revised ed., Int. Zeolite Assoc. Biston: Butter worth-Hoinemann, 1992.

30. Chen, N. Y., Garwood, W.E. and Dwyer, F. G., Shape Selectivity Catalysis in Industrial Application, 2nd ed. New York: Marcal Dekker, 1996.

31. Tsai, t., Liv, S. and Wang, I., Appl. Catal. A, 181 (1991): 355-398.

32. Ashton. A. G., Batamanian, S. and Dwyer, J., "Acid in Zeolite" (Lmelik, B. et al.) Catalysis by Acid-Bases, Amsterdam: Elesvier, 1985.

33. Sano, T.; Fujisawa, K. and Higiwara, H. " High Stream Stability of H-ZSM-5 Type Zeolite Containing Alkaline Earth Metals" Catalyst Deactivation, (Delmon, B. and Froment, G. F. eds), Stu. Surf. Sci. Catal., p. 34, Amsterdam: Elsevier, 1987.

34. N. Viswanadham, A.R. Pradhan, N. Ray, S.C. Vishnoi, Uma Shanker, T.S.R. Prasada Rao, Appl. Catal. A, 137 (1996): 225-233.

35. Inui, T. Yamase, O., Fukada, K., Itoh, A. Tarmuto, J. Morina, N., Hagiwara, T., and Takegami, Y., Proceedings 8 th International Congress on Catalysis, Berlin, 1984. Vol.3, Dechema Frankfult-am-Main, 1984.

36. Meier, Olson and Baerlocher, Atlas of Zeolite structure Type (1996): 525.

37. J.Connerton, R. Joyner, and M. Padley, J. Chem. Soc. Faraday Trans., 91 (1995): 1841-1844.

38. M. Campbell, M. Bibby, M. Coddington, F. Howe, and H. Meinhold, J. Catal. A, 161 (1996): 349-358

39. Ikusei Nakamura and Kaoru Fujimoto, Catal. Today, 31 (1996): 335-344.

40. S. Phatanasri, P. Praserthdam and A. Sripusitto, Korean J. Chem. Eng., 17 (4) (2000): 409-413.

41. M.Guisnet, N.S. Gnep and F. Alario, Appl. Catal. A, 89 (1992): 1.

42. S. Fukase, H. Kumagai and T. Suzuka, Appl. Catal. A, 93 (1992): 35.

43. G. Giannetto, A. Montes, N.S. Gnep, A. Florentino, P. Cartraud and M. Guisnet, J. Catal., 145 (1993): 86.

44. Kanai, J. and Kawata, N., J. Catal, 55 (1989): 115-122.

APPENDICES

APPENDIX A
SAMPLE OF CALCULATIONS

A-1 Calculation of Si/Metal Atomic Ratio for Metallosilicates Preparation

The calculation is based on weight of Sodium Silicate ($Na_2O.SiO_2.H_2O$) in G2 and S2 solutions.

Molecular Weight of Si = 28.0855

Molecular Weight of SiO_2 = 60.0843

Molecular percent of SiO_2 in Sodium Silicate = 28.5

Using Sodium Silicate 69 g with 45 g of water as a G_2 and S_2 solution.

$$\text{mole of Si used} = \text{wt.} \times \frac{(\%)}{100} \times \frac{(\text{M.W. of Si})}{(\text{M.W. of } SiO_2)} \times \frac{(1 \text{ mole})}{(\text{M.W. of Si})}$$

$$= 69 \times (28.5/100) \times (1/60.0843)$$

$$= 0.3273 \text{ mole}$$

ZSM-5 Catalyst

For example, to prepare ZSM-5 at Si/Al atomic ratio of 40 by using $AlCl_3$ for aluminum source.

Molecular Weight of Al = 26.9815

Molecular Weight of $AlCl_3$ = 133.3405

Si/Al atomic ratio of 40

Mole of $AlCl_3$ required = $0.3273/40 = 8.1825 \times 10^{-3}$ mole

Mole of $AlCl_3$ = $8.1825 \times 10^{-3} \times 133.3405$

= 1.0911 g

Ga.Al-silicate Catalyst

For example, to prepare Ga.Al-Silicate with Si/Ga atomic ratio of 40 by using $Ga_2(SO_4)_3$ for aluminum source.

Molecular Weight of Ga = 69.723

Molecular Weight of $Ga_2(SO_4)_3$ = 427.63

Si/Ga atomic ratio of 40

Mole of $Ga_2(SO_4)_3$ required = $0.3273/40 = 8.1825 \times 10^{-3}$ mole

Mole of $Ga_2(SO_4)_3$ = $(8.1825 \times 10^{-3} \times 427.63) / 2$

= 1.7495 g

Zn.Al-silicate Catalyst

For example, to prepare Zn.Al-Silicate with Si/Zn atomic ratio of 40 by using $ZnSO_4.7H_2O$ for aluminum source.

Molecular Weight of Zn = 65.39

Molecular Weight of $ZnSO_4.7H_2O$ = 287.54

Si/Zn atomic ratio of 40

Mole of $ZnSO_4.7H_2O$ required = $0.3273/40 = 8.1825 \times 10^{-3}$ mole

Mole of $ZnSO_4.7H_2O$ = $8.1825 \times 10^{-3} \times 287.54$

= 2.353 g

This is the amount of $AlCl_3$, $Ga_2(SO_4)_3$ and/or $ZnSO_4.7H_2O$ used in G1 and S1 solutions.

A-2 Calculation of Metal Ion-Exchange ZSM-5

Gallium Ion-Exchange

Determine the amount of Ga into catalyst = 2.03 wt.%

The catalyst used = X g

So that, from the equation

Ga/(X+Ga) = 2.03/100

100 x Ga = 2.03 x (X+Ga)

(100-2.03) x Ga = 2.03 x X

Thus Ga = (2.03 x X) / (100 – 2.03) g

Use $Ga_2(SO_4)_3$ (Molecular Weight = 427.63, 32.61 % Ga)

Weight of $Ga_2(SO_4)_3$ = [2.03 x X / (100-2.03)] / [100 / 32.61] g

Zinc Ion-Exchange

Determine the amount of Zn into catalyst = 1.88 wt.%

The catalyst used = X g

So that, from the equation

Zn/(X+Zn) = 1.88/100

100 x Zn = 1.88 x (X+Zn)

(100-1.88) x Zn = 1.88 x X

Thus Zn = (1.88 x X) / (100 – 1.88) g

Use $ZnSO_4.7H_2O$ (Molecular Weight = 287.54, 21.98 % Zn)

Weight of $ZnSO_4.7H_2O$ = [1.88 x X / (100-1.88)] / [100 / 22.74] g

A-3 Calculation of Reaction Flow Rate

The catalyst used = 0.25 g

Packed catalyst into quartz reactor (inside diameter = 0.6 cm)

Determine the average high of catalyst bed = H cm. So that,

$$\text{Volume of catalyst} = \pi \times (0.3)^2 \times H \text{ cc-cat.}$$

Used Gas Hourly Space Velocity (GHSV) = $2000\ h^{-1}$

$$\text{GHSV} = \frac{\text{Volumetric flow rate}^1}{\text{Volume of catalyst}}$$

$$\text{Volume of flow rate}^1 = 2000 \times \text{Volume of catalyst}$$

$$= 2000 \times \pi \times (0.3)^2 \times H \text{ cc/h}$$

$$= (2000 \times \pi \times (0.3)^2 \times H) / 60 \text{ cc/min.}$$

At STP condition:

$$\text{Volume flow rate} = \text{Volume flow rate}^1 \times (273.15 + t) / 273.15$$

Where t = room temperature, ^oC

A-4 Calculation of Conversion and Hydrocarbon Distribution of Aromatization Reaction

The n-heptane aromatization activity was evaluated in term of the conversion of n-heptane into other hydrocarbons.

$$\text{n-heptane conversion (\%)} = \frac{([\text{n-heptene}]_{in} - [\text{n-heptane}]_{out}) \times 100}{(\text{n-heptane})_{in}}$$

For example: H-Ga.Al-silicate (Si/Ga = 100, Si/Al = 40)

Reaction condition Reaction temperature 550 ^{o}C, GHSV = 2000 h^{-1},
Feed 6 % n-heptane feed

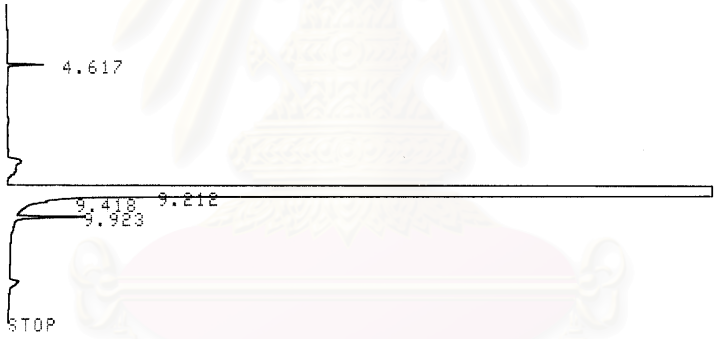

P<NO	TIME	AREA	MK	IDNO	CONC	NAME
1	9.212	244450	S		99.8436	
2	9.923	383			0.1564	
	TOTAL	244833			100	

START

From Figure A-5.1

Silicon OV-1 (feed)

Area of feed n-heptane = 244833

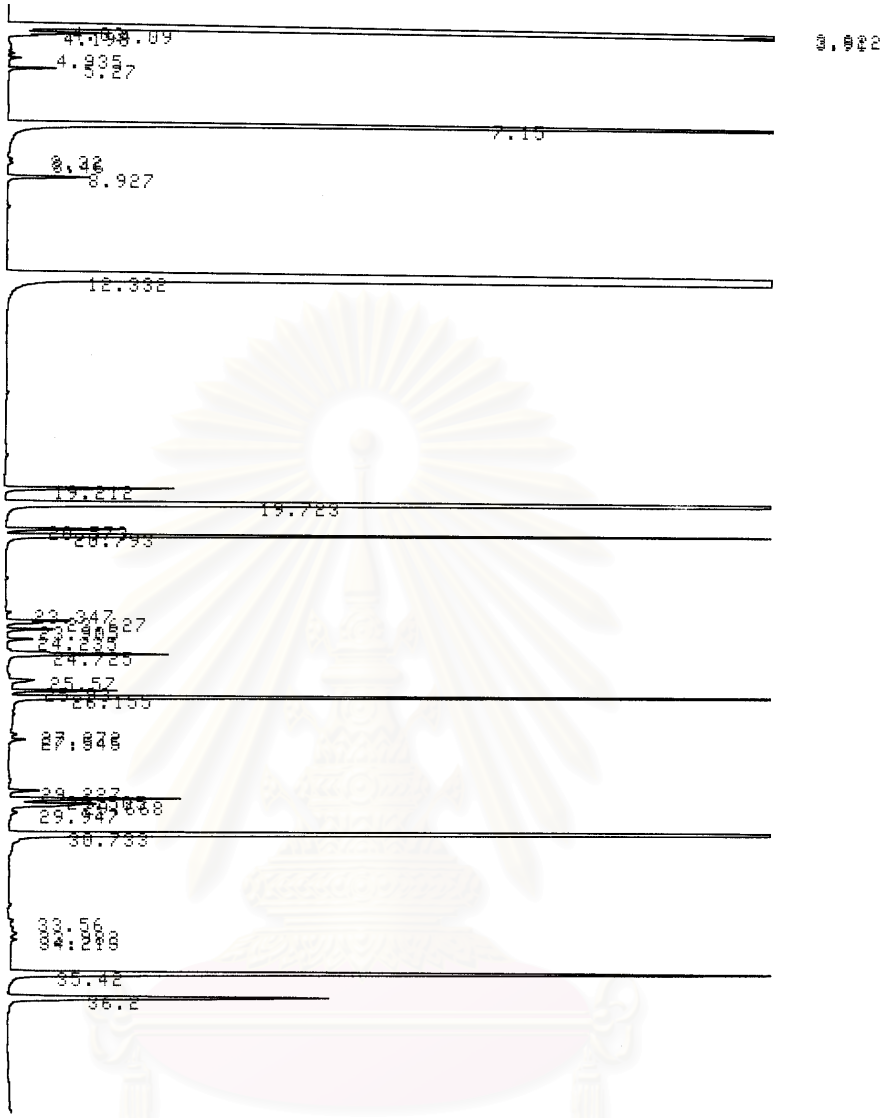

NO	TIME	AREA	MK	IDNO	CONC	NAME
1	3.822	37127			16.205	
2	3.91	14820	V		6.4687	
3	4.09	579	V		0.2528	
4	7.15	65726			28.6874	
5	8.927	451			0.1967	
6	12.332	61806			26.9763	
7	19.212	906			0.3955	
8	19.723	12117			5.2888	
9	20.573	601			0.2623	
10	20.793	4127	V		1.8013	
11	23.627	417	V		0.1819	
12	24.725	984			0.4293	
13	25.93	479	V		0.2093	
14	26.155	6129	V		2.6753	
15	29.505	983	V		0.4291	
16	29.668	748	V		0.3266	
17	30.733	12427			5.4242	
18	35.42	6162			2.6897	
19	36.2	2520			1.0999	
	TOTAL	229110			100	

From Figure A-5.2

VZ-10 (1h)

Area of CH_4, C_1 = 470000

Area of C_2 = 392794

Area of $C_2^{=}$ = 525273

Area of C_3 = 334395

Area of $C_3^{=}$ = 174367

Area of C_4^{+} = 16680

Area of C_1-C_4 = 47000+39794+525273+334395+174369+ 16680

= 1913509

Form Figure A-5.3

Silicon OV-1 (1h)

Determine all of hydrocarbons area into 3 parts

First part are the area of C_1-C_4 = 52526

Second part are the area of C_5 = 451

Third part are the area of aromatics = 176133

Total area = 229110

So that: compared the area from VZ-10 to the area of OV-1

$$\text{area of } C_1 \text{ (OV-1)} = \frac{\text{area of } C_1\text{(VZ-10)} \times \text{area of } C_1\text{-}C_4\text{(OV-1)}}{\text{area of } C_1\text{-}C_4\text{(VZ-10)}}$$

= (470000 x 52526) / 1913059

= 12902

The other were calculated as same as C_1

Area of C_2 (OV-1) = 10782

Area of $C_2^{=}$ (OV-1) = 14419

Area of C_3 (OV-1) = 9179

Area of $C_3^{=}$ (OV-1) = 4786

Area of C_4^{+} (OV-1) = 458

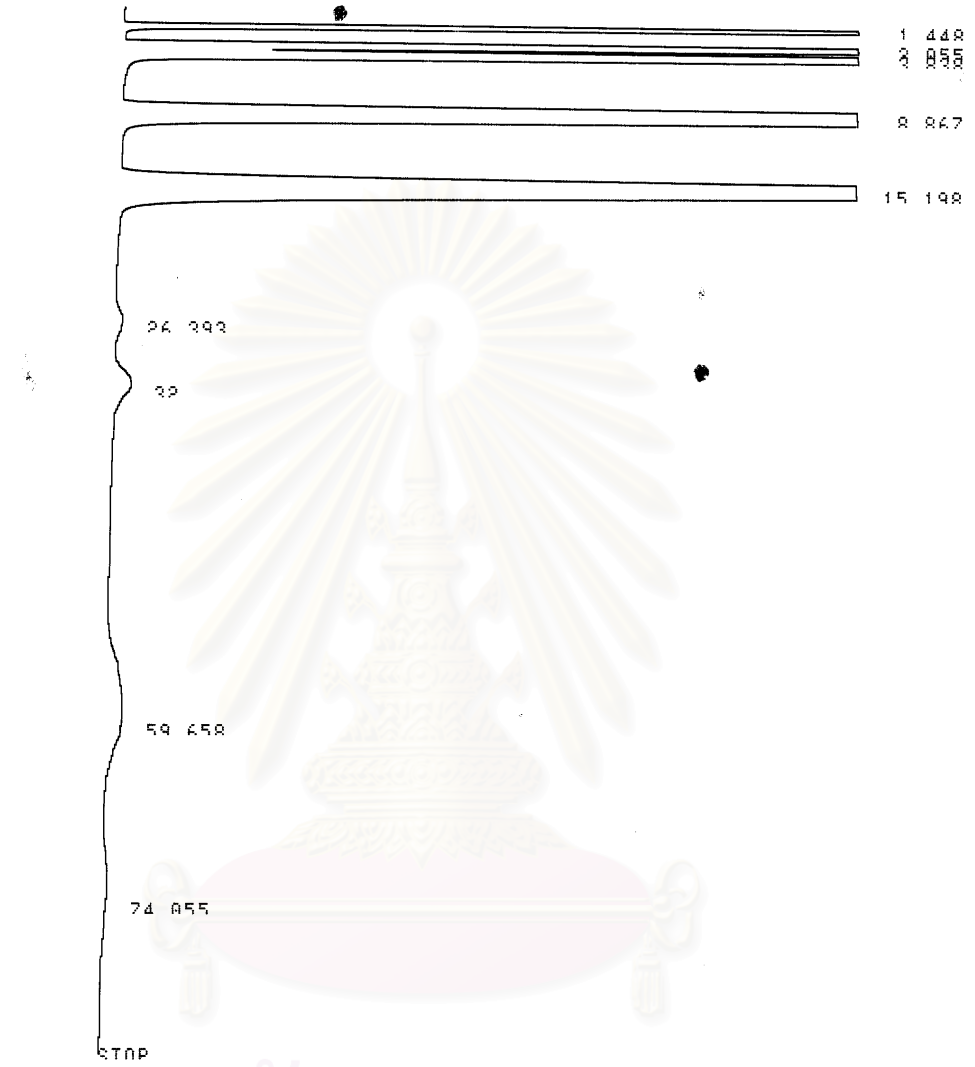

PKNO	TIME	AREA	MK	TRNO	CONC	NAME
1	1 448	470000			24 5629	
2	3 855	392794			20 5274	
3	3 838	525273	V		27 4508	
4	8 867	334395			17 4755	
5	15 198	174367			9 1124	
6	24 393	1917			0 0636	
7	39	3630			0 1897	
8	59 658	9443			0 4935	
9	74 855	2390			0 1249	
	TOTAL	1913588			100	

Hence: Product distribution (C-wt.%)

C_1	=	[area C_1(OV-1) x 100] / (total area of OV-1)
	=	(12902 x 100) / 229110
	=	5.63 %
C_2	=	4.71 %
$C_2^=$	=	6.29 %
C_3	=	4.01 %
$C_3^=$	=	2.09 %
C_4	=	0.20 %
C5	=	0.20 %

Aromatics	=	76.88 %
- benzene	=	28.69 %
- toluene	=	26.98 %
- xylene	=	7.75 %
- A_9^+ (or other)	=	13.46%

$$\text{n-heptane Conversion} = \frac{[\text{area of feed n-heptane}] - [\text{area of n-heptane rested}]}{\text{area of feed n-heptane}}$$

$$= [(244833 - 78096) \times 100] / 224833$$

$$= 100\ \%$$

VITA

Miss Nilnate Oung was born on October 6, 1976 in Bangkok, Thailand. She received the Bachelor's Degree of Science from Department of Chemical Technology, Faculty of Science, Chulalongkorn University in 1998. She continued her Master's Study at Chulalongkorn University in June, 1998.